2019

A Break In Communication: The Synthesis, Characterization, DNA Binding and Photocleavage of a Novel Ruthenium Polypyridyl Complex Containing an Electronically Isolated Pyrene Group

Samantha Klein
Bryn Mawr College

A Break In Communication: The Synthesis, Characterization, DNA Binding and Photocleavage of a Novel Ruthenium Polypyridyl Complex Containing an Electronically Isolated Pyrene Group

By

Samantha Klein

April 2019

Submitted to the Faculty of Bryn Mawr College in partial fulfillment of the requirements for the degree of Doctor of Philosophy in the Department of Chemistry

ABSTRACT

A novel complex $[Ru(bpy)_2bpy\text{-}py]^{2+}$ (where bpy= 2,2'-bipyridine and bpy-py=N-(6-(4-(pyren-1-yl) butanamido) hexyl)-[2,2'-bipyridine]-5-carboxamide))) has been synthesized. The effect of electronically isolating the pyrene from the metal core on the complex's ability to bind to and photocleave DNA was studied. Other molecules such as 1-pyreneacetic acid and $[Ru(bpy)_2dep]^{2+}$ (where dep= N-(6-aminohexyl)-[2,2'-bipyridine]-5-carboxamide), which share structural similarities to $[Ru(bpy)_2bpy\text{-}py]^{2+}$, were also studied to help determine which areas of the $[Ru(bpy)_2bpy\text{-}py]^{2+}$ molecule may be responsible for interacting with DNA. Spectroscopic experiments including isothermal and competitive binding titrations in addition to the hydrodynamic technique of viscometry were used to show that $[Ru(bpy)_2bpy\text{-}py]^{2+}$ binds to DNA with a binding constant of 8×10^5 and 1×10^6 M^{-1} (binding constants calculated using isothermal and competitive binding experiments, respectively). Agarose gel electrophoresis, used to assess photocleavage, gave ambiguous results. Additional fluorometric experiments revealed that a transfer of energy from the pyrene portion of the complex to the ruthenium core may be occurring.

ACKNOWLEDGEMENTS

I am extremely grateful to my two advisors, Drs. Jonas Goldsmith and Sharon Burgmayer. They guided me through my research and all of the other requirements and nuances of completing my degree. I consider myself very lucky to have benefited from the perspectives of these two mentors. They showed me how scientists can work together to take ideas from theory, through experimentation to a meaningful conclusion that can benefit the wider scientific community.

I would like to thank Dr. Ryan Fealy for his friendship, guidance and patience in helping me through this journey. Dr. Fealy along with Michele Seiler and doctors Ben Williams, Doug Gieswhite, Maria Winters, Sarah Burke Church, Andy Krasley and Alyssa Bohen served as my wider community of graduate students who commiserated and celebrated with me along our journeys at Bryn Mawr. Dr. Shannon Dalton, while no longer on campus during my time, left an indelible mark within the Burgmayer group and my project was partially based off of her work. I thank her for making a path for others to explore. Undergraduates are such an important part of the Bryn Mawr experience and special thanks go to Maggie Ahrens, Meredith Skiba and Alex Gaudette who either worked with the complex used in my project or the wider ruthenium DNA project in the Burgmayer group.

At the beginning of my journey at Bryn Mawr, I did not fully understand the importance of community. Still now, I fight against it trying to act as a loner, but this community at Bryn Mawr helped me during some of my darkest times. My path to earning my PhD has been effected by several losses in my immediate family, including the loss of my dear father, Tibor Klein and my grandmother, Vera Klein. I have lost more than I could imagine during my time at Bryn Mawr, but through this loss I am trying to find my strength and my ability to contribute to

the scientific community. I know that through the mentorship I have received I will be a better scientist and work towards meaningful resolutions to the problems that I am confronted with. Thank you to all who have helped, including my mother- Johanne Klein, my husband, Travis Uyeno and my new family: Pat, Steve and Elizabeth Uyeno.

This work is dedicated to
Tibor, Johanne, Vera and Travis

Table of Contents

List of Figures

LIST OF TABLES

LIST OF REACTION SCHEMES

LIST OF ABBREVIATIONS

ACN	**Acetonitrile**
Anhyd	**Anhydrous**
Bp	**Base pairs**
^{1}H-NMR	**Proton Nuclear Magnetic Resonance**
bpy	**2,2'-bipyridine**
bpy-py	**N-(6-(4-(pyren-1-yl) butanamido) hexyl)-[2,2'-bipyridine]-5-carboxamide**
$CDCl_3$	**Chloroform-*d***
CT DNA	**Calf Thymus DNA**
DCM	**Methylene Chloride**

DMF	**Dimethyl Formamide**
DNA	**Deoxyribonucleic Acid**
DPPZ	**Dipyrido[3,2-a:2',3'-c]phenazine**
EB	**Ethidium Bromide**
EDTA	**Ethylenediaminetetraacetic acid**
ESI-MS	**Electrospray Ionization Mass Spectrometry**
FRET	**Fluorescence Resonance Energy Transfer**
FT-NMR	**Fourier-transform Nuclear Magnetic Resonance**
$\mathbf{K_{app}}$	**Apparent Binding Constant**
$\mathbf{K_b}$	**Binding Constant**
$\mathbf{K_{EB}}$	**Binding Constant of Ethidium Bromide**
LFSE	**Ligand Field Stabilization Energy**
MeOD	**Methanol-d_6**
MeOH	**Methanol**
MLCT	**Metal to Ligand Charge Transfer**
PCR	**Polymerase Chain Reaction**
phen	**1,10- phenanthroline**
TLC	**Thin Layer Chromatography**
$\mathbf{T_m}$	**DNA melting temperature**
TPP	**Triphenylphosphite**
UV	**Ultraviolet**
UV-Vis	**Ultraviolet-Visible**

1.0 Introduction

1.1 Purpose of Studying Compounds That Interact With DNA

Over the last several decades, extensive research has been conducted on compounds capable of binding to and photocleaving DNA. (Biver, Seco and Venturrini 2008), (Liu, et al. 1995). Photocleavage occurs when the energy from photons causes reactions that break some of the bonds in DNA. This research had been motivated by the desire to find more effective and safer chemotherapeutic drugs, as well as by the need for better molecular diagnostics. (Erkkila, Odom and Barton 1999), (Zhang and Lippard 2003), (Friedman, et al. 1990) These compounds include transition metal complexes, such as those containing platinum or ruthenium, in addition to small molecules such as ethidium bromide. Following irradiation, these compounds promote the generation of reactive oxygen species (ROS) localized to the base pairs of DNA, which can trigger oxidation of the base pairs of DNA and ultimately lead to strand breakage. (Caitino, Mella and Cardenas-Jiron 2014) This provides a potential mechanism to destroy cancerous tissue. This thesis will focus on the way in which ruthenium polypyridyl complexes interact with DNA. Since ruthenium polypyridyl complexes often contain polycyclic aromatic hydrocarbons, the interaction of polyaromatic hydrocarbons with DNA will also be investigated in order to better understand how different constituents of the complex may contribute to DNA binding and photocleavage. For the purpose of clarity in this work ligand will refer to something bound to a metal center. When used the term molecule refers to a covalently bound collection of atoms which is not connected to a metal center.

Molecular structure plays an important role in determining whether or not a species will bind to DNA, and if so, in what manner. When transition metal complexes are examined for their interactions with DNA, one of two primary modes of binding are usually observed:

intercalation and groove binding. Intercalation typically occurs when an extended aromatic system inserts itself between the base pairs of DNA, whereas groove binding involves the attachment of the complex or molecule to the exterior grooves of DNA. (Biver, Seco and Venturrini 2008), (Murphy and Barton 1993) (Barton, et al. 1986) (Rehmann and Barton 1990) DNA has both major and minor grooves binding, usually via electrostatic interactions, may transpire at either site.(Barton, et al. 1986) Figure 1 below illustrates molecules binding to DNA through either intercalation or grove binding. (Turro, Barton, & Tomalia, 1991)

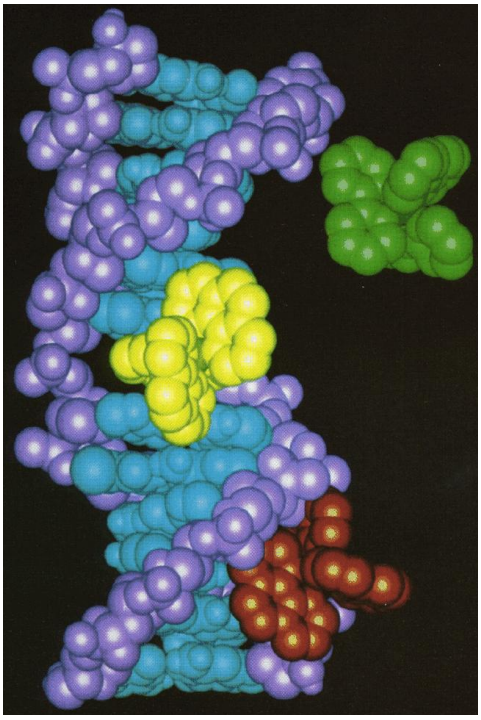

Figure 1. Model of DNA and complexes- $[Ru(bpy)_3]^{2+}$ (where bpy= 2,2'-bipyridine) in green shown not binding to DNA, Δ-$[Ru(phen)_3]^{2+}$ (where phen= 1,10- phenanthroline) in yellow is binding through intercalation to DNA and red Λ-$[Ru(phen)_3]^{2+}$ to the surface of DNA through the minor groove. (Turro, Barton, & Tomalia, 1991)

Before considering specific examples of complexes and how they interact with DNA, it is important to establish which experimental techniques are commonly used to demonstrate the existence of DNA binding and photocleavage.

1.2. Methods of Analyzing DNA Interactions

Many of the techniques used to characterize the binding of a coordination complex or polyaromatic hydrocarbon to DNA utilize the light-absorbing properties of such compounds to indicate binding. (Barone, et al. 2013) (Kelly, et al. 1987) When binding occurs, the light-absorbing behavior of the coordination complexes and polyaromatic hydrocarbons are often altered due to, in part, the electronic interaction with DNA. (Barone, et al. 2013) Isothermal binding titrations demonstrate binding to DNA (Smith, et al. 2013), by exposing a molecule to increasing amounts of DNA. When transition metal complexes bind to DNA, the functional group of the complex bound to DNA no longer receives an electron originating from the metal center, thereby decreasing the absorbance. This occurs because the new binding interactions with DNA through electrostatic or intercalative binding prevent the ligand centered molecular orbital from being available to accept an electron from the metal centered orbital. This experiment is most useful for complexes with light-absorbing properties at wavelengths longer than 300 nm. (Smith, et al. 2013) This is due to the fact that at wavelengths shorter than 300 nm, it becomes difficult to distinguish if changes in absorption are due to the binding molecule or DNA, which absorbs around 260 nm. Therefore, this experiment is particularly useful for transition metal complexes with MLCT bands centered around 400-500 nm. (Smith, et al. 2013) The isothermal binding experiment generally supports that binding to DNA is occurring when there is a hypochromic shift (a decrease in absorbance intensity) in the absorbance of the MLCT as DNA is added. (Carter, Rodriguez and Bard 1989) . When such a hypochromic shift is

observed, isothermal binding titrations can also provide a quantitative measure of the strength of binding in the form of a binding constant, K_b. (Carter, Rodriguez and Bard 1989)

In addition to isothermal binding titrations other spectroscopic experiments can be used to help understand DNA binding behavior of complexes and molecules. (Smith, et al. 2013), (Friedman, et al. 1990) If a complex or molecule is able to absorb light, then that energy must be released in some manner. One possible decay pathway for the release of energy is through emission. Emission spectroscopy can be used to probe complex or molecule binding properties with DNA in a manner similar to that used with isothermal binding titrations and absorption spectroscopy. (Friedman, et al. 1990) The emission of light is not the only way that a system can release absorbed energy; therefore fluorescence enhancement experiments may not be suitable for all complexes to study their DNA binding behavior.

Complexes are commonly emissive in organic solvents and often have their emission quenched when in aqueous systems. (Sabatani, et al. 1996) This quenching typically occurs due to the excited state transition metal complex donating a proton to water. (Liu, et al. 2001) This reaction with water provides a non-radiative decay pathway that reduces emission from the complex . For systems that have low emission in aqueous solutions it is sometimes possible for their emission to be enhanced when DNA is added. When a complex binds to DNA this interaction can shield the ligand from interacting with water, thereby preventing the excited state proton transfer that causes the complex's emission to be quenched. (Liu, et al. 2001) This results in the emission of the complex going from weak to more intense, as if DNA is able to turn on a "light switch" for the complex or molecule. (Liu, et al. 2001) This fluorescence enhancement experiment is widely used in the literature to show that binding to DNA is occurring. (Erkkila, Odom and Barton 1999) Just like the absorption-based isothermal binding titration, the

fluorescence enhancement experiment can also determine a quantitative value for DNA binding strength by consideration of what concentration of DNA is necessary to cause a particular amount of fluorescence enhancement. (Carter, Rodriguez and Bard 1989)

In some circumstances where a complex exhibits strong fluorescence in aqueous solutions, the addition of DNA does not enhance the emission of the complex. In such a situation a competitive binding experiment that uses a second emissive species to study a compound's ability to bind to DNA can be employed. Competitive binding experiments are based on similar principles as the fluorescence enhancement experiment; in order for the experiment to work a molecule must have its emission enhanced when in contact with DNA. Ethidium bromide (EB) has weak emission when excited at 520 nm in aqueous solutions. When DNA is added to an aqueous solution of EB, a marked increase in the emission is observed. (LePecq and Paoletti 1967) When EB interacts with DNA, it does so by binding through intercalation and this shields the molecule from the solvent and thereby prevents water molecules from quenching its emissive state. (Lee, et al. 1993) (LePecq and Paoletti 1967) When a third complex or ligand is added to the solution of DNA and EB, the added complex can cause a decrease in the emission of EB if the complex is also binding to DNA. (Haworth, et al. 1991) This is due to the fact that the new complex competes for space on DNA with EB, effectively displacing the EB out of its shielded environment and therefore diminishing some of its emission. (Haworth, et al. 1991) Such an experiment is useful for determining binding and calculating and apparent binding constant. (Lee, et al. 1993) The binding strength is determined by finding the concentration of complex that results in a 50% decrease in the emission of EB and comparing this value to the concentration of EB used and its binding constant of $1 \times 10^7\ M^{-1}$. (Ganeshpandian, Loganathan, Suresh, Riyasdeen, Akbarsha, & Palaniandaver, 2014) Complexes

that compete strongly with EB for space on DNA will decrease EB's emission even with relatively low concentrations of complex added.

The isothermal binding studies carried out using either fluorescence or UV-Vis (ultraviolet-visible) spectroscopy were once thought to be able to definitively indicate that the mode of binding was through intercalation. Further study has revealed that in most circumstances theses experiments are not sensitive enough to distinguish the mode of binding to DNA. (Eriksson, et al. 1992) (Rehmann and Barton 1990) (Liu, et al. 2001). (Eriksson, et al. 1992) (Rajalakshmi, et al. 2011) Another technique, Fluorescence Resonance Energy Transfer (FRET) can show if a complex or ligand is binding to DNA through intercalation.(Paoletti and Le Pecq 1971) The experiment works by first exciting the DNA. (Reinhardt, Roques and Le Pecq 1982) When a complex that binds to DNA does so in the correct orientation, the energy absorbed by DNA can be transferred to the complex, resulting in its excitation and then subsequent emission. (Reinhardt, Roques and Le Pecq 1982) This can only work if the complex is in close contact with DNA and in the correct orientation such as it would be if it was binding through intercalation. The Resonance Energy Transfer Jablonski Diagram below illustrates how the transfer of energy occurs between molecules in the FRET experiment. (Herman, et al. 2012) First the donor molecule must accept a photon which results in its excitation. A portion of the energy absorbed is released through vibrational relaxation or other non-radiative pathways that result in energy transfer to the acceptor molecule. The excited acceptor molecule then releases energy as emission of light.

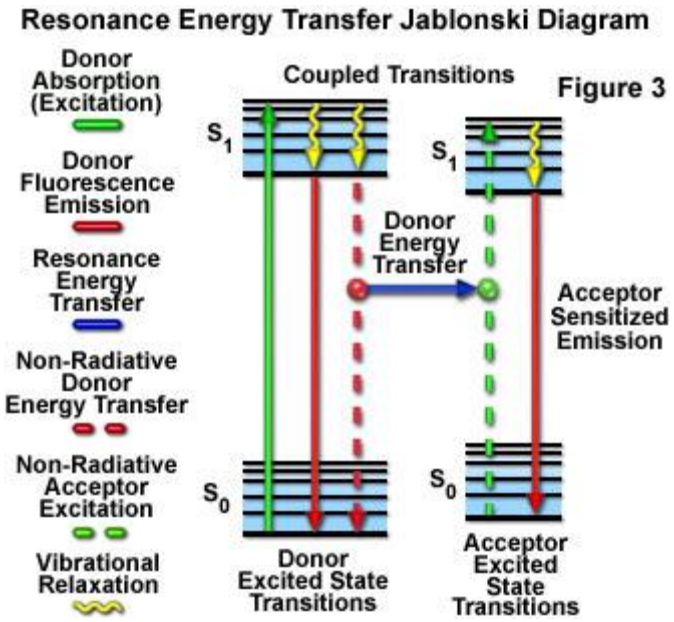

Figure 2. Transfer of energy between species used in a FRET experiment. (Herman, et al. 2012)

Molecules must be in close contact and correctly oriented in order for energy transfer to occur. Due to the constraints of this experiment, there are a limited number of systems in which FRET can successfully show that intercalation is occurring but it is still useful. (Herman, et al. 2012)

When spectroscopic studies support that a molecule is binding to DNA the hydrodynamic technique of viscometry can demonstrate conclusively whether or not intercalation is taking place. (Satyanarayana, Dabrowiak and Chaires 1992) When a complex is added to a solution of DNA and binds through intercalation, this causes an overall lengthening of the DNA helix due to space on the helix now being occupied by the binding compound. This lengthening results in an increase in the viscosity of DNA. (Satyanarayana, Dabrowiak, & Chaires, 1992)

Once evidence of binding of a complex or ligand to DNA is established through either spectroscopic or hydrodynamic techniques, researchers often turn to electrophoretic experiments

to investigate whether or not the molecules are able to damage DNA. Molecules that damage DNA are good candidates for use as chemotheraputics.

Due to their d- π^* energy transfers transition metal complexes with medium to large aromatic groups generally have absorption profiles that extend well into the visible region of the electromagnetic spectrum. This increases potential energy absorption compared to a complex lacking aromatic groups, or small polyaromatic hydrocarbons which generally only absorb between 200- 300 nm. (Tan, et al. 2007) (Swavey and Wilson 2015) After light is absorbed a common result is the generation of reactive oxygen species (ROS) that can go on to oxidize DNA and cause photocleavage. (Poteet, et al. 2013) (Swavey and Wilson 2015) (Belvedere, et al. 2002) The most widely used technique for determining whether or not photocleavage of DNA has happened is agarose gel electrophoresis. In this experiment a specific pattern of bands can be imaged on the gel substrate and this pattern corresponds to how much damage to DNA has occurred.

Through the analysis of spectroscopic, hydrodynamic and photocleavage experiments, researchers can show whether or not a compound is binding to DNA, by which mode and if that compound is capable of damaging DNA. Not every experiment may be applicable for a complex or ligand under investigation. For example, a chemical entity's absorption properties will greatly dictate the usefulness of the isothermal binding titrations and the various fluorescence experiments discussed.

1.3 Compounds Studied for DNA Binding

Transition metal complexes, polyaromatic hydrocarbons (PAHs), and simple organic molecules are all capable of interacting with DNA. (Erkkila, Odom and Barton 1999) Each of these different types of molecules have the potential to be used as chemotherapeutics, molecular

imaging dyes or models to help understand how molecules interact with and break down DNA. (Zhang and Lippard 2003) By comparing how small molecules interact with DNA alone and when ligated to transition metals a better understanding of the key structural elements for DNA binding may be obtained.

One of the the first transition metal complexes to be used as a chemotherapeutic drug was cisplatin, a square planar platinum complex. (Sherman & Lippard, 1987) Prior to its discovery most therapeutics were derived from organic compounds lacking metal centers. Cisplatin laid the foundation for much of the research that continues today involving transition metal complexes as possible therapeutics. (Sundquist and Lippard 1990) The complex in this work contains an octahedral complex of ruthenium, therefore a review of prior research involving similar complexes that interact with DNA will be provided. The complex of interest also contains a pyrene functional group, therefore small molecules that bind to DNA will be reviewed to better understand how the pyrene portion of the complex affects any DNA binding.

1.3.1 Square Planar Complexes Interacting with DNA

Early work performed by Lippard and coworkers discovered that the square planer complex $[(2,2',2''\text{-terpyridine})PtCl]^{+}$ was capable of interacting with DNA. (Jennette, et al. 1974) The group found that the complex was able to bind to DNA when its planar terpyridine ligand intercalated between the base pairs of DNA. (Jennette, et al. 1974) Fluorescence studies showed that the complex was able to decrease the emission of EB bound to DNA through a competitive process. (Sundquist and Lippard 1990) This result, coupled with viscosity experiments showed that the complex was binding to DNA through intercalation. (Jennette, et al. 1974) While this complex showed reactivity that would make the it an attractive candidate for medicinal purposes, the use of coordination complexes as theraputic agents was not yet a

common practice. (Sundquist and Lippard 1990) It was not until the discovery of the square planar complex Cisplatin, *cis*-$[Pt(NH_3)_2(Cl)_2]$, that coordination complexes began to be viewed as viable candidates for drugs such as antitumor agents. Once in vivo Cisplatin works by exchanging one of its chloride ligands for water. (Wang & Lippard, 2005) (Rosenberg, 1978) This water ligand is rather labile and able to be exchanged for one of the bases on DNA. (Crul, van Waardenburg, Beijnen, & Schellens, 2002) (Gust, Beck, Jaouen, & Schonenberger, 2009) The resulting adduct causes distortion of the tumor cell's DNA and can inhibit the tumor cells' ability to transcribe and replicate. This promotes apoptosis which leads to the breakdown of cells and inhibits tumor growth.

Cisplatin is not very specific as to what kind of DNA it targets and as a result it can also damage DNA in healthy tissue. Cisplatin possesses significant nephrotoxicity which can limit its utility for cancer patients. (Zhang & Lippard, 2003) Research continues on platinum complexes for their ability to treat cancer. In order to develop chemotherapeutics with lower toxic effects carboplatin was developed. (Gust, Beck, Jaouen, & Schonenberger, 2009) Carboplatin is a square planar complex of platinum and is structurally similar to cisplatin except it lacks the labile chloride ligands of its predecessor. (Jakupec, Galanski, & Keppler, 2003) In place of the chloride ligands is a modified dicarboxylate moiety which binds to platinum as a bidente ligand. (Jakupec, Galanski, & Keppler, 2003) This structural change results in slower aquation of carboplatin when compared to cisplatin. (Kim, Roh, Wee, & Kim, 2016) The rate constants for aquation of cisplatin and carboplatin were found to be $8 \times 10^{-5}\ s^{-1}$ and $7.2 \times 10^{-7}\ s^{-1}$, respectively (when tested in vitro at 37°C). (Knox, Friedlos, Lydall, & Roberts, 1986) DNA binding cannot occur in either Cisplatin or Carboplatin until aquation takes place and allows for monofunctional or difunctional adducts to form with DNA. The initial monoaquation of carboplatin results in

monoadducts of carboplatin to form with DNA, it is not until over 12 hours later that difunctional adducts of carboplatin form with DNA in vivo. (Oliveria, Caquito, & Rocha, 2018) In cisplatin both chloride ligands are exchanged for water quickly and difunctional adducts of cisplatin with DNA are formed. While the binding constants for cisplatin and carboplatin are similar, $(2.4 \pm 0.4) \times 10^4\ M^{-1}$ and $(1.6 \pm 0.2) \times 10^4\ M^{-1}$ (for cisplatin and carboplatin, respectively) the differences in rates accounts for a reduction in unwanted side effects in carboplatin. (Oliveria, Caquito, & Rocha, 2018)

The work involving Cisplatin and its analogs helped show the utility of transition metal complexes for therapeutic purposes. Today the vast majority of medicinal products are still small organic molecules. (Sundquist and Lippard 1990) Despite this trend cisplatin has been on the market as a chemotheraputic for decades. More recent studies now examine square planar complexes of Cu^{2+}, Zn^{2+} and Ni^{2+} for DNA binding and chemotheraputic properties in an effort to improve on drug resistance of cisplatin. (Selvakumaran, Bhuvanesh, Endo, & Karvembu, 2014) The Irving-Williams series states that complex stability increases as ionic radius decreases across across the period. (Haas & Franz, 2009) This is an important consideration when creating first row divalent complexes for DNA binding. Complexes will generally exhibit the following stabiliy: $Ni^{2+} < Cu^{2+} > Zn^{2+}$(LFSE or ligand field stabilization energy is used to explain the increased stability of copper). (Haas & Franz, 2009) If the goal is to synthesize complexes that are more labile so that they can interact with DNA in a manner similar to cisplatin or carboplatin, then working with Ni^{2+} may be more desirable than Cu^{2+}. Conversly, if the desire is to synthesize a more inert complex, Cu^{2+} may be a more suitable choice. One structural feature found in modern square planar complexes is the incorporation of Schiff bases as ligands. (Barone, et al., 2013) Schiff bases are a subclass of imines and bind to metals

through their imine nitrogens. One benefit of using Schiff bases as ligands in complexes is that when cojugated, the absorbance of Schiff bases extends into the visible spectrum, which can be probed through spectroscopic studies to determine DNA binding. (Barone, et al., 2013)

1.3.2- Octahedral Complexes Interacting with DNA

The work involving cisplatin and its remarkable contribution to medicine helped open the door for other coordination complexes to be considered for potential pharmaceutical targets. (Sundquist and Lippard 1990) Early examples of inorganic complexes being used in biological systems are DNA foot printing reagents which were used to help determine the size of protein binding sites within DNA. (Sundquist and Lippard 1990) (Tullius 1989) Octahedral complexes of zinc, cobalt and ruthenium, among others, have been studied for their interactions with DNA. (Erkkila, Odom and Barton 1999), (Barton, Dannenberg and Raphael 1982) The spectroscopic properties such as their visible and UV (ultraviolet) light absorption of these complexes make them ideal candidates to be used as molecular probes for applications such as diagnostic imaging. (Strianese 2016) If preferential binding to sequences of DNA can be achieved, then the complex's spectroscopic properties can signal this binding through luminescence enhancement and aid in the detection of diseased tissue. (Murphy & Barton, 1993) The focus of this dissertation will be on the interaction of an octahedral complex of ruthenium with DNA. The target complex consists of two bipyridine ligands and a third modified bipyridine ligand. It is therefore prudent to focus on prior research based on similar complexes to understand the similarities and differences between past work and the complex of interest.

Jacqueline Barton has contributed a great deal of research to understanding how complexes, particularly ruthenium polypyridyl complexes interact with DNA.(Murphy and Barton 1993) The fact that such complexes are coordinatively saturated and inert to substitution and that their octahedral structure, with three bidente ligands, makes these species chiral (a

structural aspect that allows for enhanced DNA binding studies) makes them excellent candidates for probing DNA. (Murphy & Barton, 1993) (Xiong & Ji, 1999) A complex that is coordinatively saturated and inert to substitution prohibits the exchange of ligands which may complicate experiments by making it more difficult to determine what form of a complex is actually interacting with DNA. Much of this type of study focuses on how structurally related complexes differ in their ability to interact with DNA. By making subtle changes to functional groups of related complexes researchers can discern what structures are necessary for DNA binding. Chiral species used in DNA studies can bind selectively to certain sequences of DNA, this type of selective binding is helpful for making complexes that target diseased tissue.

Barton's early studies investigated octahedral complexes that bind to DNA and used tris(1,10-phenanthroline) ligands bound to metals to facilitate this interaction with DNA. (Barton, Goldberg, et al. 1986) The complex $[Ru(phen)_3]^{2+}$ had already been extensively studied in other contexts and was chemically well understood. (Erkkila, Odom and Barton 1999),(Friedman, et al. 1990) Researchers presumed the extended aromatic structure of the phenanthroline ligand would make it an attractive candidate for intercalation into the base pairs of DNA. (Erkkila, Odom and Barton 1999) It was discovered that the mode of binding to DNA was influenced by which enantiomer of $[Ru(phen)_3]^{2+}$ was present, the Δ-isomers preferred binding to right handed DNA via intercalation while the Λ-isomers were found to bind complementarily against the right handed groove. (Erkkila, Odom and Barton 1999) (Barton, Goldberg, Kumar, & Turro, 1986)

The claim that $[Ru(phen)_3]^{2+}$ binds to DNA was substantiated with luminescence studies. (Bouskila, et al. 2004) In an aqueous solution, the complex had minimal emission upon excitation of light corresponding to the complex's MLCT. When the complex was exposed to

DNA, there was a modest increase in its emission. This fluorescence enhancement experiment did show that the complex binds to DNA, however the binding was weak as characterized by limited emission enhancement upon addition of DNA. Therefore Barton and coworkers explored modified forms of the $[Ru(phen)_3]^{2+}$ complex to try to develop a complex that binds to DNA with greater affinity. (Friedman, et al. 1990) Barton performed a great deal of research on the complex $[Ru(bpy)_2DPPZ]^{2+}$(bpy- 2,2'-bipyridine, DPPZ = dipyrido[3,2-a:2',3'-c]phenazine). This complex was an excellent candidate for intercalative DNA binding due to the extended aromatic DPPZ ligand. Barton found that $[Ru(bpy)_2DPPZ]^{2+}$ by itself in aqueous solution displayed no appreciable emission. (Hartshorn and Barton 1992) When the emission of $[Ru(bpy)_2DPPZ]^{2+}$ was monitored at 628 nm, there was a 10^4 factor enhancement in its emission using a 1:10 solution of complex with poly[d(GC)d(GC)] DNA. (Friedman, et al. 1990) Barton's group was able to show that $[Ru(bpy)_2DPPZ]^{2+}$ was undergoing a "molecular light switch" effect making the complex an excellent candidate to be used as a molecular reporter. (Hartshorn and Barton 1992) A molecular reporter is a molecule that undergoes a measurable change that can be used to detect the presence of an enzyme, tumor or specific type of DNA. (Murphy & Barton, 1993) In aqueous solutions, the nonradiative decay pathway for $[Ru(bpy)_2DPPZ]^{2+}$ involves protonation of the phenazine nitrogens when the complex is in an excited state. (Friedman, et al. 1990) When the complex is put into solution with DNA, it binds to DNA through the phenazine ring. Once bound, DNA shields the phenazine nitrogens from protonation from the solvent and allows for a radiative pathway to occur. (Friedman, et al. 1990) In contrast to this result, a similar polypyridyl complex, $[Ru(bpy)_3]^{2+}$, did not experience any enhancement in emission upon exposure to DNA, making the complex an ideal negative control for future fluorescence enhancement experiments. (Friedman, et al. 1990)

Barton's group went on to study a host of modified ruthenium polypyridyl complexes to try to understand how the structure of complexes affects DNA binding and luminescence behavior. The group made a series of $[Ru(phen)_2X]^{2+}$ complexes where X represents a modified phenazine ring, which are shown in the figure below. (Hartshorn and Barton 1992)

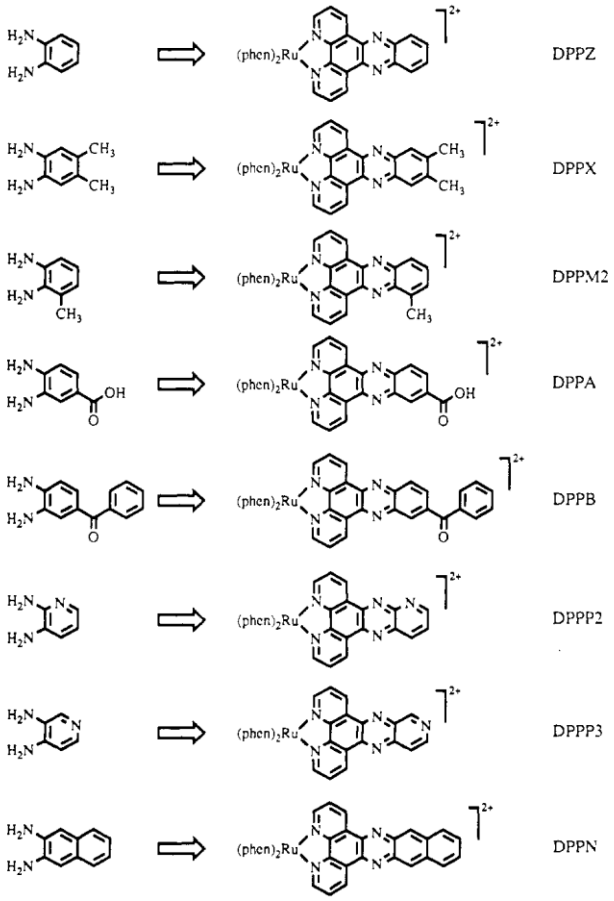

Figure 3. Ortho-diamines (from left to right) used to construct DPPZ derivatives. (Hartshorn and Barton 1992)

All of the $[Ru(phen)_2X]^{2+}$ complexes showed some luminescence in aqueous solutions in the absence of DNA. Though none of the new complexes were capable of achieving an emission enhancement as significant as the one observed for $[Ru(bpy)_2DPPZ]^{2+}$. (Hartshorn and Barton 1992) Barton and coworkers suggest that the limited fluorescence enhancement for the new

complexes may have resulted in part due to steric bulk around the phenazine nitrogens. (Hartshorn and Barton 1992) This would prevent water from getting close enough to quench the phenazine nitrogens, even in the absence of DNA. The greatest emission enhancement upon exposure to DNA occurred for complexes containing DPPX, DPPM2 or DPPA. (Hartshorn & Barton, 1992) The group concluded that this increase in emission was likely due to the ligand becoming protected from solvent quenching upon intercalation. This work showed that even subtle changes to known DNA intercalator/light switches can have a profound effect on the photophysical parameters. This highlights the importance of performing structure function studies to better understand how complexes behave both in the presence and absence of DNA. To further investigate how the DPPZ ligand interacted with DNA Claudia Turro and coworkers went on to study the quenching of racemic, Δ- and Λ-$[Ru(phen)_2(DPPZ)]^{2+}$ excited states both in the presence and absence of DNA in order to correlate electronic transitions within the complex to possible binding modes with DNA. (Turro, Bossman, Jenkins, Barton, & Turro, 1995) By studying racemic mixtures as well as, Δ- and Λ-$[Ru(phen)_2(DPPZ)]^{2+}$ the group could assign how the isomeric forms of the complex effected DNA binding.

Upon excitation of complexes with the structure $[Ru(L)_2DPPZ]^{2+}$ the lowest energy MLCT transition promotes an electron to the DPPZ ligand. (Myrick, DeArmond, & Blakley, 1989), (Juris, Barigeletti, Campagna, Balzani, Belser, & Zelewsky, 1988) This is thought to occur because DPPZ is the most easily reduced ligand in the complex. (Turro, Bossman, Jenkins, Barton, & Turro, 1995) Therefore, by monitoring the emission of the lowest energy MLCT transition in different chemical environments, information can be obtained for the movement of electrons originating from the DPPZ region of the complex. A biexponential decay was observed for $*[Ru(phen)_2DPPZ]^{2+}$ with both short and long lifetime components in aqueous

solutions with DNA. (Turro, Bossman, Jenkins, Barton, & Turro, 1995). This provided evidence that *$[Ru(phen)_2DPPZ]^{2+}$ exists in two different chemical environments to give rise to the observed biexponential decay. The group used hydroquinone and *o*-chlorophenol as quenchers of the emissive state of *$[Ru(phen)_2DPPZ]^{2+}$ to better understand how differences in chemical environment would result in the different lifetime components. (Turro, Bossman, Jenkins, Barton, & Turro, 1995) While both hydroquinone and *o*-chlorophenol are proton donors, hydroquinone is more likely to reside in the aqueous phase and *o*-chlorophenol is better able to interact with hydrophobic regions of DNA. (Turro, Bossman, Jenkins, Barton, & Turro, 1995) By examining the solvent dependence of quenching *$[Ru(phen)_2DPPZ]^{2+}$ they found that the complex is bound to the hydrophobic base pairs of DNA and is therefore protected from quenching by hydroquinone (rather than being bound to the grooves of DNA where the complex would be more exposed to the aqueous solvent and therefore hydroquinone. When the quenching effects of *o*-chlorophenol with racemic *$[Ru(phen)_2DPPZ]^{2+}$ were studied the short lifetime component of the complex bound to DNA showed no solvent dependency indicating that it is not as closely associated with the protected environment of DNA. (Turro, Bossman, Jenkins, Barton, & Turro, 1995) In contrast the long lifetime component of decay was associated with a form of the complex that has the DPPZ intercalated into DNA. These experimental results provide evidence that $[Ru(phen)_2DPPZ]^{2+}$ binds to DNA in two different ways. In one binding geometry the complex is fully intercalated into the base pairs of DNA, and in the other intercalation occurs but DPPZ does not extend as deeply into DNA. Turro and coworkers work helped prove how isomeric differences can effect DNA binding, similar to Barton's work involving $[Ru(phen)_3]^{2+}$.

This new understanding of how the shape of a complex affects DNA binding would aide in creating new complexes with improved binding strength. (Turro, Bossman, Jenkins, Barton, & Turro, 1995)

The body of work involving ruthenium polypyridyl complexes that bind to DNA is vast. This introduction is not meant to be an exhaustive analysis of all of this work, but rather provide insight into the remarkable effects the structure of complexes can have on DNA binding. A group at Bryn Mawr College under the supervision of Dr. Sharon Burgmayer has performed research involving ruthenium complexes bound to DNA that is representative of the wider research performed on such complexes. In order to explore the ability of ruthenium polypyridyl complexes to bind to DNA, this research group constructed DPPZ modified ligands with pterin groups attached to them. (Dalton, et al. 2008) A pterin is a bicyclic N-heterocycle containing a pyrimidine ring substituted by an amino group at the 2 position and a keto group at the 4 position. (Basu & Burgmayer, 2011) The structure of a DPPZ-pterin molecule can be found in Figure 4 below.

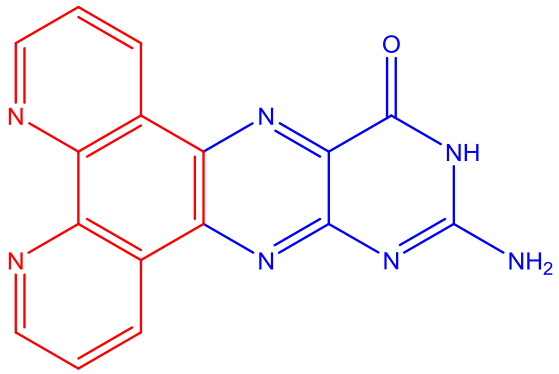

11-aminopteridino[6,7-
f][1,10]phenanthrolin-13(12*H*)-one
"DPPZ-Pterin"

Figure 4. Structure of a DPPZ-pterin molecule used as a ligand in ruthenium complexes. The red and blue portions of the molecule represent the DPPZ and pterin sections; respectively.

The goal of this work was to explore the effects of the pteridynl group on the complex's interaction with DNA. All of the complexes contained a modified phenanthroline group, the terminal portion of which had either a modified pterin or something else such as an alloxazine moiety, which were the areas of the ligand that would be responsible for DNA binding. Some of the pterins contained functional groups capable of hydrogen bonding to the base pairs of DNA and the group questioned what, if any, effect this would have on the complex binding to DNA. (Dalton, et al. 2008) The design of these new complexes probed two different types of binding. The extended aromatic pterin should bind DNA through intercalation. At the same time, the functional groups positioned on the pterin could promote binding similar to complementary base pair binding observed in DNA.

The complexes were synthesized after considering the favored base pairing in native DNA. The different forms of the pterin based complexes could serve as analogs for base pairs such as guanine, which bind to cytosine as show in the following figure.

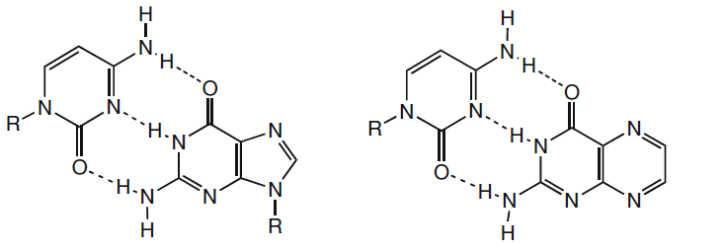

Figure 5. Comparison of Watson-Crick hydrogen bonding in a CG base pair and between C and pterin. (Dalton, et al. 2008)

The group found that all 5 complexes studied were able to bind to DNA and that the mode of binding was through intercalation. (Dalton, Glazier, Leung, Win, Megatulski, & Burgmayer, 2008) The group noted that further experimentation would be necessary to determine if hydrogen bonding between the pterin functional groups and the DNA base pairs was occurring. (Dalton, et al. 2008) The data obtained from both absorption and fluorescence experiments agreed in that all of the complexes bind to DNA but with a lower affinity when compared to $[Ru(bpy)_2(DPPZ)]^{2+}$. (Dalton, Glazier, Leung, Win, Megatulski, & Burgmayer, 2008) This suggests that the electronic extension of the DPPZ ligand in the form of substituted pterins did not result in significant enhancement in DNA binding strength. Viscosity experiments performed on the series of complexes showed that each caused an increase in viscosity of DNA. (Dalton, Glazier, Leung, Win, Megatulski, & Burgmayer, 2008) This result is consistent with intercalative binding.

Thermal denaturation experiments were also used by Burgmayer and coworkers to further their understanding of the complexs' interaction with DNA. When a complex intercalates into DNA, the binding results in the stabilization of the helix. This stabilization has an effect on the temperature necessary to cause the DNA to denature or melt. (Dalton, Glazier, Leung, Win, Megatulski, & Burgmayer, 2008) When an increase in stabilization occurs from intercalation, the temperature necessary to cause DNA to denature will increase. (Dalton, Glazier, Leung, Win, Megatulski, & Burgmayer, 2008) The L-pterin complex showed a biphasic melting curve, which is indicative that the complex undergoes two modes of binding to DNA, presumably through intercalation as well as groove binding. (Dalton, Glazier, Leung, Win, Megatulski, & Burgmayer, 2008) The work performed by Burgmayer and her group introduced five new complexes that were capable of binding to DNA with similar binding affinities to previously synthesized complexes. The electronic extension of the DPPZ ligand and ligands possessing the ability to complimentarily bind to DNA did not significantly enhance DNA binding.

Another prominent researcher who studied DNA binding and photocleavage of ruthenium polypyridyl complexes was Karen J. Brewer. Brewer studied both monometallic and bimetallic DNA binders (Jain, Slebodnick, Winkel, & Brewer, 2008)., (Holder, Swavey, & Brewer, 2004) She researched how changes in the ligand substitution of ruthenium polypyridyl complexes affected DNA photocleavage efficiency. (Mongelli, Heinecke, Shatara, Okyere, Winkel, & Brewer, 2006) Brewer's early work focused on polyazine complexes of ruthenium with the goal of utilizing polyazine groups to act as bridging ligands between two metal centers.

Brewer and coworkers studied $[(Ph_2phen)_2Ru(dpp)]^{2+}$, $[(phen)_2Ru(dpp)]^{2+}$ and $[(bpy)_2Ru(dpp)]^{2+}$ (where dpp= 2,3-bis(2,3-dihydropyridin-2-yl)pyrazine) in an effort to find a

strong DNA binder with improved DNA cleavage efficiency. The structure of the ligands incorporated into complexes used in the study can be found in the figure below.

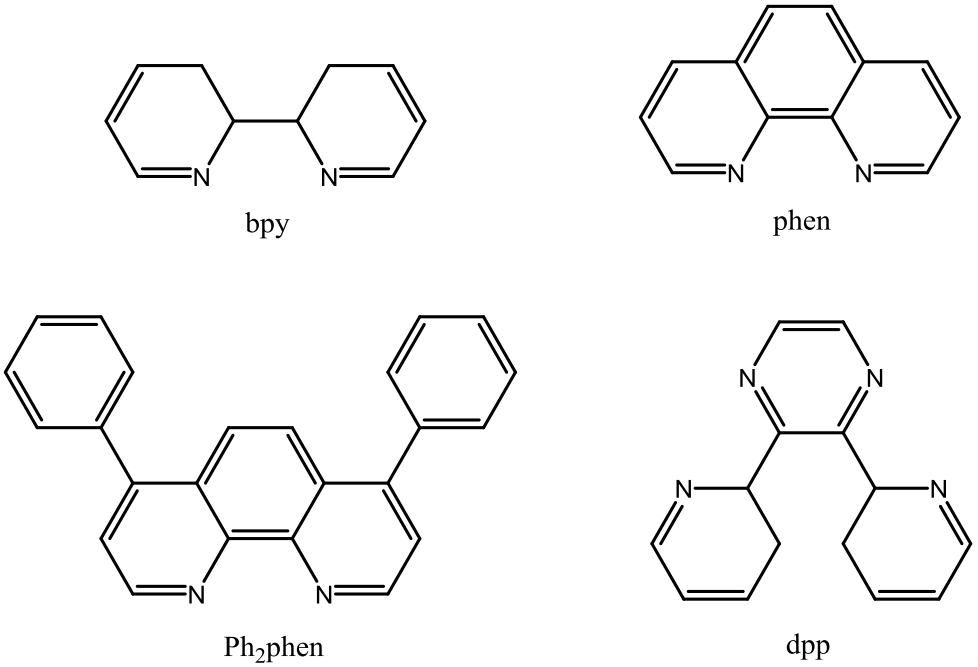

Figure 6. Ligands of Brewer's ruthenium complexes studied for DNA photocleavage.

The structure of Brewer's complexes were chosen due to a separate study that showed that $[(bpy)_2Ru(dpp)]^{2+}$ acted as a strong generator of $^1O_2$. (Abdel-Shafi, Worrall, & Ershov, 2004) (Mongelli, Heinecke, Shatara, Okyere, Winkel, & Brewer, 2006) In addition by creating complexes containing larger extended aromatic ligands, the group hoped that there would be stronger association to DNA and therefore increased photocleavage. (Mongelli, Heinecke, Shatara, Okyere, Winkel, & Brewer, 2006)

Brewer's complexes were studied by means of UV-Vis and fluorescence spectroscopies. The greatest amount of photocleavage was observed for the Ph_2phen complex, followed by the phen complex and the bpy complex. (Mongelli, Heinecke, Shatara, Okyere, Winkel, & Brewer, 2006) The group noted that the extent of quenching by O_2 being converted to $^1O_2$ observed in

the emission studies was very similar for all three complexes, therefore the trend in photocleavage observed for the complexes is likely due to differences in DNA binding affinity between the complexes rather than differences in the amount of reactive oxygen species produced from the ^{3}MLCT of the three complexes. (Mongelli, Heinecke, Shatara, Okyere, Winkel, & Brewer, 2006) The Ph_2phen complex had the largest extended aromatic system of the complexes, and this attribute makes it more likely to be able to intercalate deeply into the base pairs of DNA. (Mongelli, Heinecke, Shatara, Okyere, Winkel, & Brewer, 2006) The results of this study show that variations of the terminal ligand on ruthenium polypyridyl complexes, in particular extension of the aromatic chain, are able to modulate the extent of DNA binding and photocleavage. (Mongelli, Heinecke, Shatara, Okyere, Winkel, & Brewer, 2006)

Bhaskar G. Maiya also researched how extension of the aromaticity of a binding ligand altered DNA binding efficiency. Maiya was interested in finding new DNA intercalating ligands and ones that possibly acted as bifunctional intercalators, with more than one site on the complex involved in intercalative binding. The complex below, $[Ru(phen)_2(acdppz)]^{2+}$ (where acdppz= 8-(acridin-9-yl)-6-methyl-[1,4]diazecino[2,3-f][1,10]phenanthroline), was synthesized and studied for its binding behavior with DNA.

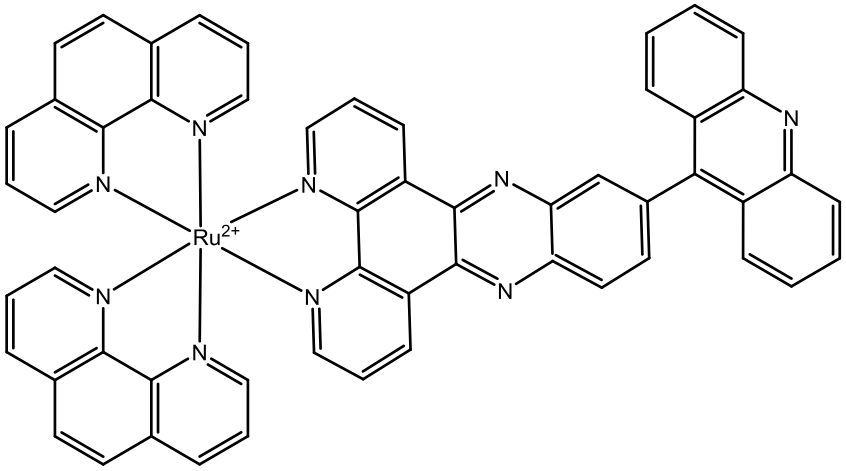

$[Ru(phen)_2(acdppz)]^{2+}$

Figure 7. Structure of Maiya's Title Complex, $[Ru(phen)_2(acdppz)]^{2+}$

Mayia noted that the complex shown above had two possible sites for intercalation, through the dppz ligand and through the acridine ligand which are linked via a single C-C bond. The group postulated that by incorporating the acridine functional group onto the DPPZ ligand, more intercalative binding would be able to occur due to the increased aromaticity, either through deeper intercalative binding or by the DPPZ and acridine portions occupying different regions on the helix (i.e.- two separate intercalation sites or extension through the major groove). (Mariappan, Suenaga, Mukhopadhyay, Raghavaiah, & Maiya, 2011) The intent of studying a complex capable of bifunctional intercalation was to find a complex capable of enhanced DNA binding. However, from absorption studies a binding constant 2 orders of magnitude smaller than that of $[Ru(phen)_2(DPPZ)]^{2+}$ was determined. (Mariappan, Suenaga, Mukhopadhyay, Raghavaiah, & Maiya, 2011), (Hartshorn & Barton, 1992) The dppz and phen ligands were planar however the acridine ring was not coplanar with the dppz moiety. (Mariappan, Suenaga,

Mukhopadhyay, Raghavaiah, & Maiya, 2011) The lack of coplanarity between the acridine and dppz portions of the complex likely hindered the complex's ability to bind to DNA.

DNA melting studies suggested that the mode of binding was through intercalation. This evidence of intercalative binding was further supported by viscosity studies however $[Ru(phen)_2(acdppz)]^{2+}$ did not yield as strong of a viscosity response as was observed with EB. (Mariappan, Suenaga, Mukhopadhyay, Raghavaiah, & Maiya, 2011) The group proposed that since the dppz and acridine moieties were not coplanar, both groups could not simultaneously intercalate into DNA, resulting in the lower than expected change in viscosity. (Mariappan, Suenaga, Mukhopadhyay, Raghavaiah, & Maiya, 2011)

Once the DNA binding behavior of $[Ru(phen)_2(acdppz)]^{2+}$ was established, its ability to photocleave DNA was studied. The group found that the complex produced low photocleavage of DNA when kept in the dark or exposed to light in the presence of room air. Inhibitor studies showed that DABCO, a $^1O_2$ quencher, largely inhibited the photocleavage of DNA in D_2O with $[Ru(phen)_2(acdppz)]^{2+}$, leading the group to conclude that the photocleavage observed was the result of a $^1O_2$ pathway. (Mariappan, Suenaga, Mukhopadhyay, Raghavaiah, & Maiya, 2011) The photocleavage being driven by $^1O_2$ was further supported with another experiment involving D_2O. D_2O increases the excited state lifetime of $^1O_2$, when the buffer was exchanged for D_2O and the solution of DNA and complex was purged with O_2 prior to irradiation, the amount of photocleavage observed was much greater. (Mariappan, Suenaga, Mukhopadhyay, Raghavaiah, & Maiya, 2011) The group went on to claim that the increase in photocleavage of DNA by $[Ru(phen)_2(acdppz)]^{2+}$ in D_2O purged with O_2 was supportive of oxygen being involved in the photocleavage mechanism. (Mariappan, Suenaga, Mukhopadhyay, Raghavaiah, & Maiya, 2011)

One common feature shared by the complexes studied by Barton, Brewer, Burgmayer, Mayia and Turro is that the ruthenium polypyridyl complexes studied for DNA binding have at least one ligand with an extended aromatic region. (Dalton, et al. 2008) (Hartshorn and Barton 1992) (Erkkila, Odom and Barton 1999) (Mongelli, Heinecke, Shatara, Okyere, Winkel, & Brewer, 2006) (Mariappan, Suenaga, Mukhopadhyay, Raghavaiah, & Maiya, 2011) Complexes are synthesized in this way to increase the chances of intercalative binding with DNA. (Kumar, Reddy and Satyanarayana 2010) (Zhen, et al. 1999) (Xiong and Ji 1999) Burgmayer and coworkers noted that since the discovery of $[Ru(bpy)_2DPPZ]^{2+}$, second generation complexes have been synthesized with extension of the dppz π- system to promote tighter intercalative binding. (Dalton, Glazier, Leung, Win, Megatulski, & Burgmayer, 2008), (Chouai, et al., 2005) Another commonality of complexes studied for their ability to interact with DNA is that they are synthesized with their extended aromatic ligand in direct electronic communication with the metal center.

Extended aromatic ligands and small molecules do not always need to be bound to a metal center in order to interact with DNA. (Tse & Boger, 2004) There is a large amount of research pertaining to free ligands or molecules such as polyaromatic hydrocarbons that bind to DNA without any metal centers. (Tse & Boger, 2004) (Brun & Harriman, 1992) (Guo & Wei, 2009) These ligands share structural similarities with polyaromatic hydrocarbons. Therefore, it can be helpful to examine small molecules by themselves without being attached to a metal to assist in determining what structural elements are necessary for something to bind to DNA. (Tse and Boger 2004) (Brun & Harriman, 1992) (Guo & Wei, 2009) Studying these smaller and simpler molecules can serve as models to aide in understanding how and why more complicated systems such as transition metal complexes behave both with and without DNA.

1.3.3 Polycyclic Aromatic Hydrocarbons and DNA

The ligands present in transition metal complexes that are often responsible for binding to DNA are modified or unmodified phenazines, bipyridines and other polycyclic aromatic functional groups such as pyrano groups. As the works by Barton and Turro showed, even subtle changes in the phenazine ring of $[Ru(bpy)_2DPPZ]^{2+}$ or $[Ru(phen)_2DPPZ]^{2+}$ can significantly modulate binding strength of the complex with DNA. (Hartshorn & Barton, 1992) The extended aromaticity of bipyridine and phenazine are what make them such ideal candidates for intercalative binding, the aromatic structures are more likely to bind between the base pairs of DNA rather than in either the major or minor groove because binding between the base pairs will result in stabilization of the helix through π- stacking. However complexes with the most extended aromatic character do not always translate to the best DNA binders as was evident in Mayia's study discussed above. (Mariappan, Suenaga, Mukhopadhyay, Raghavaiah, & Maiya, 2011) By studying how small polycyclic aromatic molecules interact with DNA, the knowledge may be used to serve as a model for how their incorporation into new complexes may effect DNA binding. The next section will compare a series of polyaromatic hydrocarbons that are known to bind DNA to highlight what molecules or functional groups are likely to enhance DNA binding when incorporated into a complex.

While Ethidium bromide (EB) and Hoechst 33258 both possess functional group substitutions beyond simple aromatic rings they will be considered here as examples of polyaromatic hydrocarbons (PAHs) capable of binding to DNA. Both EB and Hoechst 33258 are utilized in many biochemical experiments. (Brun and Harriman 1992) The structure of these two compounds can be seen in the Figure below.

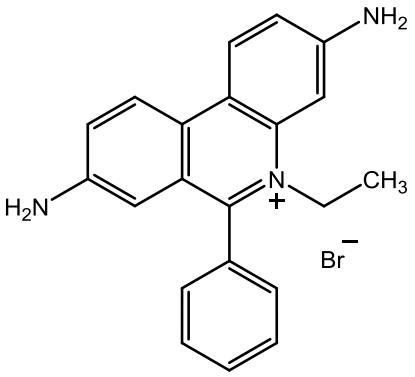

Ethidium Bromide

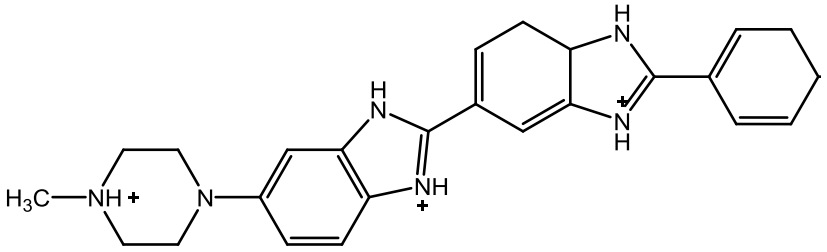

Figure 8. Structure of the polyaromatic DNA binding molecules EB and Hoechst 33258.

EB is an indispensable reagent for many basic biochemical assays, including imaging for gel electrophoresis. (Sutherland, et al. 1987), (Olmstead and Kearns 1977) EB binds to DNA in an intercalative fashion through its phenanthridine rings. Hoechst 333258 is a known DNA groove binder that can also be used as a stain for DNA. (Meyer-Almes & Dietmar, 1993) (Bresloff & Crothers, 1975) The region of Hoechst 33258 that binds to DNA is still debated. One binding mode has been shown to occur through electrostatic interactions from the phenol and modified piperazine portions of the molecule. (Fornander, Billeter, Lincoln, & Noran, 2013) At higher Hoechst 33258:DNA ratios there appears to be a second binding mode through the nonpolar region of the molecule. (Fornander, Billeter, Lincoln, & Noran, 2013)

The mechanism that makes these compounds useful for imaging DNA is similar to the fluorescence enhancement reaction described earlier. Kearns and coworkers found that the excited state of EB is responsible for protonation of polar solvents resulting in low fluorescence yields. (Olmstead and Kearns 1977) When EB comes into a hydrophobic environment, such as the one created when it is surrounded by DNA, the excited state does not transfer protons to the solvent molecules. (Olmstead and Kearns 1977) This allows for the radiative pathway of the electronic energy decay to occur and this is what is taken advantage of experimentally to allow for the imaging of DNA.

Hoechst 33258 is spectroscopically active and does not bind to DNA through intercalation; instead it binds to DNA through groove binding. (Sibirtsev 2005). (DeFlaun and Paul 1986) The emission intensity of Hoechst 33258 is increased when the dye comes in contact with DNA. (Cosa, Focsaneanu, McLean, McNamee, & Scaiano, 2001) This enhancement occurs because interactions with DNA prevent emission quenching by water molecules. Hoechst can exist in a number of different protonation states depending on the pH of the media and these forms undergo different quenching processes. (Cosa, Focsaneanu, McLean, McNamee, & Scaiano, 2001) Hoechst can be used in some experiments to help distinguish between electrostatic or intercalative binding to DNA. Both EB and Hoescht 33258 are used in a variety of experiments in this dissertation. For this reason it is important to understand the spectroscopic properties and DNA binding modes of these molecules for use in the experiments to be discussed later on in this work.

The focus of this dissertation is the synthesis and binding characteristics of a ruthenium complex containing a pyrene moiety. For this reason, the interactions of pyrene with DNA will be discussed in greater detail to provide a background as to how different forms of the molecule

behave by themselves without being bound to a metal. The structure of a pyrene molecule can be found in the figure below.

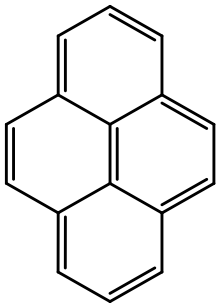

Pyrene

Figure 9. Structure of an unmodified pyrene molecule.

Benzo[a]pyrene is a carcinogen and mutageic agent that is found in cigarette smoke. (Zhang, et al. 2016) Its metabolically active form, n 7r,8t-dihydroxy- 9t, 10t-epoxy-7,8,9,10-tetrahydrobenzo[a]pyrene (BPDE) has been studied for its interactions with DNA, and the structures of both molecules can be found in the Figure below. (O'Connor, Shafirovich and Geacintov 1994), (Guo and Wei 2009)

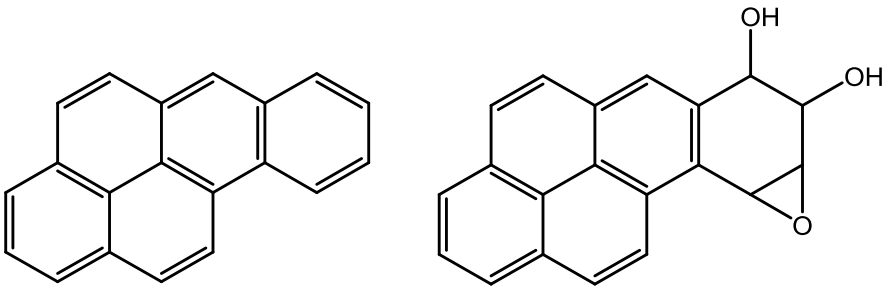

Benzo[a]pyrene BDPE

Figure 10. Structure of Benzo[a]pyrene and its metabolite BDPE

Once formed the metabolite BPDE is able to form both non-covalent and covalent adducts with DNA, as determined through spectroscopic studies. (O'Connor, Shafirovich and Geacintov 1994) When the pyrene species comes in contact with DNA or specific nucleic acid residues, its fluorescence can become quenched. This is believed to occur due to electronic transitions from

the pyrene to the nucleic acid residues. (O'Connor, Shafirovich and Geacintov 1994) The degree of quenching and electronic properties of the pyrene metabolites are very sensitive to the microenvironment that the molecule finds itself in when in contact with DNA. (O'Connor, Shafirovich and Geacintov 1994)

To understand the differences in DNA binding behavior between various PAHs, a study was performed by Guo and coworkers which examined a variety of different PAHs focusing on the effects of their side chains on their DNA binding behavior. (Guo and Wei 2009) In the study the group examined whether or not 1-hydroxypyrene, 1-aminopyrene and 1-pyrenebutyric acid were able to bind to DNA and in which mode. (Guo and Wei 2009) This work serves an excellent survey to demonstrate how pyrenes with minimal functional group modification behave with DNA.

The group used a fluorescence displacement assay with a secondary dye bound to DNA to examine whether the pyrenes were interacting with DNA. The secondary dyes used were thiazole orange (TO) a known intercalator, and 4',6-diamidino-2-phenylindole (DAPI) and Hoechst 33258 which are known groove binders. (Guo and Wei 2009) These dyes were used to help determine if the mode of DNA binding was through intercalation or groove binding. When either TO, DAPI or Hoechst 33258 are titrated into DNA, the emission resulting from the dye is enhanced. Adding another molecule to the dye/DNA solution can potentially displace some of the dye from its protected environment within DNA and cause a decrease in its emission as a result. The group found that when 1-hydroxypyrene, 1-aminopyrene or 1-pyrenebutyric were titrated into thiazole orange (TO) bound to DNA a significant reduction of the TO emission was observed. (Guo and Wei 2009) Since TO binds to DNA through intercalation the group concluded that the pyrenes must also be intercalating in order to compete in this manner. (Guo &

Wei, 2009) When these results were compared to other PAHs studied, the group found that the presence of polar groups on the periphery of the ligands were more likely to result in enhanced DNA binding than increasing the number of fused aromatic rings in the PAH. (Guo and Wei 2009) The study of PAHs' interaction with DNA is often limited by solubility problems experienced by the largely hydrophic molecules when they are dissolved in aqueous solutions. Therefore the reason why PAHs with polar groups led to greater DNA binding is likely due to the fact that these molecules were more soluable in the aqueous solution. (Guo & Wei, 2009) This work serves an excellent survey to demonstrate how pyrenes with minimal functional group modification behave with DNA.

Other experiments involving pyrene molecules and DNA have studied functionalized nanoparticles with pyrene molecules to act as biosensors. (Wang, et al. 2005) Some groups have attached pyrene moities to larger aromatic molecules to try and develop better theraputic drugs. (Hartley, et al. 1995) This functionalization of molecules with pyrene is done for a number of reasons, including to take advantage of pyrene's emissive properties as well as to enhance pyrene's inherent poor water solubility. (Niko, Kawauchi and Konishi 2011) The body of work showing that pyrene molecules are capable of binding to DNA is supportive that incorporating this functional group into transition metal complexes should enhance the complex's ability to bind to DNA. (Tse & Boger, 2004) (Hartley, Weber, Wyatt, Bordenick, & Lee, 1995) (Hariharan, Joseph, & Ramaiah, 2006)

1.3.3.1 Polyaromatic Hydrocarbons Incoprorated Into Pharmaceuticals

Tse and Boger examined a number of small molecules for their ability to bind to DNA in a selective manner highlighting their potential for use as sequence specific drug targets. (Tse & Boger, 2004) Their review categorizes molecules as intercalators, minor groove binders and major groove binders. All of the intercalators discussed contain polyaromatic subunits in their

structure and it is this structural feature that is identified as the portion of the molecule responsible for DNA binding through intercalation. (Tse & Boger, 2004) The aromatic portions of these small molecules promote binding through π-stacking and stabilizing electrostatic interactions. (Tse & Boger, 2004) The intercalating molecules that are cited consist of two or more fused aromatic rings. One example given is the anthracycline chemotheraputic drug doxorubicin whose structure is shown below.

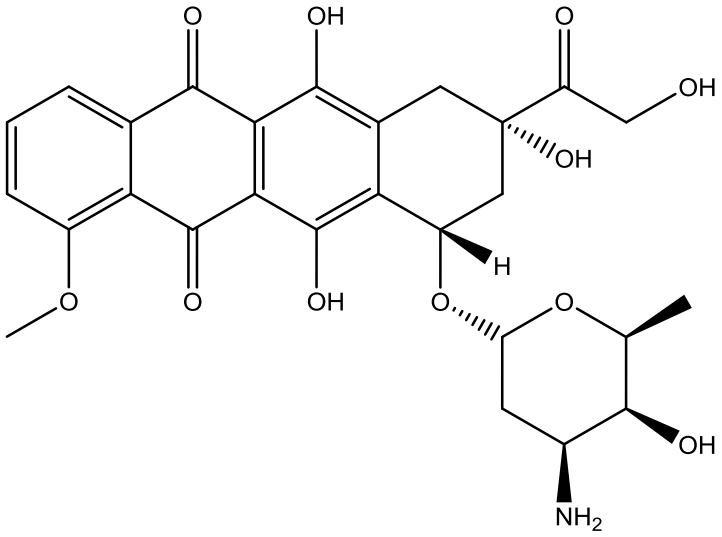

Figure 11. Structure of the chemotheraputic drug Doxorubicin

Anthracyclines such as Doxorubicin bind via intercalation an do so by extending end to end through DNA from the minor groove to the major groove. (Tse & Boger, 2004) Generally these molecules bind at alternating pyrimidine-purine sites. (Tse & Boger, 2004) Actinomycin is a tricyclic heterocycle that is a good example of polyaromatic hydrocarbons incorporated into larger molecular strucures. The structure of Actinomycin is shown below.

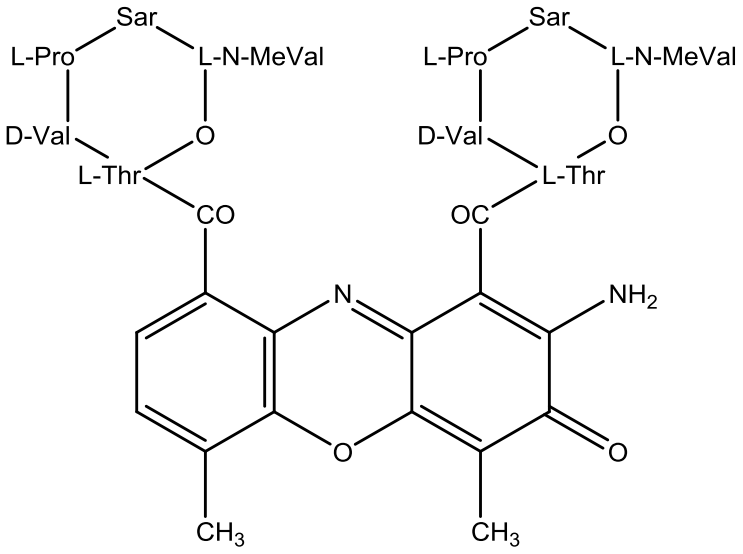

Actinomycin D

Figure 12. Structure of intercalating and minor groove binding Actinomycin D

The extended aromatic portion of Actinomycin D results in maximal base pair overlap while the peptide residues bind to the minor groove of DNA. (Tse & Boger, 2004) (Tse & Boger, 2004) The work by Tse and Boger highlighted polyaromatic hydrocarbons being used in extended molecular systems to help increase DNA binding. (Tse & Boger, 2004) Another research group led by Moses Lee examined how pyrene groups incorporated into larger molecular systems effected DNA binding. (Hartley, Weber, Wyatt, Bordenick, & Lee, 1995)

Lee was interested in finding molecules that were able to bind to DNA with sequence selectivity. A portion of his research used molecules with pyrene groups attached to take advantage of their light absorbing properties and to promote light driven pathways that could degrade DNA.

Lee and coworkers focused on how chemotherapy treatments often lack selectivity for target cancerous cells. To combat the effects of non-specific DNA binding of common chemotheraputics Lee attempted to design compounds that could be photoactivated at target

sites. (Hartley, Weber, Wyatt, Bordenick, & Lee, 1995) This work was inspired by psoralens which are photoactive and phototoxic to microorganisms. Lee's group noted that conjugates of psoralens with netropsin were more phototoxic than previously researched psoralens. Netropsin is a naturally found polyamide antibiotic which binds to DNA preferentially through the minor groove. The group continued this research and tried to futher optimize DNA affinity and sequence selectivity by creating the neotropsin analogue or lexitropsins that were bound to pyrene. (Hartley, Weber, Wyatt, Bordenick, & Lee, 1995) Lexitropsins are semi-synthetic DNA binders derived from netropsin. They share similar properties to that of netropsin, including minor groove binding to DNA. The general structure of psoralen and some of the target complexes in Lee's studies are shown below.

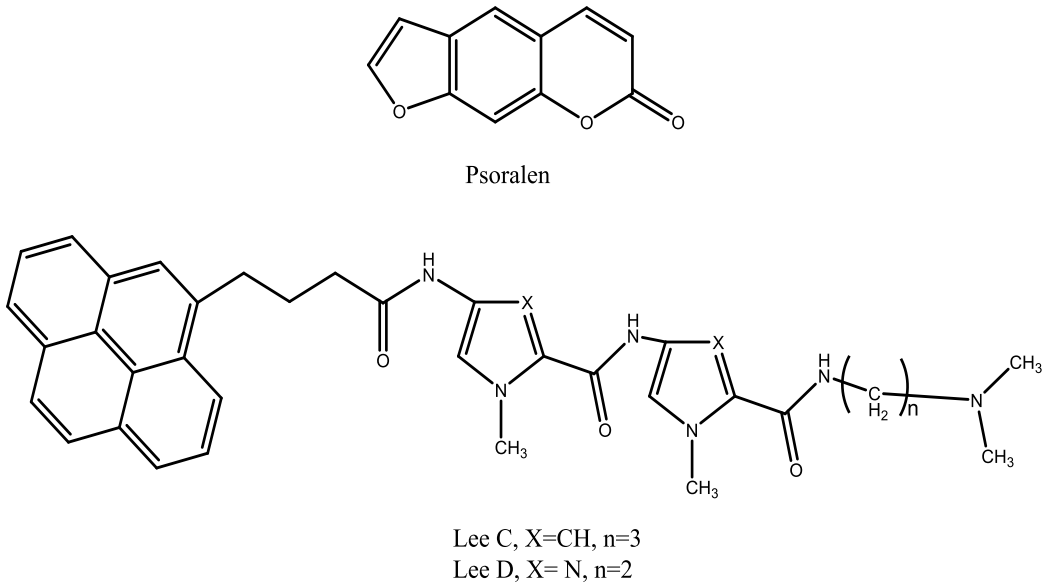

Figure 13. Moses Lee and coworker's. complexes. Psoralen depicted on top is a photoactive compound. Lee C and Lee D are neotropsin analogs of lexitropsin conjugated to 1-pyrenebutyric acid. (Hartley, Weber, Wyatt, Bordenick, & Lee, 1995)

Lexitropsin analogs were incorporated into the molecular structure due to their DNA binding capability and also because they exhibit sequence selectivity for binding to AT rich

sequences of DNA. The group incorporated pyrene moieties not to act as intercalators but rather they were selected to act as photosensitizers for the molecules because pyrene-phosphatidyl conjugates had been shown to be photocytotoxic in prior studies and due to the fact that the pyrene has a different cytotocix mechanism. (Hartley, Weber, Wyatt, Bordenick, & Lee, 1995)

Competitive binding experiments performed using T4 DNA showed both Lee C and Lee D bind strongly. (T4 DNA is a bacteriophage, or viral species that infects E. Coli). (Becker, Kleinsmith, & Hardin, 2006) Binding of the complexes to T4 DNA must occur through the minor groove since α-glycosylation of the cytidine residues at the major groove of blocks access. (Hartley, Weber, Wyatt, Bordenick, & Lee, 1995) The results of the competitive binding experiments produced larger binding constants for both Lee C and Lee D when compared to distamycin. The group postulated that both the lexitropsin and pyrene portions of the molecule were binding to DNA and this accounted for the increased binding affinity. (Hartley, Weber, Wyatt, Bordenick, & Lee, 1995)

Emission studies were carried out with Lee C and Lee D by exciting the pyrene moiety. The group noted the pyrene emission of Lee C and Lee D was enhanced 5 times when exposed to DNA. (Hartley, Weber, Wyatt, Bordenick, & Lee, 1995) Classical intercalators such as EB can have their emission increased by 25 times when bound to DNA. (Hartley, Weber, Wyatt, Bordenick, & Lee, 1995) The comparison of the emission enhancement of Lee C and Lee D to EB suggests that the pyrene portion of complexes may be pseudointercalated or binding in the minor groove. (Hartley, Weber, Wyatt, Bordenick, & Lee, 1995) If the complexes are binding in this way, then they would not be fully protected from the quenching effects of the aqueous solvent which would result in the lower emission enhancements observed. (Hartley, Weber, Wyatt, Bordenick, & Lee, 1995)

Photocleavage experiments using either Lee C or Lee D caused strand breakage. (Hartley, Weber, Wyatt, Bordenick, & Lee, 1995) Cleavage experiments carried out in the dark showed that neither complex was able to damage DNA. When Lee C was irradiated for longer than 4 minutes the amount of linear DNA imaged increased. Lee D did not produce linear DNA when irradiated for longer periods of time. (Hartley, Weber, Wyatt, Bordenick, & Lee, 1995)

Complexes Lee C and Lee D bind to DNA as was shown through competitive binding experiments and flouroescence titrations. The emission enhancement was lower for the complexes when compared to EB and the binding strength was lower when compared to $[Ru(bpy)_2DPPZ]^{2+}$. (Hartley, Weber, Wyatt, Bordenick, & Lee, 1995) The work performed by Lee and coworkers is an example of how polyaromatic hydrocarbons and more specifically pyrene, are used in larger molecular systems. Just as the ruthenium polypyridyl complexes discussed previously require tuning to optimize their binding with DNA, so do pyrene molecules attached to larger molecular systems. The Lee complexes are good comparators for the complex of interest in this dissertation and show that there is a precedent to study pyrenes as part of larger molecules but there is much room to improve on their DNA binding properties. (Hariharan, Joseph, & Ramaiah, 2006)

1.3.4 DNA Binding Using Sensitizer/ Cosensitizer Systems-

One potential problem for molecules that can act as photocleavers is that the energy absorbed from light may decay back to the ground state prior to generating ROS or acting on DNA. Alternatively, the excited electron may go on to perform other chemistry that does not result in photocleavage. One way to combat such reactions is to generate charge separated molecules using sensitizer/cosensitizer systems. (Hariharan, Joseph, & Ramaiah, 2006) Sensitizer and cosensitizer systems generally have two molecular regions that perform two separate functions when interacting with DNA . The sensitizer is responsible for absorbing

energy from light and then using that energy to react with a second species, known as the cosensitizer. This system is utilized to try to maximize photocleavage of DNA. (Hariharan, Joseph, & Ramaiah, 2006)

One competitive process known as back electron transfer occurs when an excited electron decays back to the ground state through thermal radiation. (Stemp, Holmlin, & Barton, 2000) This reduces the amount of damage a complex can impose on DNA because the excited electron is no longer available for other chemical reactions. One way to combat this competitive process is to use sensitizer/cosensitizer molecular systems. The sensitizer is a photoactivatable group such as the extended aromatic region of a complex that usually binds to DNA through intercalation. The cosensitizer receives charge from the excited state photosensitizer and also binds to DNA (usually through groove binding). The cosensitizer can go on to generate singlet oxygen from its excited state that can damage DNA. The oxidized sensitizer can receive an electron from one of the bases of DNA such as guanine, thereby inducing DNA damage at two sites. The structure of sensitizer/cosensitizer system is such that the cosensitizer can be tethered to the sensitizer through an alkyl chain although this is not a structural requirement. (Dunn, Lin and Kochevar 1992) Research performed by Dunn and coworkers looked at a system that used EB bound to DNA through intercalation as the photosensitizer and methyl viologen (MV) externally bound to DNA as the cosensitizer. (Dunn, Lin and Kochevar 1992) (Fromherz and Rieger 1986)

In Dunn and coworker's research solutions containing EB with methyl viologen resulted in an increase in the amount of DNA single strand breakage by a factor of ten when compared to solutions consisting of DNA and EB alone. (Dunn, Lin, & Kochevar, 1992). One explanation for this effect is that EB in its singlet excited state cannot oxidize any of the bases in DNA. EB

lacks the potential energy to overcome redox potentials of the base pairs of DNA. A cosensitation mechanism where charge transfer occurs between methyl viologen and EB may occur, after which EB would be able to oxidize one of the base pairs of DNA. (Dunn, Lin, & Kochevar, 1992)

In other related studies the photosensitizer can be tethered to the cosensitizer in some manner, usually through an alkyl chain. (Hariharan, Joseph and Ramaiah 2006) This allows the two portions of the compound to be in close contact, but prohibits processes that compete with cleavage of DNA such as transfer of electrons between the two portions of the molecule. In a study performed by Ramaiah and coworkers, a series of viologen linked pyrene molecules with the general formula PYL_nV^{2+} (where L_n= methylene spacer units) were examined for their interactions with DNA. (Hariharan, Joseph and Ramaiah 2006) A depiction of the PYL_nV^{2+} can be seen in the Figure below.

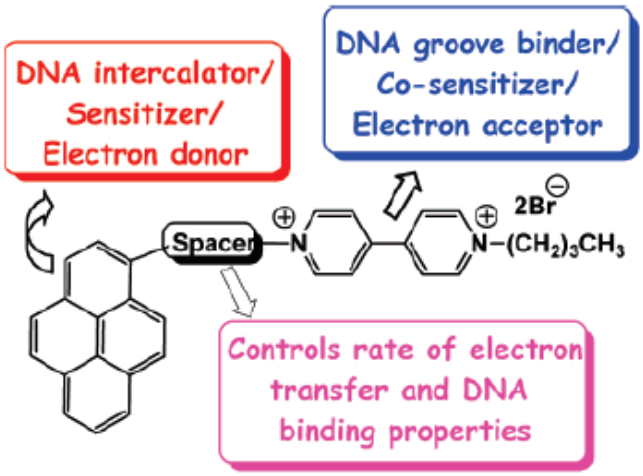

Figure 14. Representation of the PYL_nV^{2+} sensitizer/cosensitizer system used to cause the photodegradation of DNA. (Hariharan, Joseph and Ramaiah 2006)

When studied with DNA PYL_1V^{2+}, PYL_7V^{2+} and $PYL_{12}V^{2+}$ each underwent a hypochromic shift in their absorption spectra. (Hariharan, Joseph and Ramaiah 2006) This result

suggests that each molecule was capable of binding to DNA. The group noted that the greater the spacer length in PYL_nV^{2+} the higher the value of the DNA binding constant. (Hariharan, Joseph and Ramaiah 2006) This is likely due to the bulk of the larger molecules, which serve to stabilize the DNA-ligand complexes and result in the higher binding constants when compared to the molecules with smaller spacer lengths. (Hariharan, Joseph and Ramaiah 2006). Viscosity experiments supported this finding and showed that the $PYL_{12}V^{2+}$ species produced the greatest change in relative viscosity of DNA, presumably due to the bulk of the molecule occupying more space on DNA. (Hariharan, Joseph and Ramaiah 2006) Electron transfer studies showed that the most likely route for DNA oxidation involved a pathway in which an excited electron on pyrene gets transferred to the viologen moiety before a second electron from a DNA base pair reduces the radical cation pyrene. (Hariharan, Joseph and Ramaiah 2006).

The photosensitizer/cosensitizer systems show that spatially separated portions of a molecule can still act in concert to bind to and cleave DNA. (Hariharan, Joseph, & Ramaiah, 2006) (Dunn, Lin, & Kochevar, 1992) Absorption and fluorescence studies are often used to help determine the movement of electrons within these systems and how oxidation or damage to DNA ultimately occurs. (Hariharan, Joseph and Ramaiah 2006) (Bassani, et al. 1996) These systems are important to consider when studying the complex of interest, which also has two molecular regions that are spatially separated.

1.4 Study of a Novel complex – A Pyrene Terminated Ruthenium Complex

The goal of this dissertation was to synthesize and characterize a novel ruthenium complex and determine whether or not it is capable of binding to DNA and causing photocleavage. The complex under investigation, $[Ru(bpy)_2bpy\text{-}py]^{2+}$ (where bpy= 2,2'-

bipyridine and bpy-py=N-(6-(4-(pyren-1-yl) butanamido) hexyl)-[2,2'-bipyridine]-5-carboxamide) is depicted in the figure below.

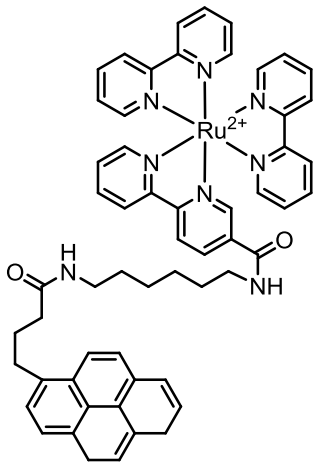

Figure 15. Structure of the target complex, $[Ru(bpy)_2bpy\text{-}py]^{2+}$

The portion of the complex that should bind to DNA is the pyrene moiety. Based on the findings of prior research performed by Barton and coworkers involving $[Ru(phen)_3]^{2+}$ and $[Ru(bpy)_2DPPZ]^{2+}$ as well as research by Brewer, the extended aromatic portion of the complex (the pyrene) is predicted to interact with the base pairs of DNA in an intercalative mode. (Erkkila, Odom, & Barton, 1999) (Mongelli, Heinecke, Shatara, Okyere, Winkel, & Brewer, 2006) The pyrene was connected to a ruthenium complex in order to take advantage of the favorable photochemistry and water soluble properties of ruthenium complexes. In addition the overall positive charge of the resulting complex should assist in the complex being able to bind to DNA which has an overall negative charge. The effect of electronically isolating the pyrene from the metal core on the complex's ability to bind to and photocleave DNA was studied. Viscometry and spectroscopic techniques were used to explore the complex's ability to bind to DNA and photocleavage was assessed by agarose gel electrophoresis. Molecules and complexes that are structurally related to the target complex were studied to better understand the structure-

function relationship in this system and how specific portions of the complex affect its DNA binding and photocleavage abilities. These compounds are the well known DNA experimental controls; $[Ru(bpy)_3]^{2+}$ (which is known not to bind to DNA) and $[Ru(bpy)_2DPPZ]^{2+}$ (where DPPZ= dipyrido[3,2-*a*:2',3'-c]-phenazine) (which binds strongly acting as a positive control). $[Ru(bpy)_2dep]^{2+}$ (where dep= N-(6-aminohexyl)-[2,2'-bipyridine]-5-carboxamide) is analogous to $[Ru(bpy)_2bpy\text{-}py]^{2+}$except that it is lacking the pyrene group. Finally, the bpy-py ligand and 1-pyreneacetic acid were studied for their DNA binding and photocleavage behavior. By studying complexes and molecules that have structural similarities to the complex of interest, we were able to better understand the structure-function relationship of the complex and how specific regions of the complex affect its DNA binding and photocleavage.

2.0 Experimental

In order to study the behavior of the $[Ru(bpy)_2bpy\text{-}py]^{2+}$, synthesis and characterization were necessary first steps. One method of synthesis involved the preparation of the bpy-py ligand followed by attaching it to $[Ru(bpy)_2Cl_2]$. The other added the pyrene moiety to an intermediate ruthenium complex ($[Ru(bpy)_2dep]^{2+}$) in its final step. All materials synthesized were characterized using proton NMR spectroscopy as well as Electrospray Ionization Mass Spectrometry (ESI-MS). The complexes used in this work can be seen in the figure below.

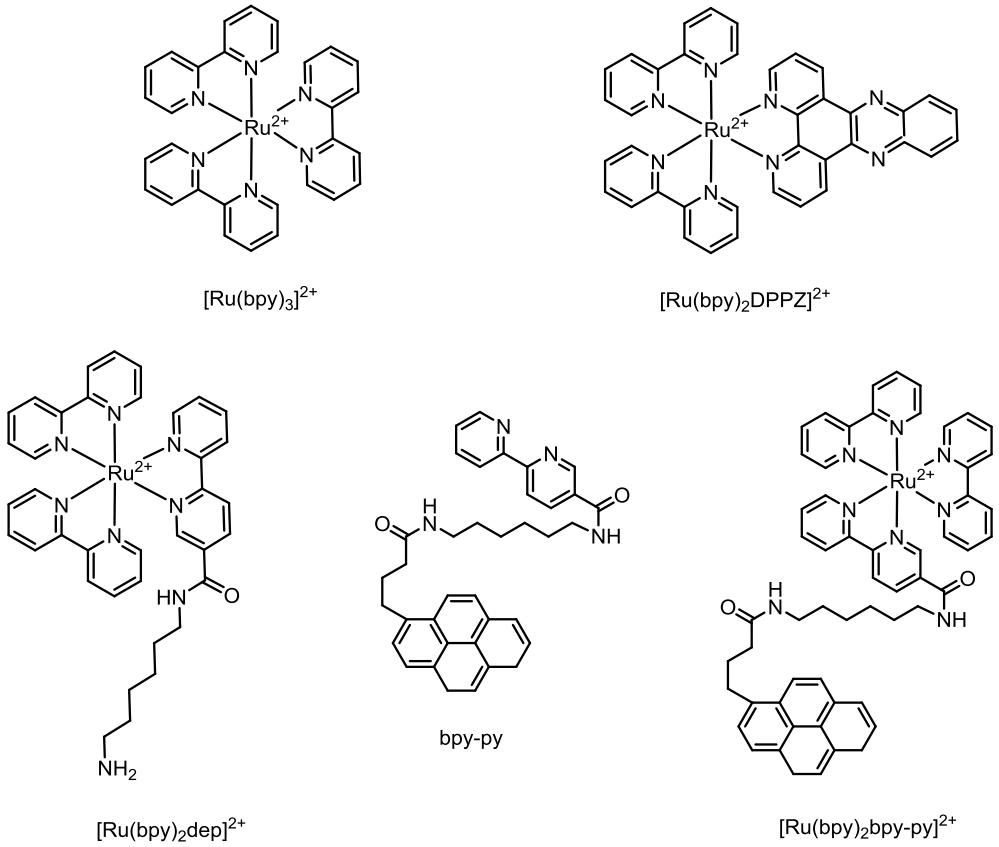

Figure 16. Complexes and molecules used for DNA binding and photocleavage studies.

After synthesizing the series of complexes and ligands above they were used for DNA binding studies. The ability of the compound to damage DNA was determined by using gel electrophoresis. For both of these studies intermediates and other control complexes were also studied for comparative purposes.

2.1 Materials and Instrumentation

2.1.1 Materials

The preparation of $[Ru(bpy)_3][PF_6]_2$ was performed according to the synthesis outlined by Broomhead and Young. (Fackler, et al. 1982) The synthesis of cis-$[Ru(bpy)_2Cl_2]$ was performed according to the procedure by Meyer et al. (Eggleston, et al. 1985) The $[Ru(bpy)_2DPPZ]^{2+}$ complex was provided by the Burgmayer lab. All other chemicals were

purchased from Sigma-Aldrich, Amfinecom Inc, Matrix Scientific and Pharmco-Aaper and were used without further purification.

2.1.2 Instrumentation

Electrospray Ionization- mass Spectrometry (ESI-MS) was performed in house on a Waters Micromass-ZQ mass spectrometer, ^{1}H-NMR (proton nuclear magnetic resonance) was performed in house on a Bruker 400 MHz FT-NMR (Fourier-transform Nuclear Magnetic Resonance) spectrometer. The UV-Visible measurements were taken using an Agilent 8453 UV-Vis spectrophotometer and a Varian Cary 100 Bio UV-Visible spectrophotometer. The luminescence studies were performed using a Horiba Jobin-Yvon Fluoromax3 with a Xenon arc-lamp.

2.2 Synthetic Procedures

A multistep process was used to synthesize the modified bipyridine molecule to which the pyrene functional group would be attached. Scheme 1 below shows the synthetic route to form the modified bipyridine.

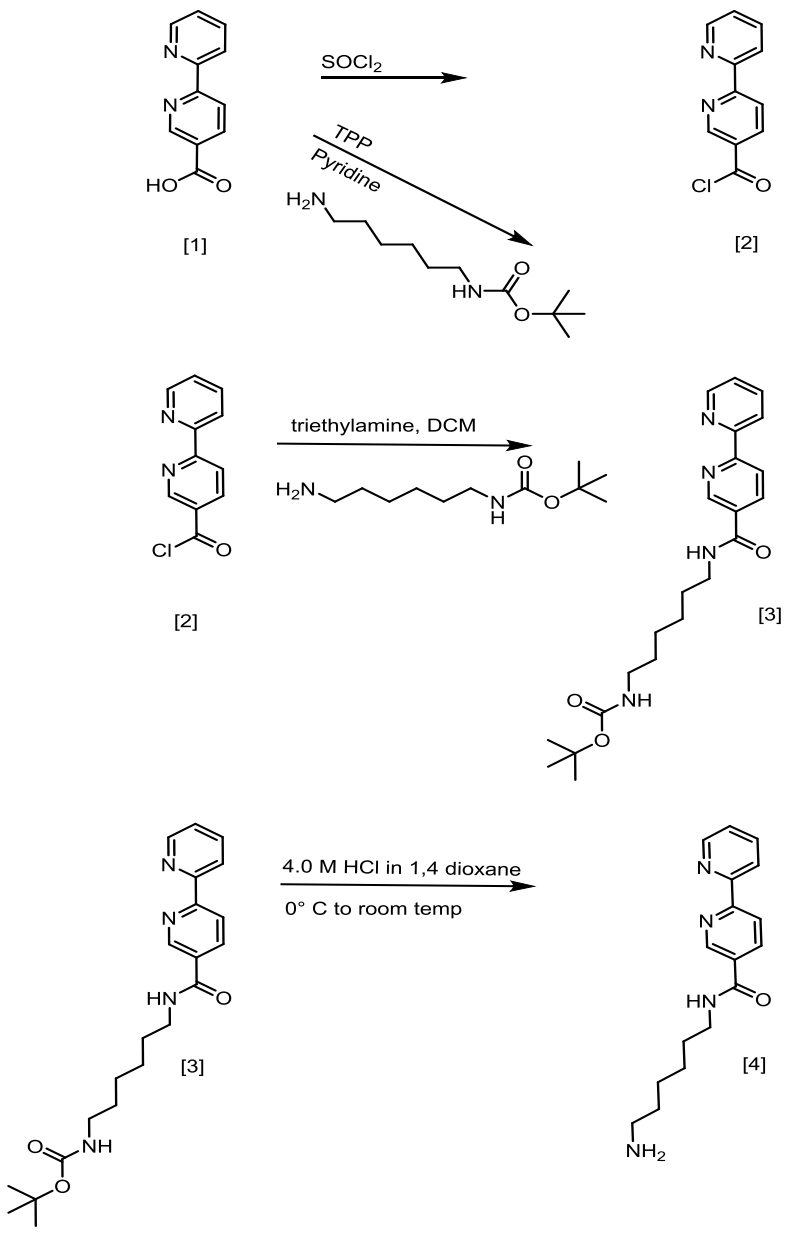

Scheme 1. Synthesis of modified bipyridine ligand

2,2'-Bipyridine-5-carbonyl chloride [2]

Solid 2,2'-bipyridine-5-carboxylic acid (0.50 g, 2.5 mmol) was added to a 100 mL 3 neck round bottom flask that had been oven-dried and fitted with septa and a condenser that had a drying tube attached. Next thionyl chloride (50 mL) was added to the flask and the mixture was

refluxed overnight. Thionyl chloride was removed from the peach colored solution by rotary evaporation and the resulting solid was used in the next step without further preparation. Since the acid chloride degrades over time, the next step in the reaction scheme was performed immediately, keeping the product under nitrogen to prevent atmospheric moisture from reacting with the product.

tert-butyl (6-([2,2'-bipyridine]-5-carboxamido)hexyl)carbamate ("protected bpy") [3]

Two synthetic routes were used to produce the protected bipyridine.

A 3 neck 100 mL round bottom flask containing 0.54 g (2.70 mmol) of 2,2'-bipyridine-5-carbonyl chloride[2] was fitted with septa and degassed under nitrogen for 20 minutes then (10 mL) of dichloromethane (DCM) (anhyd.) was added to the flask. Triethylamine (0.33 mL, 2.4 mmol) and n-boc-1,6-diamino hexane (0.57 mL, 2.4 mmol) were added to the flask via syringe. The mixture was stirred overnight under nitrogen. The following morning more DCM (10 mL) was added to the flask and the mixture was washed twice with 30 mL portions of saturated sodium bicarbonate and twice with 50 mL portions of DI H_2O. Sodium sulfate was added to the organic layer containing the product in order to remove any residual water. The organic solution was filtered to remove solids. The product was isolated by rotary evaporation and dried under vacuum. Yield 0.564 g 60%. ^{1}H-NMR (chloroform-*d*, ppm): 8.68 (s, 1H), 8.45 (d, 1H), 8.22 (m, 2H), 7.85 (d, 1H), 7.76 (td, 1H), 7.33 (td, 1H), 6.64 (s, 1H), 3.49 (s, 1H), 1.63 (m, 2H), 1.57 (d, 2H). ESI-MS *m/z* 399 ($M + H^+$) 421 ($M + Na^+$).

Alternate Synthesis for tert-butyl (6-([2,2'-bipyridine]-5-carboxamido)hexyl)carbamate ("protected bpy") [3]

A second synthetic route to produce the protected bipyridine was used due to difficulties synthesizing the protected-bpy in the manner described above. Based on Ryan Fealy's success

using triphenylphosphite (TPP) in reactions where amides were formed, the mechanism described in this alternate synthesis was attempted. This new method was successful in creating the desired ligand and was used depending on reagents available at the time of synthesis.

A 50 mL three neck round bottom flask containing 2,2'-bipyridine-5-carboxylic acid [2] (0.250g, 1.25 mmol) was fitted with a condenser and septa, then degassed under nitrogen for 20 minutes, and then 25 mL of pyridine was added. Next n-boc-1,6-diaminohexane (0.30 mL, 1.25 mmol) and triphenylphosphite (0.56 mL, 2.1 mmol) were added to the flask. The contents of the flask were purged with nitrogen for an additional 20 minutes. The reaction was allowed to reflux overnight, under nitrogen. The pyridine solvent was removed by rotary evaporation yielding an oil which was dissolved in diethyl ether. A copious amount of white precipitate with a copper tint formed and was collected via vacuum filtration. The solid product was washed three times with 10 mL portions of diethyl ether. The product was used in the next step without further purification. Yield 0.461 g 89%. ^{1}H-NMR (chloroform-*d*, ppm) δ 9.16 (s, 1H), 8.72 (s, 2H), 8.47 (t, 2H), 8.32 (dd, 1H), 8.11 (m, 1H), 7.86 (t, 1H), 7.65 (t, 1H), 7.39, (t, 1H), 7.26 (m, 2H), 7.16 (d, 2H), 7.06 (t, 2H), 6.84 (d, 1H), 3.46 (t, 2H), 3.13 (2, 2H),

N-(6-aminohexyl)-[2,2'-bipyridine]-5-carboxamide ("Deprotected bpy") [4]

Tert-butyl (6-([2,2'-bipyridine]-5-carboxamido)hexyl)carbamate [3] , (0.564 g, 1.4 mmol) was added to a 100 mL 3 neck round bottom flask fitted with septa and then degassed under nitrogen. Next 10 mL of DCM (anhyd.) was added to the flask. The contents were stirred over ice. 4 M HCl in dioxane (3.0 mL) was slowly added to the solution in small increments over several hours. A white precipitate formed during the reaction. The reaction was monitored by TLC (SiO_2, 2:3 hexane:ethyl acetate) and ESI-MS. After 7 hours of stirring the reaction was stopped and the solution was added to 40 mL of cold DI H_2O and the precipitate dissolved immediately.

NaOH (1 M) was added drop wise to a pH of 13, resulting in the precipitation of the desired product which was an off-white flakey solid. The solution was extracted three times with 50 mL portions of DCM, the organic layer was collected and dried over sodium sulfate, and the solvent was removed by rotary evaporation. The product was purified by column chromatography (SiO_2, 2:3 hexane:ethyl acetate). Yield 0.068 g 16%. ^{1}H-NMR (chloroform-*d*, ppm) δ 8.46 (s, 1H) 8.21 (d, 1H), 8.18 (m, 2H), 7.86 (dd, 1H), 7.83 (td, 1H), 7.35 (td, 1H), 6.45 (s, 1H), 3.50 (t, 2H), 2.67 (t, 2H). ESI-MS *m/z* 299 ($M + H^+$) 597 ($2M + H^+$).

Alternate Synthesis for N-(6-aminohexyl)-[2,2'-bipyridine]-5-carboxamide ("Deprotected bpy") [4]

Due to the low synthetic yield of [2,2'-bipyridine]-5-1,6-diaminohexane, an alternate approach to isolate the product was attempted. The procedure outlined below also resulted in a low yield, around 26%. One benefit of the alternate workup is that the product obtained was more pure and did not require column chromatography for purification.

Tert-butyl (6-([2,2'-bipyridine]-5-carboxamido)hexyl)carbamate [3] (0.3454g, 1.16 mmol) was put into an oven dried 3 neck 100 mL round bottom flask fitted with septa and suspended in a solution of 10 mL DCM, 5 mL methanol and 7 mL of 4 M HCl in dioxane. The solution was cooled in an ice bath and the HCl/ dioxane was added in small increments over a period of 7 hours with continuous stirring. The reaction mixture was centrifuged to produce a white sediment that was retained; the clear supernatant was discarded. The precipitate was added to water and was sparingly soluble, the resulting solution had a light pink color. NaOH (1.2 g, 30 mmol) was added to increase the pH to 13. The solution containing the product was extracted with three 50 mL portions of DCM and the resulting organic solution was dried with sodium sulfate. The solvent was removed by rotary evaporation. Yield 0.091 g 26%. ^{1}H-NMR

(chloroform-*d*, ppm) δ 9.09 (ds, 1H), 8.70 (d, 1H), 8.44 (m, 2H), 8.34 (dd, 1H), 8.00 (td, 1H), 7.51 (dd, 1H), 3.46 (t, 2H), 2.78 (t, 2H), 1.62 (m, 2H), 1.57 (m, 2H), 1.49 (m, 4H). ESI-MS *m/z* 299 ($M + H^+$) 597 ($2M + H^+$).

Both deprotection reactions resulted in low yields; 16% and 26%, respectively. One benefit of the latter procedure is that the product obtained was of high purity and therefore column chromatography was not necessary.

Once the deprotected bipyridine ligand [4] was synthesized it was reacted with a pyrene molecule [5] to create the final form of the pyrene ligand to be attached to the metal center. Scheme 2 shows the reaction of the modified bipyridine with the pyrene.

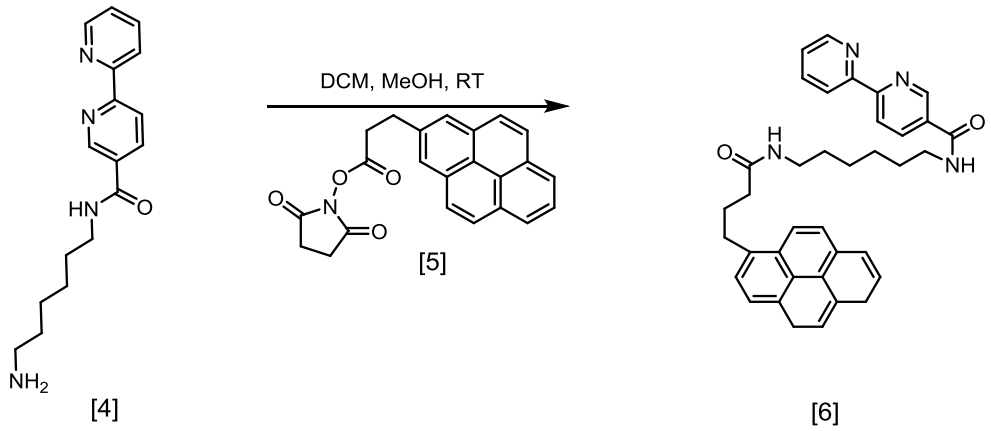

Scheme 2. Synthesis of [6] (bpy-py ligand)

***N*- (6-(4-(pyren-1-yl)butanamido)hexyl)-[2,2'-bipyridine]-5-carboxamide (bpy-py) [6]**

N-(6-aminohexyl)-[2,2'-bipyridine]-5-carboxamide [4] (0.068 g, 0.23 mmol) was dissolved in 10 mL of DCM (anhyd.) and 3 mL of MeOH (anhyd.) in a scintillation vial fitted with a septum. The solution was degassed under N_2 for 20 minutes and then transferred by cannula to a dry 100 mL 3 neck round bottom flask fitted with septa. At the same time 0.092 g (0.24 mmol) of 1-pyrenebutyric acid n-hydroxy succinimide ester [5] was dissolved in 10 mL DCM (anhyd.) in a scintillation vial, degassed and then transferred by cannula to the round bottom flask containing

N-(6-aminohexyl)-[2,2'-bipyridine]-5-carboxamide . The solution was stirred overnight. The reaction mixture was extracted with 20 mL portions of 1 M HCl 5 times. The aqueous portions were combined, 6.9 g of NaOH pellets were added and precipitation was observed. The neutralized aqueous solution was extracted 3 times with 50 mL portions of DCM and methanol, and the precipitate dissolved in the organic solvent. The organic layer was washed with 100 mL portions of DI H_2O three times and then dried over Na_2SO_4. The product was isolated by rotary evaporation. Yield 0.07g, 54%. ^{1}H-NMR (chloroform-*d* & methanol- d_4) δ 8.99 (s, 1H), 8.61 (s, 1H),), 8.43 (s, 2H), 8.24 (d, 1H), 8.16 (d, 1H), 8.10 (d, 2H), 8.03 (d, 2H), 7.94 (m, 3H), 7.79 (d, 2H), 7.31 (s, 1H), 6.14 (s, 1H), 2.19 (m, 6H), 1.54 (t, 2H). ESI-MS *m/z* 569 ($M + H^+$) 591 ($M + Na^+$)

Once the bpy-py ligand had been synthesized the related ruthenium polypyridyl complex was made. Through an alternate preparation of $[Ru(bpy)_2bpy\text{-}py]^{2+}$a related complex was synthesized to be used as a comparator in the DNA binding studies. Scheme 3 below shows the process of making the ruthenium complexes.

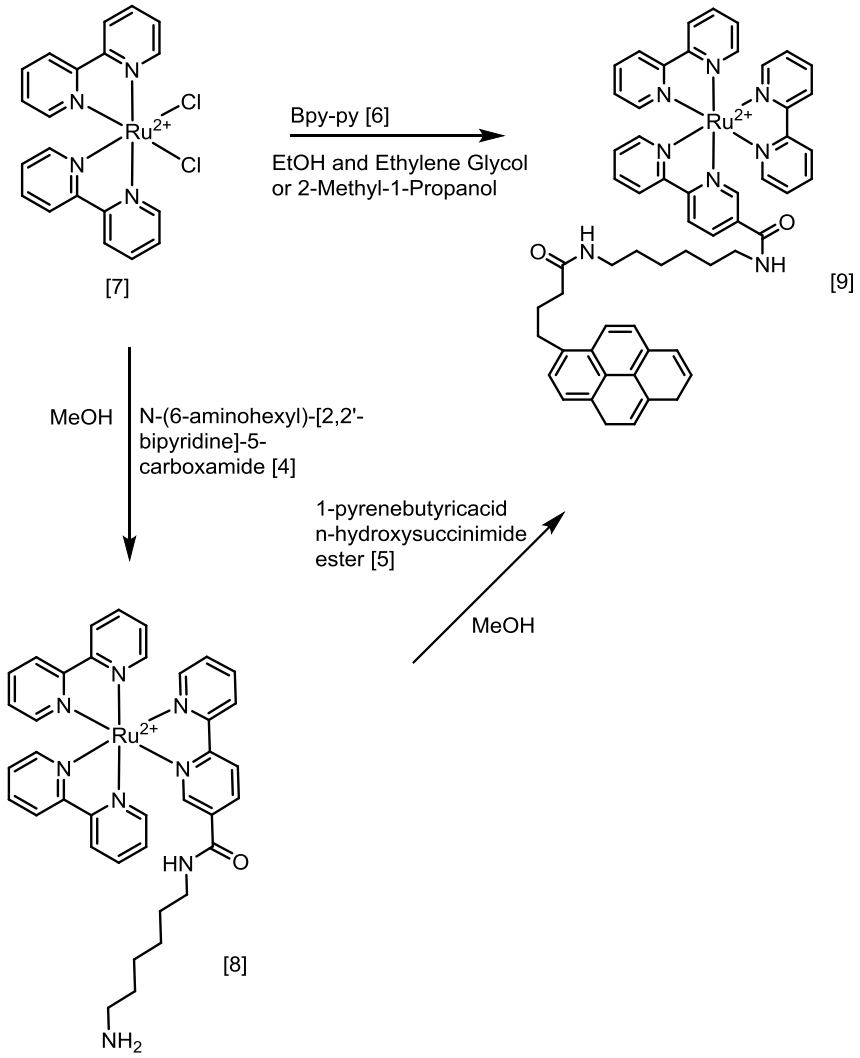

Scheme 3. Synthesis of $[Ru(bpy)_2bpy\text{-}py]^{2+}$ and $[Ru(bpy)_2dep]^{2+}$

$[Ru(bpy)_2dep][Cl_2]$ [8]

The precursor $[Ru(bpy)_2Cl_2]$ (0.0433g, 0.083 mmol) and N-(6-aminohexyl)-[2,2'-bipyridine]-5-carboxamide [4] (0.0487g, 0.16 mmol) were added to a 50 mL 3 neck round bottom flask fitted with two septa and a condenser. The flask was degassed with nitrogen for 20 minutes. Next 25 mL of methanol (anhyd.) was added to the flask and the mixture was brought to reflux. The solution changed from purple to red. The reaction was monitored using TLC (Al_2O_3, 5:1 DCM/MeOH) and ESI-MS. After 3 days of refluxing the reaction was stopped and the solvent was removed by rotary evaporation. The resulting solid product was dissolved in a minimal

amount of dichloromethane and chloroform and extracted with three 50 mL portions of water. The aqueous layer containing the product was dried by rotary evaoporation. ESI-MS indicated that the desired product was synthesized however the ^{1}H-NMR had undefined peaks in the aromatic region indicative of contamination. The solid product was dissolved in DCM and extracted with 1 M NaOH to remove any unreacted bpy-deprotect ligand. The product was present in the aqueous layer as evident by its red coloration. The product was isolated by rotary evaporation. ^{1}H-NMR performed on this product confirmed that it was pure. Yield 0.037g 56%. ^{1}H-NMR (Acetonitrile-d_3) δ 9.07 (s, 1), 8.62 (m, 3H), 8.49 (m, 2H), 8.06 (M, 3H), 7.88 (dd, 2H), 7.70, (dd, 2H), 7.39 (m, 3H). ESI-MS *m/z* 711 $(M)^+$, 356 $(M)^{2+}$.

$[Ru(bpy)_2bpy\text{-}py][PF_6]_2$ [9]

Two synthetic routes were used to produce $[Ru(bpy)_2bpy\text{-}py][PF_6]_2$. The reaction of $[Ru(bpy)_2dep][Cl]_2$ [8] with 1-pyrenebutyric acid n-hydroxy succinimide ester [5]was attempted due to difficulties purifying $[Ru(bpy)_2bpy\text{-}py][PF_6]_2$ from $[Ru(bpy)_2Cl_2]$and bpy-py [6]. The reaction pathway involving $[Ru(bpy)_2dep][Cl]_2$ [8] created $[Ru(bpy)_2bpy\text{-}py][PF_6]_2$ however purification of the desired complex was not successful and this synthetic route was abandoned. The precursor $[Ru(bpy)_2Cl_2]$ (0.017 g, 0.033 mmol) was placed in a 50 mL 3 neck round bottom flask fitted with septa and a condenser and degassed under N_2. The ligand bpy-py [6] (0.013g, 0.023 mmol) was dissolved in 10 mL ethanol in a scintillation vial and degassed under N_2. Sub-stoichiometric ligand was used because of difficulty removing unreacted ligand from the product due to the ligand's inherent poor solubility. The contents of the scintillation vial were transferred via syringe into the round bottom flask. The flask was heated and one hour into reflux 1 mL of ethylene glycol was added. The temperature was increased to maintain reflux and product formation was monitored with TLC (Al_2O_3, 5:1 DCM/MeOH) and ESI-MS. The mixture was allowed to reflux for 3 days after which the reaction mixture was removed from heat and the

solvents were removed using high vacuum rotary evaporation. 20 mL of DI H_2O was added to the product. An excess of NH_4PF_6 (about 0.1 g) was added to the aqueous solution containing the product to ensure that all of the chloride ions on the complex were exchanged for PF_6 and a red-orange precipitate formed. The product was collected via vacuum filtration and washed 3 times with 50 mL portions of water and 3 times with 50 mL portions of ether and allowed to dry under vacuum. Crude yield 0.032g 77%. Purification was performed using aluminum oxide chromatography with a 50:50 ACN:H_2O (ACN= acetonitrile) eluent to remove starting material. The fractions containing product were combined and the ACN and water were removed with rotary evaporation. The product was dissolved in 10 mL of acetone and filtered through a glass pipette filter. The product in acetone was concentrated using rotary evaoporation. The solution of the product in acetone was then recrystallized by ether vapor diffusion. ^{1}H-NMR (Acetonitrile-d_3) δ 8.46 (m, 3H), 8.22 (d, 1H), 8.19 (d, 2H), 8.13 (m, 4H), 8.03 (d, 1H), 8.01 (td, 1H), 7.99 (d, 1H), 7.98 (t, 1H), 7.91 (d, 1H), 7.74 (d, 1H), 7.71 (t, 1H), 7.64 (t, 1H), 7.39 (m, 4H). ESI-MS *m/z* 491 $(M - 2PF_6)^{2+}$. Yield after purification 0.016g 38%.

2.3 DNA Binding Studies

Buffers used to prepare DNA solutions were made using Millipore pure DI H_2O that had been autoclaved. Vials and tubes used to prepare and contain DNA solutions were sterile. Calf-thymus DNA (CT-DNA) type I fibers (purchased from Sigma-Aldrich) prepared as a sodium salt were used for viscosity, luminescence and isothermal binding studies. For these experiments the CT-DNA was prepared in 10 mM sodium phosphate buffer (pH 7) with 50 mM NaCl by sonicating the fibers for several hours and periodically vortexing. The sample was then centrifuged for 12 min and the supernatant was retained. The concentration of the stock DNA solution was determined by monitoring its absorption at 260 nm and using the extinction

coefficient of 13,100 $M^{-1}cm^{-1}$ to calculate the concentration of DNA in units of mM x base pairs. (Reichmann, Rice, Thomas, & Doty, 1954) Ruthenium complexes used for viscosity studies were prepared to a concentration of 400 μM in acetonitrile. Ruthenium complexes used for spectroscopic studies were prepared in 10 mM sodium phosphate buffer 50 mM NaCl pH 7 and no more than 10% by volume of acetonitrile was used when necessary to promote solubility.

2.3.1 Viscosity

An Ubbelohde viscometer was used in a non-circulating water bath at room temperature to measure the viscosity of DNA solutions with different ruthenium complexes. First, a background measurement was taken by using only buffer. This was performed by adding 3 mL of buffer to the viscometer. The solution was aspirated into one arm of the viscometer which had two lines imprinted on the glassware. A measurement was made by recording the time it took for the solution to travel from one line to the next. This procedure was repeated for 3 measurements and an average was taken. Following this background measurement 1 mL of the buffer was removed from the viscometer using a glass pipette and 1 mL of 0.9 mM per BP CT-DNA was added to the remaining 2 mL of 10 mM phosphate buffer. The solution was mixed by bubbling N_2 into the solution, after mixing the solution was allowed to equilibrate for 10-20 minutes. Measurements were taken in triplicate as described above and averaged for each run. Next 10 μL aliquots of the complex under investigation were added to the viscometer and mixed by bubbling with N_2 (the total volume in the viscometer increased after each 10 μL addition). Solutions were allowed to equilibrate prior to measuring and triplicate measurements were recorded The concentration range of complex:DNA studied was varied and the optimal range was found to be 0-0.2. The data was plotted as intrinsic viscosity $(\eta/\eta_\circ)^{1/3}$ vs. the ratio of complex to DNA in accordance with the theory of Cohen and Eisenberg. (Cohen and Eisenberg

1969) In Eq. 1, η is the viscosity of DNA and complex, t_f is the average flow time of the respective trial in seconds, t_o is the flow time of the buffer in seconds. $\eta_\circ$ is the viscosity of the DNA solution, either with or without complex.

$$\eta = t_f - t_{o/} t_o \quad (1)$$

2.3.2 Isothermal Binding

Isothermal binding experiments were conducted at room temperature using fixed concentrations of complex and titrating DNA into the solution of complex. The fixed concentration of complex used for each experiment was in the range of 12-25 μM. A stock solution of DNA was prepared and 10 μL aliquots were added to the complex solution to achieve final DNA concentrations ranging from 0- 120 μM were used. (The effect of the DNA aliquots on the complex concentration was neglected because the volume added was small compared to the total sample volume) After the addition of DNA the solutions were vortexed and then allowed to equilibrate for up to 20 minutes. Prior to analysis solutions were transferred into a quartz cuvette with a 1 cm path length. The analysis was performed by first measuring the absorption spectrum of the complex without DNA. For the solutions containing increasing amounts of DNA any changes in the absorbance spectrum of the resulting solutions were monitored. For most of the complexes studied the region around 450 nm was where the greatest change in the intensity of absorption bands was observed. The wavelength that had the greatest change upon addition of DNA was determined and the absorption at this wavelength was used to determine a binding constant using equations 2 and 3 (below) which were developed by Carter and coworkers. (Carter, Rodriguez and Bard 1989) K and s are the binding constant and site size, respectively. The site size provides a measure for how much space on DNA the complex occupies. C is the concentration of complex used, [DNA] is the total concentration of DNA used with the concentration

expressed as M x BP. ε_a is the apparent absorption or extinction coefficient of the complex in the presence of DNA, ε_f is the extinction coefficient of the free complex. The absorption of free complex at each wavelength was determined and used with the concentration of complex to calculate the extinction coefficient using Beer's Law. ε_b is the extinction coefficient of DNA-bound complex and was calculated by taking the absorbance of the DNA saturated complex and dividing by C. The DNA saturated complex is defined by the point at which additional aliquots of DNA do not cause further decrease in the absorption of the complex-DNA adduct.

$$(\varepsilon_a - \varepsilon_f)/ (\varepsilon_b - \varepsilon_f) = b-(b^2-2K^2C[DNA]/s)^{1/2}/2K \quad (2)$$

$$b= 1 +KC + K[DNA]/2s \quad (3)$$

2.3.3 Fluorimetry

Entrance and exit slit widths were 1 nm for solutions containing pyrene and 2.5 nm for all other experimental solutions. Samples were incubated for a minimum of 10 minutes prior to analysis.

2.3.3.1 Fluorescence Enhancement Experiments

For each experiment background spectra of DNA and the complex under investigation were collected separately. The emission spectrum of a solution of 10 μM of complex was recorded then DNA was titrated into the solution. A concentrated DNA solution was used and 10 μL aliquots were added to the complex solution to achieve DNA concentrations ranging from 0- 120 μM. After each addition of DNA the solutions were mixed and allowed to equilibrate for 10 minutes. For complexes that had an MLCT transition the solutions were excited at the λ_{max} for the MLCT and the emission was monitored around 600 nm or wherever it emitted. For molecules lacking an MLCT transition, such as pyrene compounds, an absorption spectra was first collected then the λ_{max} was identified and used as the excitation wavelength for emission studies.

2.3.3.2 Competitive Binding

Emission spectra were collected using 520 nm, the λ_{max} for EB, as the excitation wavelength. A solution of 10 μM of EB was prepared in 10 mM phosphate buffer. DNA was added so that its final concentration was 25 μM. The resulting solution was mixed and allowed to equilibrate for 20 minutes. EB was excited in both the absence and presence of DNA. Following excitation of each solution the emission spectra was monitored and a broad peak was observed around 600 nm. Complex was added into the EB/DNA samples to achieve concentrations of complex in the range of 0-20 μM. Each solution was mixed and allowed to equilibrate prior to analysis. The resulting solutions were excited at 520 nm and the emission recorded. A plot of complex concentration vs. emission intensity was made. The concentration of complex that caused a 50% decrease in EB's emission was used to calculate the binding constant using equation 4. In the equation below K_{EB} is the binding constant of EB, 1 x 10^7 M^{-1}, [EB] is the concentration of EB (10 μM), K_{app} is the apparent binding constant of a given complex and [complex] is the concentration of complex that resulted in a 50% decrease in the emission intensity. (Lee, et al. 1993)

$$K_{EB}[EB]=K_{app}[complex] \quad (4)$$

2.3.3.4 Fluorescence Resonance Energy Transfer

The molecules used for FRET experiments were calf thymus DNA, Hoechst 33258 and a third molecule such as EB or a complex under investigation. Initially control experiments were performed using EB with DNA and then Hoechst 33258 with DNA. EB was used as the intercalator control whereas Hoechst 33258 was used as the groove binder control. All of the solutions were prepared in 10 mM phosphate buffer. The CT-DNA was prepared to concentrations from 10 μM to 20 μM in order to find the optimal experimental conditions. EB and Hoechst 33258 were prepared to concentrations of 10 μM. The concentration of complex

used ranged from 4 µM to 25 µM. Prior to performing FRET experiments absorption spectroscopy was performed on solutions of either EB, Hoechst 33258, or a complex in order to obtain information to correct for the inner filter effect and to calculate the extinction coefficient for each wavelength. The λ_{max} was identified for each molecule and solutions were excited using this information. During the FRET experiments each solution was excited using sweeping excitation from 240 nm – 350 nm and the emission spectra were recorded. The data obtained was analyzed using the method of Le Pecq and Paoletti found in equation 5.

$$(Q_\lambda/Q_{310}) = (I_\lambda/I_{310} \times \varepsilon_{310}/\varepsilon_\lambda)_b \times (I_{310}/I_\lambda \times \varepsilon_\lambda/\varepsilon_{310})_f \quad (5)$$

In the equation above Q_λ is the quantum yield of the DNA bound species at a given excitation wavelength and Q_{310} is the quantum yield of the DNA bound species at an excitation wavelength of 310 nm. The quantum yield is defined as the number of photons absorbed at a given excitation wavelength vs. the number of photons emitted as a result of that excitation. The wavelength at 310 nm was used to normalize the data because DNA does not absorb at this wavelength. *I* and ε are the measured fluorescence intensity and molar extinction coefficients respectively of free (f) and bound (b) complex at a given wavelength. In the FRET experiment a correction was made for the inner filter effect for each wavelength. The inner filter effect describes the difference in absorption of molecules in a cuvette depending on their position relative to the incident light. (LePecq & Paoletti, 1967) Molecules at the front of the cuvette will absorb photons that will no longer be available to excite molecules further way from the incident light. The fluorescence intensity was corrected by calculating the logarithm of half of the absorption at a given wavelength.

2.4 DNA Photocleavage Studies

Prior to performing the photocleavage experiments 1 μg/μL stock plasmid DNA pBR322, (New England BioLabs) was diluted to a concentration of 0.05 μg/μL in 50 mM Tris-HCl 18 mM NaCl at pH 7.2 buffer. Portions of plasmid were added to PCR vials and each vial was brought up to a volume of 18 μL using 50 mM Tris-HCl buffer. Vials containing the 0.05 μg/μL plasmid DNA were used for photocleavage experiments and the concentration of plasmid remained constant at 1.7 ng/μL while the concentration of complex was altered. Complexes or ligands were used in concentrations ranging from 1 μM to 200 μM. When possible the complexes and ligands were dissolved in 50 mM Tris-HCl buffer, in some cases the solutions had to be sonicated for a day prior to photocleavage studies in order for the complex to fully dissolve. Acetonitrile was used as needed to help promote solubilization. Once the DNA and complex were added to each vial, enough buffer was added to bring the volume to 15 μL and then the solutions were irradiated with a UV lamp (365 nm, 8 W) for 2 hours. After irradiation, each sample was mixed on a piece of parafilm with 5 μL of loading dye. The substrate that the DNA solutions were loaded onto was made of an agarose gel. The agarose gels were made by combining 35 mL of trisborate EDTA buffer with powdered agarose to a concentration of either 0.7% or 1% and then microwaving the resulting solution for 1 minute. As the gel began to cool 17.5 μL of a 0.5 μg/mL EB solution was pipetted into the gel solution and swirled to mix. The resulting mixture was poured into a mold that had a comb placed at one end of a rectangular container. The mold was placed in the freezer for an hour. The comb was then removed from the gel, resulting in 8 wells. Prior to the samples being loaded into the wells of the agarose gel, the mold was placed into a holder and enough 10x Tris-borate EDTA buffer solution was added to submerge the gel. For each photocleavage experiment a control consisting of only plasmid

DNA was prepared and placed into the first well, well 1. The wells of the gel were labeled 1 through 8 starting from the left side of the gel. A current was then applied and the samples were run at 80 V for 90 min. After this step the gels were imaged using Gel Doc XR+ documentation system (hardware and software) through exposure to UV light.

3.0 Results and Discussion

3.1 Synthesis of Ligands

The creation of a novel ruthenium polypyridyl complex containing an alkyl chain which terminated in a pyrenyl group was achieved through a multi-step synthesis. In order to make this complex it was necessary to first make the pyrene modified bipyridine ligand. The synthesis of the pyrene ligand is shown in Schemes 1 and 2.

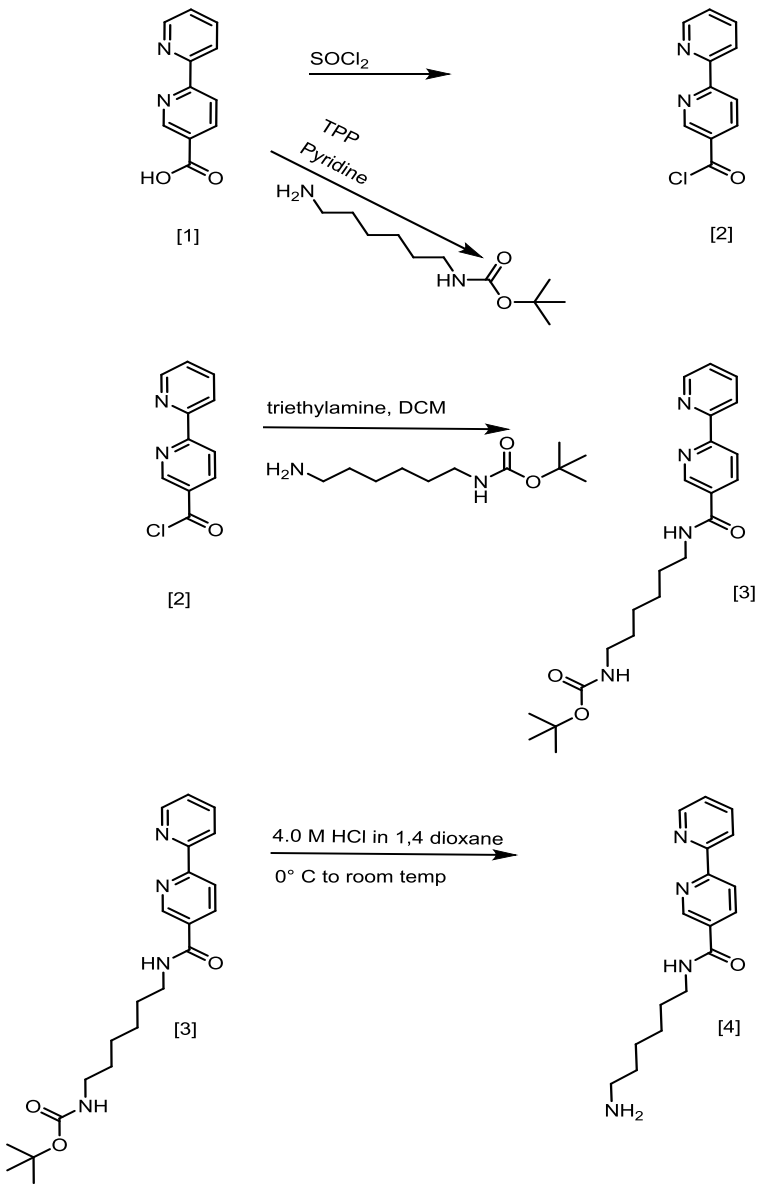

Scheme 1. Synthesis of modified bipyridine ligand

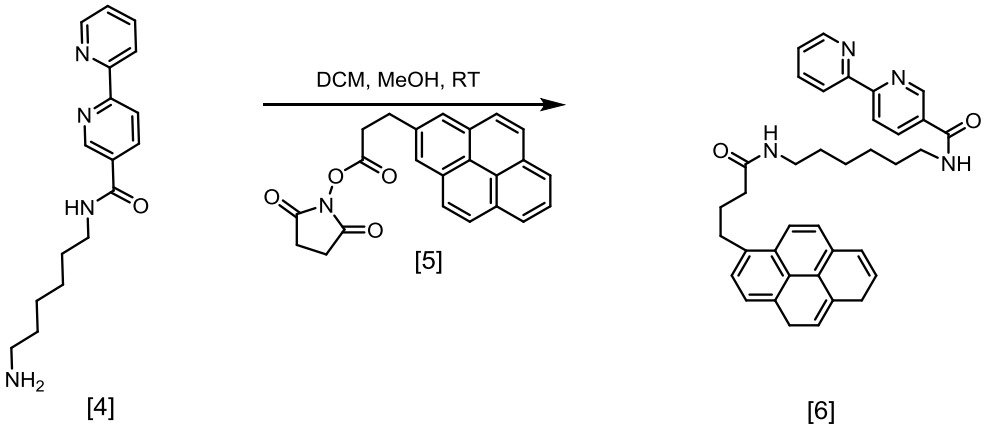

Scheme 2. Synthesis of [6] (bpy-py ligand)

The first reaction converted 2,2'- bipyridine carboxylic acid [1] into a more reactive acid chloride [2] with the use of thionyl chloride. This method was successful multiple times, however in some instances the acid chloride [2] would degrade back to starting material prior to completion of the next reaction. The acid chloride was not characterized due to the moisture reactive nature of the product. The protected amine [3] was characterized by both proton NMR and ESI-MS. In the ^{1}H-NMR shown in Figure 17 the aromatic region integrates to the 7 expected peaks from the bipyridine.

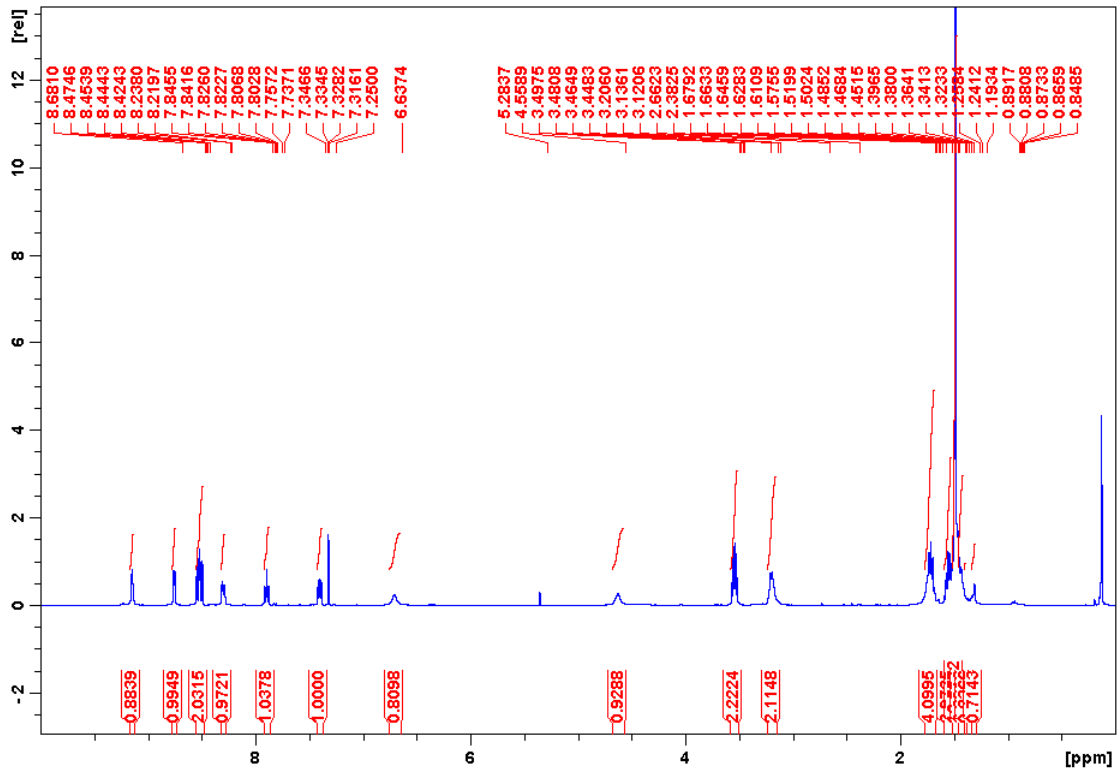

Figure 17. ^{1}H-NMR of [3] (protected bpy)

Two broad peaks can be seen further up field at δ 6.64 and 4.56, these peaks are assigned to the protons on the amide functional groups. The peaks at δ 3.48 and 3.21 are assigned to the methylene hydrogens on the carbon atoms proximal to the amide groups. These two peaks are important in determining whether the subsequent deprotection reaction goes to completion or whether residual protected ligand is left behind.

Quenching of an acid chloride occurs readily when the compound is exposed to moisture. Due to these complications an alternate method was used to synthesize the protected amine using triphenyl phosphite (TPP). This reaction was easy to set up and did not involve the use of thionyl chloride which can degrade over time. The reaction with TPP went to completion; however there were more contaminants in the resulting product than generally seen when using the thionyl chloride method. The ^{1}H-NMR revealed a higher than expected integration in the

aromatic region, the extra peaks are attributed to residual TPP left with the product see Figure 18.

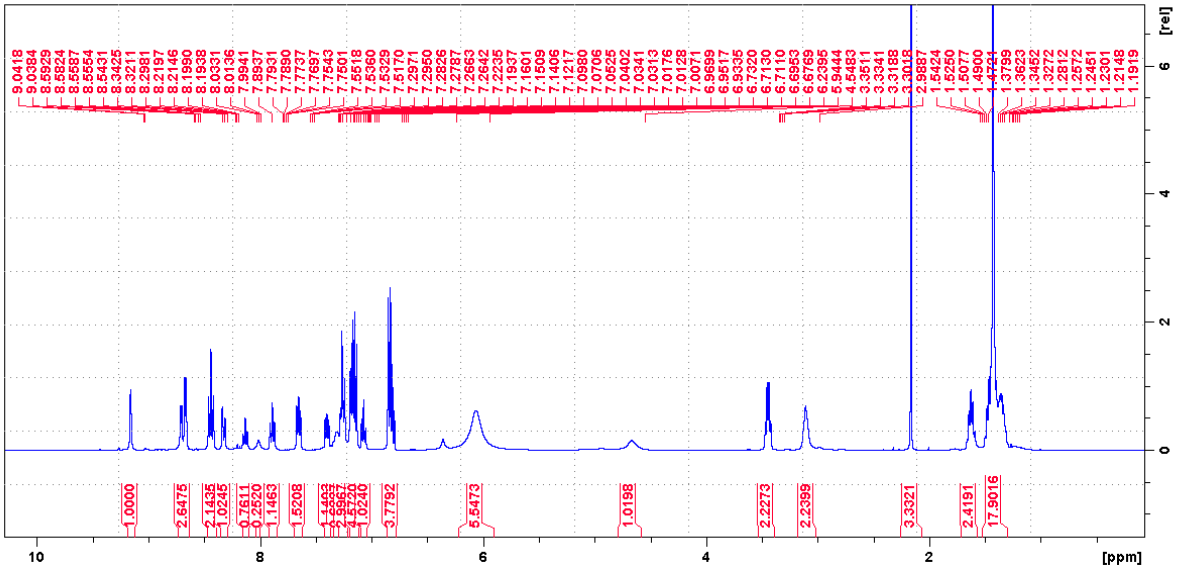

Figure 18. ^{1}H-NMR of [3] (protected bpy) from TPP

During the subsequent deprotection reaction of [3], the residual peaks arising from TPP were not seen in the ^{1}H-NMR spectra. Therefore, although contaminants are seen in [3] derived from TPP, further purification at this step was not necessary because the contaminants were removed during the course of the work up of the deprotected product [4]. Using centrifugation and multiple extractions proved to be sufficient to remove any contaminants from [4]. The pathway to produce the protected amine [3] from the thionyl chloride reaction has a crude yield of 60% compared to that of 89% when the TPP reaction is used. However the yield from the TPP reaction may be artificially high presumably due to increased mass from contamination which was seen in the ^{1}H-NMR. Purified [4] produced an ^{1}H-NMR that had 7 peaks integrated in the aromatic region, as expected. The peak at δ 4.56 which is attributed to a proton on one of the amides is now absent which is expected since one of the amides is no longer present. The peaks

from the methylene carbons proximal to the amide and amine are shifted compared to the analogous peaks in spectra of the protected ligand [3]. In the deprotection product [4] the peaks are at δ 2.71 and 3.50 as seen in Figure 19.

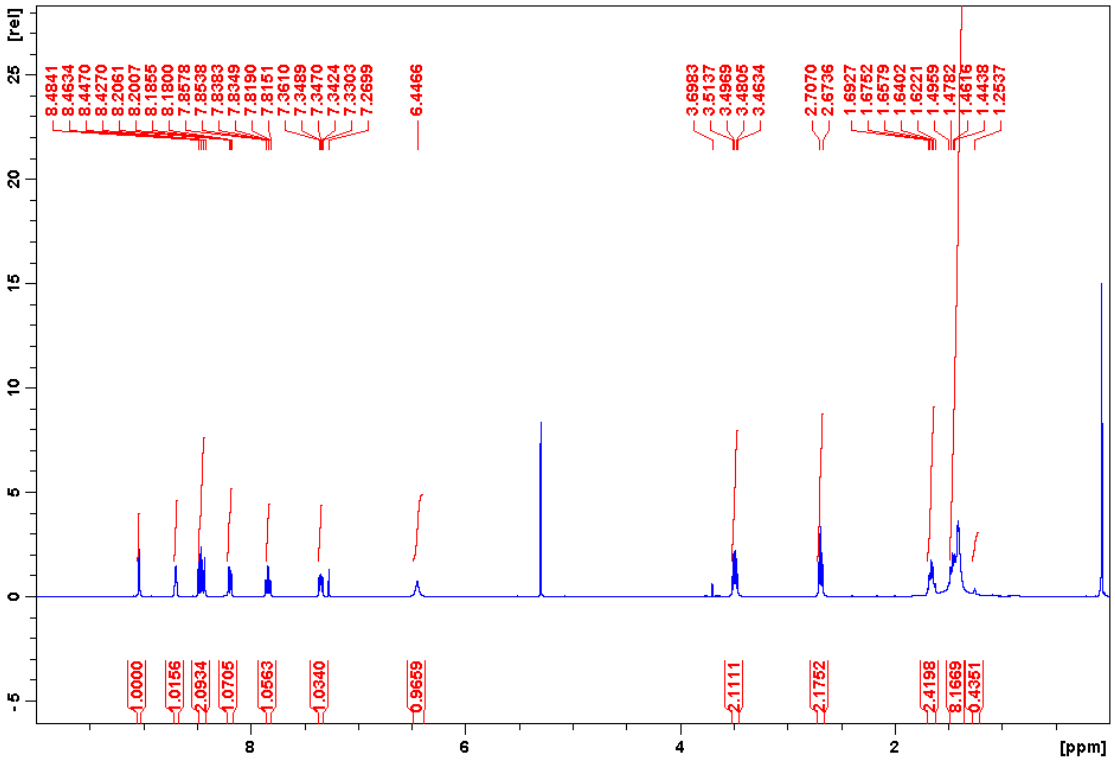

Figure 19. ^{1}H-NMR of [4] (deprotected bpy)

In comparing the two reaction pathways to synthesize and isolate the pure deprotected amine [4], the yields were 48% for [4] starting from the acid chloride reaction compared to 26% resulting from the TPP pathway.

The reaction used to synthesize the bpy-py ligand is in Scheme 2.

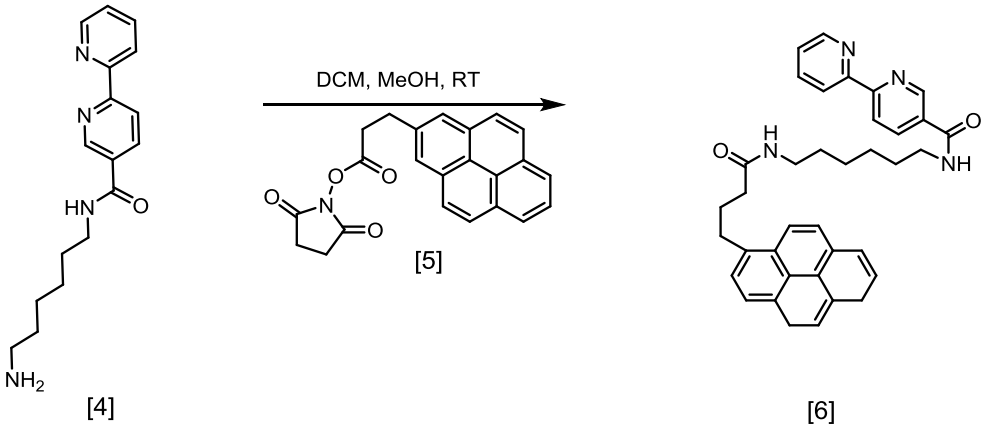

Scheme 2. Synthesis of [6] (bpy-py ligand)

The reaction took place at room temperature overnight with no complications. Isolating the product was complicated due to its limited solubility. The ligand contains a hydrophobic alkyl chain in addition to protonatable nitrogen atoms on the bipyridine. The product has limited solubility in either dichloromethane or chloroform. When a small amount of methanol was added to either of these solvents, the solubility of the ligand was greatly enhanced. Extractions were performed using a dichloromethane methanol mixture (95:5) and water in order to remove contaminants from the bpy-py [6] ligand. The use of methanol, which is miscible in water, may have contributed to the low yields of the bpy-py [6] ligand. Methanol's miscibility with both the organic and aqueous phases could have helped draw out some of the bpy-py ligand into the aqueous phase. The limited solubility of the ligand also affected its characterization with ESI-MS. The voltage of the electrospray of the MS was increased in order to visualize the ligand peak at 591 m/z ($M + Na^+$). As the voltage was increased, it became difficult to distinguish which peaks were genuine to the sample and which were created in the instrument as a result of the increased energy as can be seen in Figure 20. The ^{1}H-NMR gave greater confirmation that the ligand isolated was pure, see Figure 21.

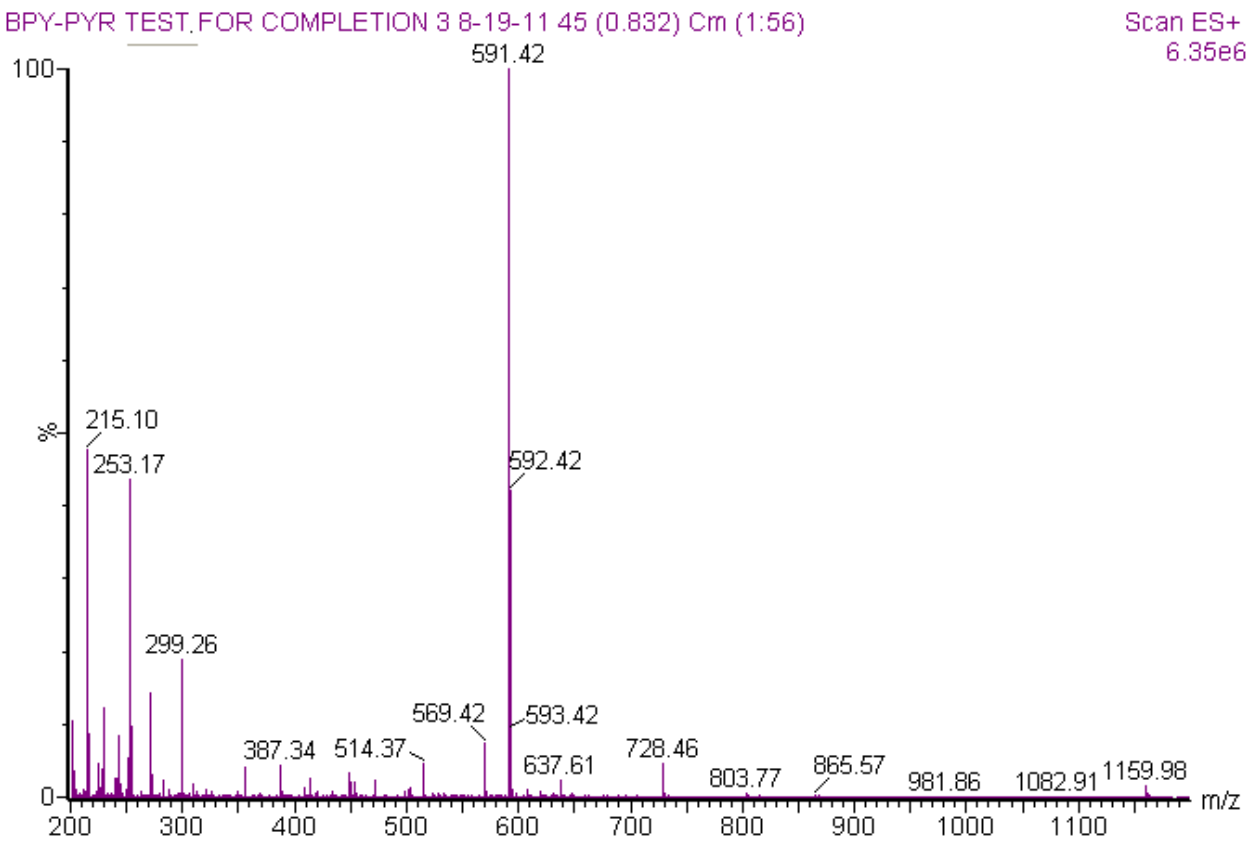

Figure 20. ESI-MS of [6]

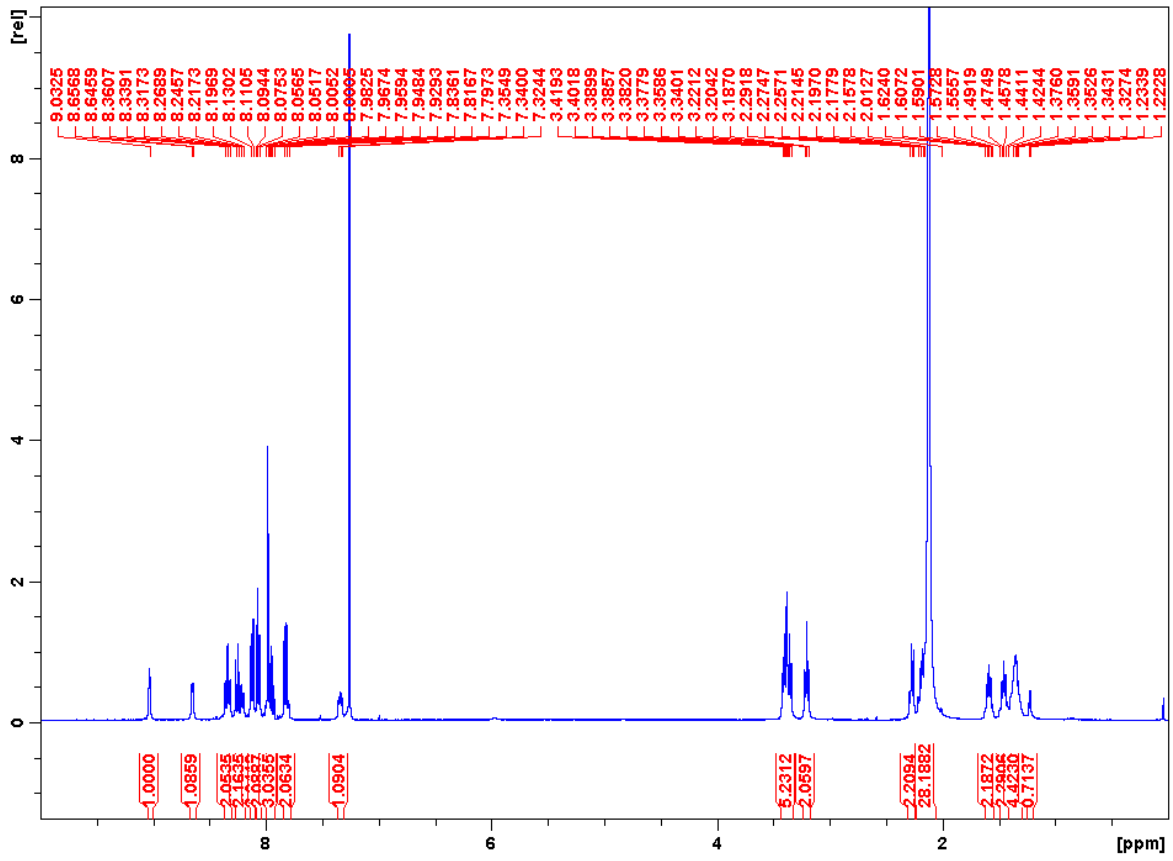

Figure 21. ^{1}H-NMR of [6] (bpy-py)

The aromatic region integrated to the expected 16 peaks, 7 coming from the bipyridine portion of the molecule and 9 from the pyrene. Further upfield the hydrogens on the methylene carbons proximal to the amides have shifted closer together at δ 3.20 and 3.39. When the incoming pyrene fragment joins to the bipyridine ligand it does so by forming a new amide bond. This new amide now has methylene carbons on either side for the amide functional group. The additional methylene carbons proximal to the amide linking the pyrene result in peaks at δ 3.39 which integrates to 6 hydrogens. While two amide functional groups are present in this molecule, two corresponding proton signals are absent. This could be due to exchange with MeOD causing broadening to the extent that the peaks are not able to be visualized.

3.2 Synthesis of Ruthenium Complexes

The complex $Ru(bpy)_2Cl_2$ was synthesized as a precursor for $[Ru(bpy)_2bpy\text{-}py]^{2+}$. The reaction of $Ru(bpy)_2Cl_2$ was performed without any complications. The limited solubility of the bpy-py [6] ligand continued to complicate its handling when reacting with $Ru(bpy)_2Cl_2$ to synthesize the final product. The choice of solvent had to both dissolve the reactants and allow for a high enough temperature during reflux to push the reaction towards product formation. Ethanol and ethylene glycol did solubilize the ligand. Methanol was able to solubilize the reactants however the boiling point was not high enough to push the reaction towards completion, as was an issue with the use of ethanol. The best choice of solvent was 2-methyl-1-propanol. This solvent both dissolved the reactants and provided a high enough boiling point to allow for product formation. In addition, the removal of 2-methyl-1-propanol did not require any special procedures such as the use of high vacuum, which is needed when using ethylene glycol as a solvent.

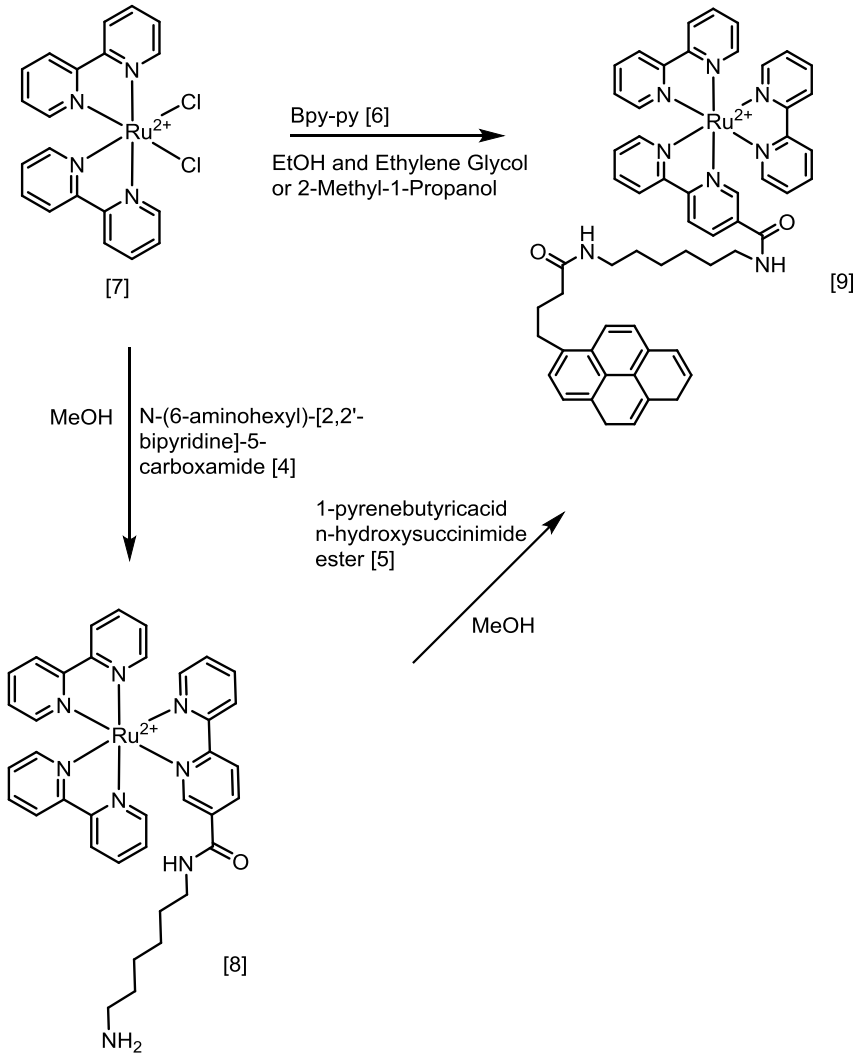

Scheme 3. Synthesis of $[Ru(bpy)_2bpy\text{-}py]^{2+}$ and $[Ru(bpy)_2dep]^{2+}$

The solution of $Ru(bpy)_2Cl_2$ and bpy-py was refluxed for a minimum of 5 days, to ensure that all of the ruthenium precursor was consumed. In some of the later synthetic attempts an excess of bpy-py ligand was added due to the fact that it was more difficult to remove unreacted $Ru(bpy)_2Cl_2$ from the product than it was to remove unreacted bpy-py [6]. The final product was converted to a PF_6^- salt and extracted with chloroform and water and then dichloromethane and water. This was not enough to remove all contamination, so an aluminum oxide column with a 50:50 solution of ACN and water used as the eluent was run. This method of purification in addition to filtering and repeated recrystallizations was successful in purifying the complex. The

crude yield was 77% however the purified yield was closer to 38%. Some of the product was lost on the column. In addition the complex [9] had limited solubility, a complication also encountered when working with the bpy-py [6] ligand. The complex and ligand were soluble in many of the same solvents and as a result extractions were not helpful in removing ligand contamination from the complex.

While the most successful method of purifying the product was using column chromatography on an aluminum oxide column, there was a major drawback with this method because the target complex would get stuck on the column and not elute off even when a variety of different solvents were used. In order to circumvent this problem an alternate synthetic pathway was developed. In the alternate preparation the deprotected bipyridine [4] was reacted with $Ru(bpy)_2Cl_2$ as shown in Scheme 3. After this step, the 1-pyrenebutyricacid n-hydroxysuccinimide ester was reacted with $[Ru(bpy)_2dep]^{2+}$ [8]. The aromatic region of the ^{1}H-NMR of purified [8] integrated to 23 hydrogens and the parent ion at 711 m/z in the mass spec both suggest that the isolated product was pure. After synthesizing $[Ru(bpy)_2dep]^{2+}$ [8] the complex was reacted with [5] to create $[Ru(bpy)_2bpy\text{-}py]^{2+}$ [9]. The rationale behind this method was that if unreacted 1-pyrenebutyricacid n-hydroxysuccinimide ester [5] or $[Ru(bpy)_2dep]^{2+}$ [8] remained at the end of the reaction, there would be enough of a difference in their polarities and solubility to make extractions more successful. The reaction of [5] and $[Ru(bpy)_2dep]^{2+}$ [8] was monitored with ESI-MS and within 24 hours $[Ru(bpy)_2bpy\text{-}py]^{2+}$ [9] was the dominant peak in the spectra. Small amounts of [5] were added during the course of the reaction to ensure all of $[Ru(bpy)_2dep]^{2+}$ [8] was consumed as any of this ruthenium precourser left over in the reaction mixture would be difficult to remove from the product. After 3 days of reflux, little change was observed in the spectra. At the end of the reaction and during work up

persistent contamination resulting from the [5] and $[Ru(bpy)_2dep]^{2+}$ [8] was unable to be removed from $[Ru(bpy)_2bpy\text{-}py]^{2+}$ [9]. While this synthetic approach resulted in the novel complex$[Ru(bpy)_2dep]^{2+}$ [8], it did not succeed in providing a reliable alternate pathway for making $[Ru(bpy)_2bpy\text{-}py]^{2+}$ [9].

3.3 - DNA Binding through Isothermal Binding Titrations

The binding behavior of ruthenium complexes with DNA can be ascertained by monitoring changes in the absorption spectra of the complex upon addition of DNA. It is well known that ruthenium polypyridyl complexes have a characteristic metal to ligand charge transfer (MLCT) absorption around 450 nm. (Bradley, Kress, Hornberger, Dallinger, & Woodruff, 1981) If a complex binds to DNA one or more of its ligands can undergo electronic interactions with DNA. The interaction can either be in the form of π stacking from one of the complex's aromatic ligands with the base pairs of DNA or from electrostatic interactions. The electronic interaction between these ligands and DNA can cause a decrease in the ligands' ability to accept an electron from the metal center, resulting in an overall decrease in the intensity of the MLCT band. As more DNA is titrated into a solution of complex, the MLCT absorption proportionally decreases. This is known as a hypochromic shift in the intensity of the MLCT. In some instances hyperchromicity of a peak is observed, this is characterized by peak intensity increasing as the amount of DNA added increases and is associated with electrostatic binding or damage occurring to the DNA. (Chitrapriya, et al., 2010) (Zhou, et al., 2007)

When changes in the intensity of an absorption band are observed, the strength of the binding event that caused the change in intensity can be calculated as shown in Equations 2 and 3.

$$(\varepsilon_a - \varepsilon_f)/ (\varepsilon_b - \varepsilon_f) = b-(b^2-2K^2C[DNA]/s)^{1/2}/2K \quad (2)$$

$$b= 1 +KC + K[DNA]/2s \quad (3)$$

The binding constant, $K_{b,}$ indicates how strongly a complex is binding to DNA. In addition to the new complexes synthesized, the binding of $[Ru(bpy)_2DPPZ]^{2+}$ (which is a known intercalator) and of $[Ru(bpy)_3]^{2+}$(which is known not to bind to DNA) were assessed as controls. In Figure 22 below, the results from isothermal binding titrations carried out on the complexes of interest can be seen.

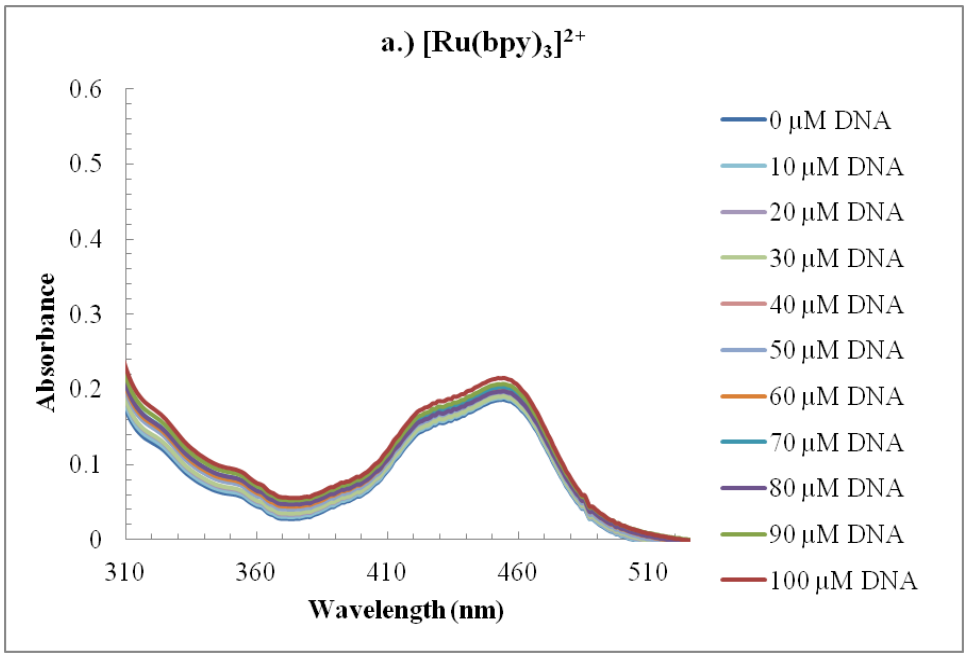
a.) [Ru(bpy)3]2+
Absorbance
0.6
0.5
0.4
0.3
0.2
0.1
0
310
360
410
460
510
Wavelength (nm)
0 µM DNA
10 µM DNA
20 µM DNA
30 µM DNA
40 µM DNA
50 µM DNA
60 µM DNA
70 µM DNA
80 µM DNA
90 µM DNA
100 µM DNA

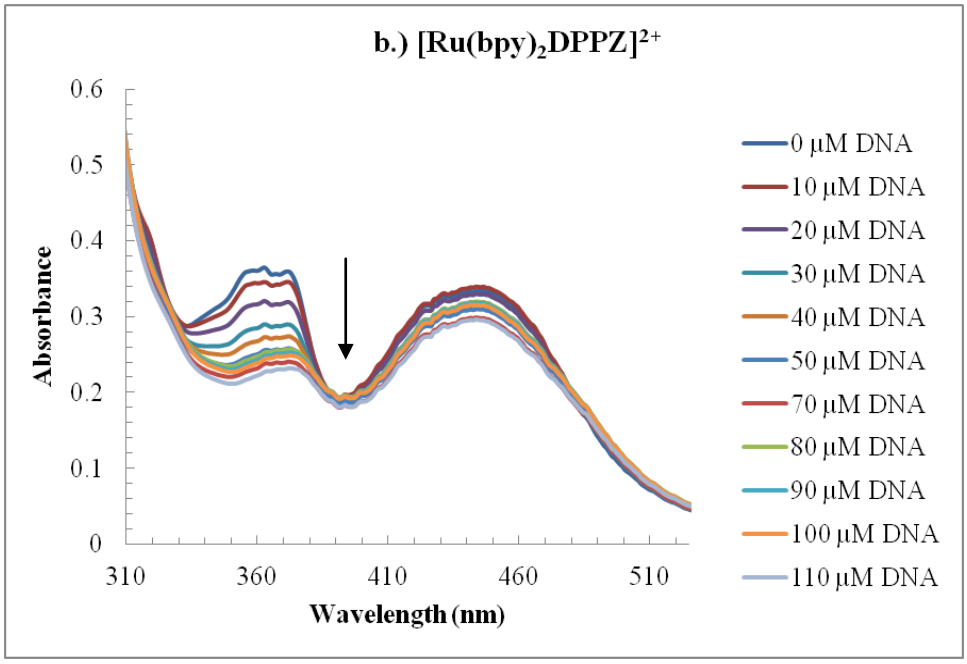
b.) [Ru(bpy)2DPPZ]2+
Absorbance
0.6
0.5
0.4
0.3
0.2
0.1
0
310
360
410
460
510
Wavelength (nm)
0 µM DNA
10 µM DNA
20 µM DNA
30 µM DNA
40 µM DNA
50 µM DNA
70 µM DNA
80 µM DNA
90 µM DNA
100 µM DNA
110 µM DNA

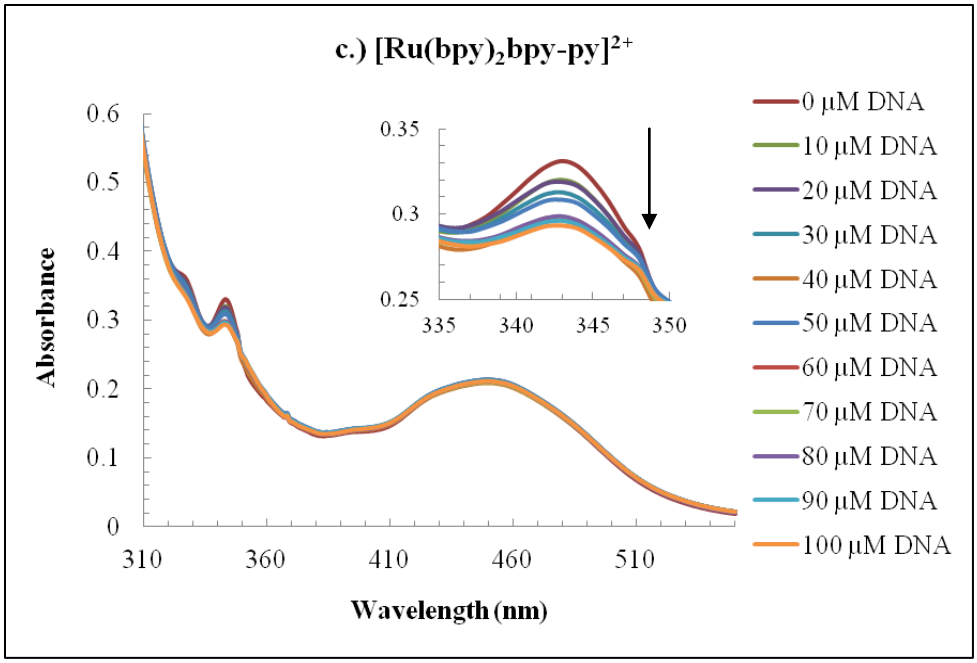
c.) [Ru(bpy)2bpy-py]2+
Absorbance
Wavelength (nm)
0 µM DNA
10 µM DNA
20 µM DNA
30 µM DNA
40 µM DNA
50 µM DNA
60 µM DNA
70 µM DNA
80 µM DNA
90 µM DNA
100 µM DNA

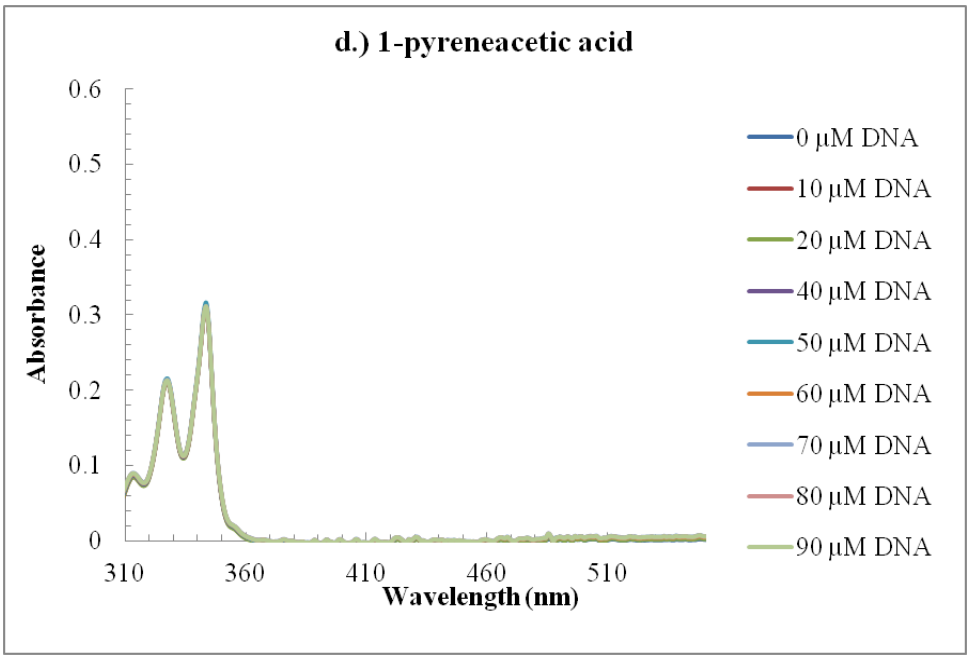
d.) 1-pyreneacetic acid
Absorbance
Wavelength (nm)
0 µM DNA
10 µM DNA
20 µM DNA
40 µM DNA
50 µM DNA
60 µM DNA
70 µM DNA
80 µM DNA
90 µM DNA

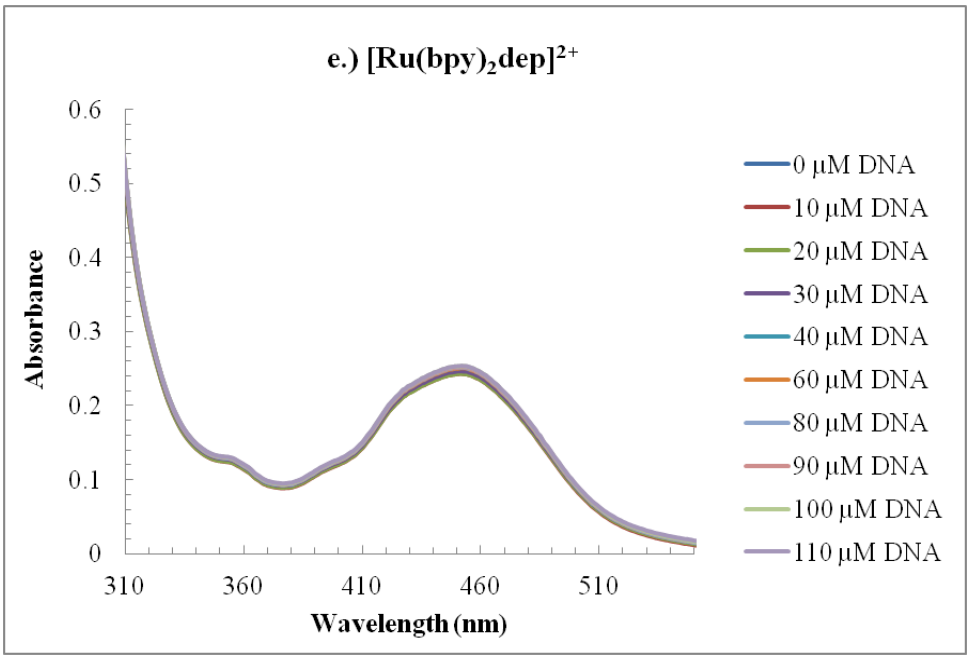

Figure 22. Isothermal binding experiments for a.) 16 µM $[Ru(bpy)_3]^{2+}$ b.) 27 µM $[Ru(bpy)_2DPPZ]^{2+}$ c.) 20 µM $[Ru(bpy)_2bpy\text{-}py]^{2+}$ with inset showing expanded view of transitions occurring around 339 nm d.) 4 µM 1-pyreneacetic acid and e.) 20 µM $[Ru(bpy)_2dep]^{2+}$ with increasing amount of DNA

When DNA was titrated into a solution of $[Ru(bpy)_3]^{2+}$ no change was observed in the intensity of the complex's absorption bands was observed. This finding is in agreement with the literature; a lack of spectral change upon addition of DNA is evidence that $[Ru(bpy)_3]^{2+}$ does not bind to DNA. (Dalton, Glazier, Leung, Win, Megatulski, & Burgmayer, 2008) The positive control, $[Ru(bpy)_2DPPZ]^{2+}$, showed a marked decrease in the intensity of the peak centered around 369 nm; this is indicative of the complex binding to DNA and is the expected result for the complex. (Barton, Goldberg, Kumar, & Turro, 1986) (Sun, Collins, Joyce, & Turro, 2010) The complex of interest, $[Ru(bpy)_2bpy\text{-}py]^{2+}$ behaves similarly, the intensity of the peak at 339 nm decreases as DNA is added, although the magnitude of change observed is not as dramatic as that observed for $[Ru(bpy)_2DPPZ]^{2+}$. The complex $[Ru(bpy)_2dep]^{2+}$ and ligand 1-pyreneacetic

acid do not exhibit any change in their peak intensities as DNA is added. This result is similar to that obtained for $[Ru(bpy)_3]^{2+}$ and indicates that either the complex or ligand are not binding to DNA or that they bind in such a manner that this experiment is not suitable to show binding. More DNA binding studies were carried out, such as fluorescence enhancement and competitive binding to determine if $[Ru(bpy)_2dep]^{2+}$ and 1-pyreneacetic acid genuinely do not bind to DNA or if the isothermal binding titration experiment using these molecules was not sensitive enough to detect binding.

$[Ru(bpy)_2DPPZ]^{2+}$ and $[Ru(bpy)_2bpy\text{-}py]^{2+}$ were the only complexes that had their absorption bands altered as DNA was added indicating that both complexes bind to DNA. The results from the experiments shown in Figure 22 were plotted against a line of best fit using equations 2 and 3, the results of this processing can be seen below in Figure 23 and binding constants for each complex were calculated using equations 2 and 3.

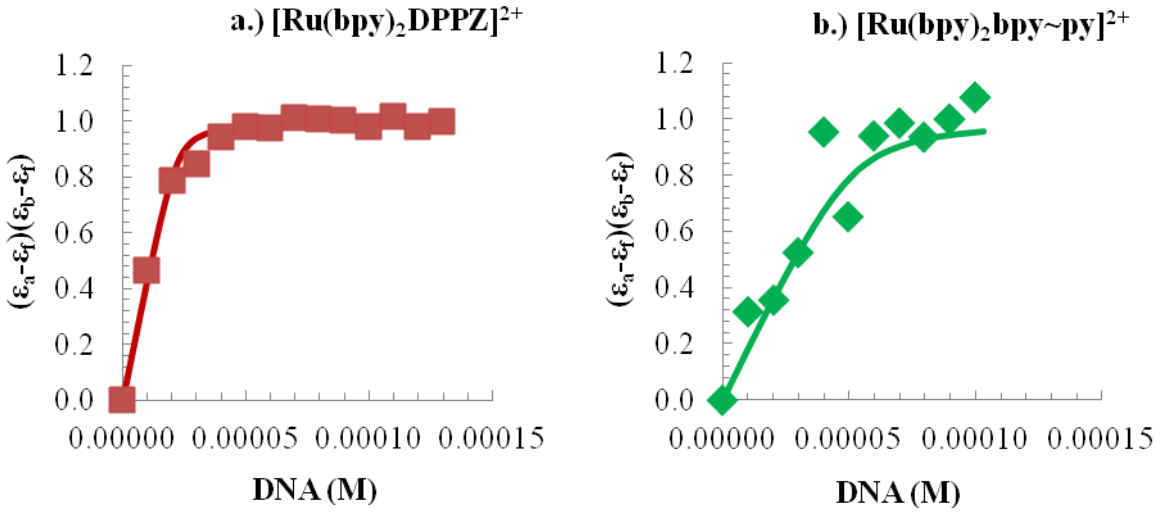

Figure 23. Binding Curves of a.) $[Ru(bpy)_2DPPZ]^{2+}$ and b.) $[Ru(bpy)_2bpy\text{-}py]^{2+}$. The filled squares are the experimental absorption data and the solid lines represent the best fit line to the equations 2 and 3. K_b values are 2.9×10^6 M^{-1} and 8.0×10^5 M^{-1} for $[Ru(bpy)_2DPPZ]^{2+}$ and $[Ru(bpy)_2bpy\text{-}py]^{2+}$ respectively.

When the absorption data from an isothermal binding experiment is plotted and is consistent with the line of best fit from equations 2 and 3, this result indicates the complex is binding to DNA and a binding constant can be extracted. The results above show that $[Ru(bpy)_2DPPZ]^{2+}$ binds to DNA and agrees with literature results for similar experiments with the complex. Using equations 2 and 3, a binding constant of 2.9×10^6 M^{-1} for $[Ru(bpy)_2DPPZ]^{2+}$ with DNA was determined, in line with the literature. (Friedman, Chambron, Sauvage, Turro, & Barton, 1990) The data in Figure 23 b indicates that the complex of interest, $[Ru(bpy)_2bpy\text{-}py]^{2+}$, also binds to DNA, though the binding constant of 8.0×10^5 M^{-1} indicates that it binds to DNA less strongly than $[Ru(bpy)_2DPPZ]^{2+}$. The data points in Figure 23 b do not fit the line of best fit as well as the corresponding data for $[Ru(bpy)_2DPPZ]^{2+}$ and may be explained due to outliers. While the results in Figure 23 indicate that the complex under investigation is binding to DNA,

the isothermal binding titration cannot offer clear evidence as to the mode of that binding. To develop a better understanding of the possible mode of binding $[Ru(bpy)_2bpy\text{-}py]^{2+}$ undergoes with DNA, further spectroscopic studies were conducted.

Binding Studies using Luminescence Spectrsocopy

Two experiments using luminescence spectroscopy were utilized to show if $[Ru(bpy)_2bpy\text{-}py]^{2+}$ is binding to DNA. One of the experiments, the molecular light switch experiment, works by monitoring the emission of a complex in the presence and absence of DNA. Another experiment, the competitive binding experiment, examines whether or not a complex is binding to DNA by monitoring the emission of a third dye, ethidium bromide (EB) for example, as complex is titrated into solution. In the competitive binding experiment the emission of EB is enhanced when it is brought into contact with DNA. As a complex under investigation is titrated into this solution, it will decrease the emission of EB if it interacts with DNA in a competitive fashion. Both experiments can provide a quantitative measure to the strength of binding.

Luminescence Enhancement of Complexes upon Addition of DNA- Excitation at 450 nm

The light switch effect of fluorescence enhancement occurs when a complex has low emission in aqueous solutions but exhibits a dramatic increase in emission upon exposure to DNA. An example of this is the behavior of the complex $[Ru(bpy)_2DPPZ]^{2+}$. When a proton from the solvent binds with the nitrogen on the phenazine ring of the DPPZ ligand, the excited state is quenched and the complex does not luminesce. In the presence of DNA, the complex fluoresces strongly due to the intercalated complex being shielded from the solvent through interactions with DNA. This behavior can be seen in Figure 24 a for the known intercalator

$[Ru(bpy)_2DPPZ]^{2+}$, excited at 440 nm (the MLCT absorbance). (McConnell, Song, & Barton, 2013) (Hartshorn & Barton, 1992)

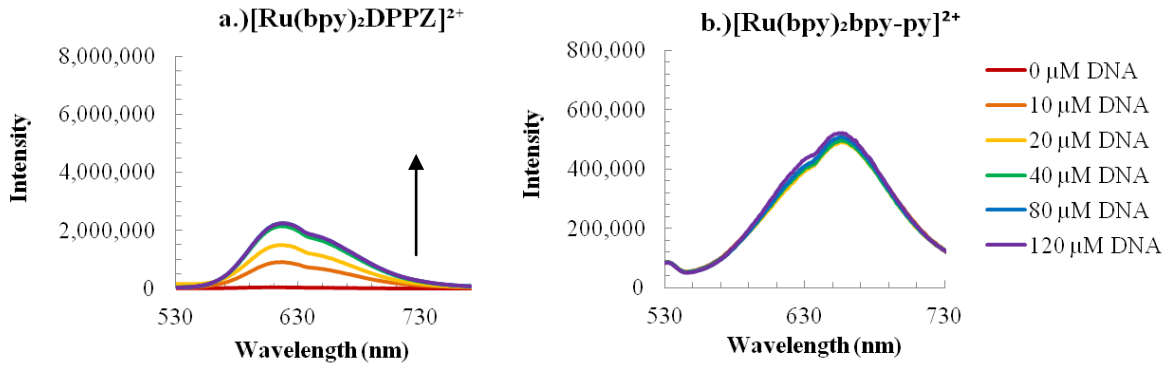

Figure 24. Fluorescence Spectrum for excitation at 440 nm for a.) $[Ru(bpy)_2DPPZ]^{2+}$, and 450 nm for b.) $[Ru(bpy)_2bpy\text{-}py]^{2+}$. The concentration of complex in each experiment is 10 µM.

When the complex $[Ru(bpy)_2bpy\text{-}py]^{2+}$ was examined for fluorescence enhancement (Figure 24 b), a markedly different response was observed. $[Ru(bpy)_2bpy\text{-}py]^{2+}$ not only exhibits fluorescence in aqueous solution (albeit weaker than that of $[Ru(bpy)_2DPPZ]^{2+}$), but its fluorescence does not change upon addition of DNA. The portion of the complex presumed to interact with DNA (the pyrene), lacks a protonatable group and consequently the observation that $[Ru(bpy)_2bpy\text{-}py]^{2+}$ does not display fluorescence enhancement under these conditions is not overly surprising. The excitation wavelength used for this experiment was 450 nm, as it is convention in the literature to excite the MLCT, because this transition is commonly able to be perturbed upon complex binding to DNA. However since the excitation wavelength used in this experiment was 450 nm, the pyrene likely didn't absorb this energy since its excitation would need to be around 339 nm. For these reasons this result does not indicate anything about the interaction between the complex and DNA.

The negative control $[Ru(bpy)_3]^{2+}$ was also studied for its ability to undergo fluorescence enhancement. The complex behaved as expected and did not produce an increase in emission upon exposure to DNA as seen in Figure 25. (Dalton, Glazier, Leung, Win, Megatulski, & Burgmayer, 2008)

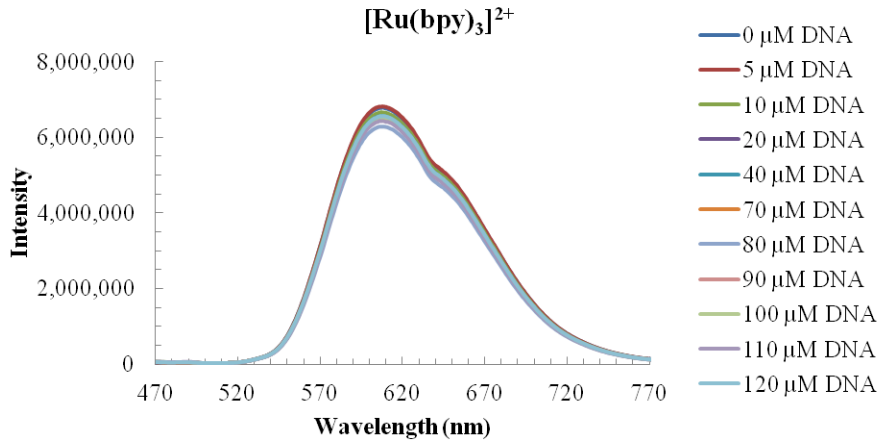

Figure 25. Fluorescence spectrum for excitation of $[Ru(bpy)_3]^{2+}$. The concentration of complex in each experiment is 10 µM with increasing concentrations of DNA.

The related complex, $[Ru(bpy)_2dep]^{2+}$, was also studied for its ability to undergo fluorescence enhancement and the results are presented in Figure 26.

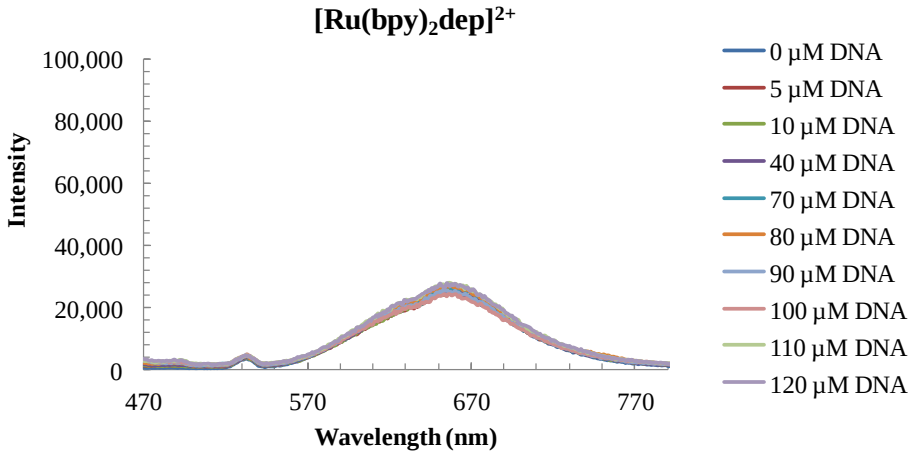

Figure 26. Fluorescence spectrum for excitation of $[Ru(bpy)_2dep]^{2+}$. The concentration of complex in each experiment is 10 µM and the concentration of DNA is noted on Figure legend.

While $[Ru(bpy)_2dep]^{2+}$ does have an amine which can hydrogen bond with water the result in Figure 26 shows that the complex does not have an appreciable emission or an increase in emission upon exposure to DNA. This result appears to agree with the data from the absorbance isothermal binding titration and suggests that $[Ru(bpy)_2dep]^{2+}$ does not bind to DNA. This is not entirely unexpected since $[Ru(bpy)_2dep]^{2+}$ is very similar to the negative control $[Ru(bpy)_3]^{2+}$, with the exception of its extended carbon chain terminating in an amine. The structural difference between $[Ru(bpy)_2dep]^{2+}$ and $[Ru(bpy)_2bpy\text{-}py]^{2+}$ is that only the latter contains a pyrene group. Therefore if $[Ru(bpy)_2bpy\text{-}py]^{2+}$ does bind to DNA it is likely to do so through its pyrene functional group since its analog $[Ru(bpy)_2dep]^{2+}$ appears to be unable to bind to DNA. In order to study the effects of the pyrene subunit of $[Ru(bpy)_2bpy\text{-}py]^{2+}$ on the complex's ability to bind to DNA, the DNA fluorescence enhancement experiment was carried out on 1-pyreneacetic acid and can be seen in Figure 27. 1-pyreneacetic acid is capable of hydrogen bonding with water through its acetic acid functional group, this bonding may allow for fluorescence quenching which could be reduced upon binding to DNA. Furthermore excitation of pyrene molecules have been shown to generate $^1O_2$ which may be able to quench the excited state of the pyrene molecule. (Hartley, Weber, Wyatt, Bordenick, & Lee, 1995) When 1-pyreneacetic acid is exposed to DNA its intercalation may prevent any $^1O_2$ from quenching pyrene's excited state.

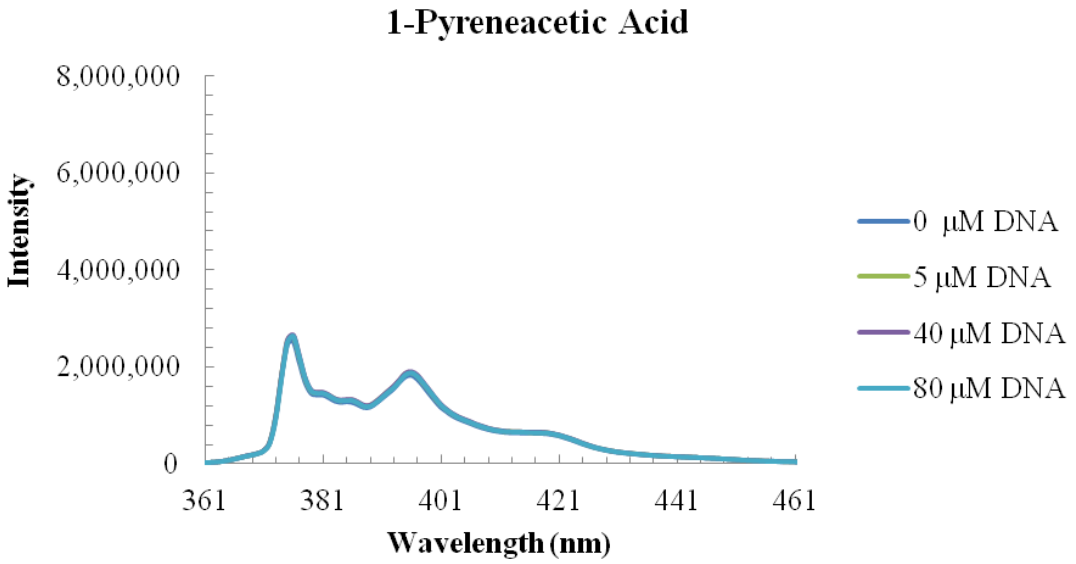

Figure 27. Fluorescence spectrum for excitation at 341 nm for 1-pyreneacetic acid. The concentration of complex in each experiment is 2 µM.

The concentration of 1-pyreneacetic acid used in this experiment was relatively low (2 µM) when compared to the concentration of complexes used for the same study (10 µM). This low concentration was still able to produce a strong emission signal in the absence of DNA. Since no emission enhancement was observed as DNA was added to the solution of 1-pyreneacetic acid it is presumed that hydrogen bonding with water molecules did not quench the excited state, which could also explain the strong emission even in the absence of DNA.

An additional fluorescence experiment interrogating the pyrene portion of $[Ru(bpy)_2bpy\text{-}py]^{2+}$, which is suspected to be the portion of the complex responsible for binding to DNA, was carried out. The absorption of the complex at 339 nm is shown in Figure 28 and is attributed to π-π* transitions within the pyrene moiety, so fluorescence experiments were conducted in the absence and presence of DNA, using 339 nm as the excitation wavelength. This experiment was

performed to examine if emission enhancement of the pyrene functional group could be observed when the functional group was incorporated into ruthenium complex.

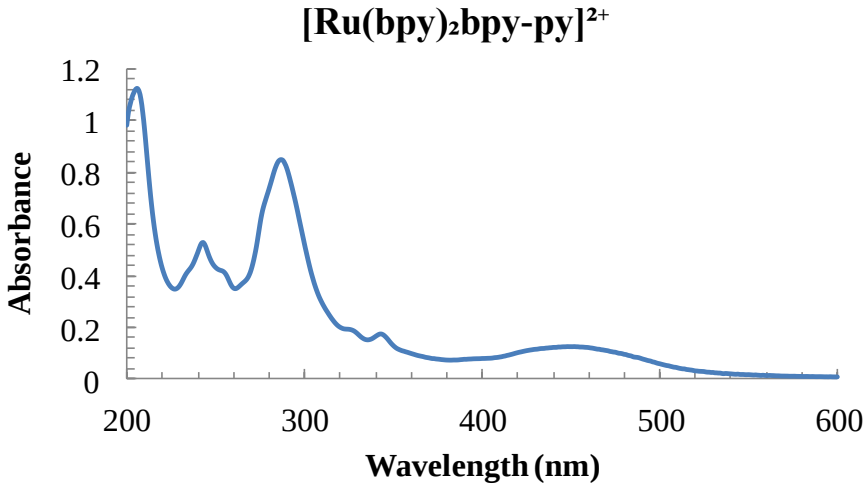

Figure 28. Absorbance spectrum of $[Ru(bpy)_2bpy\text{-}py]^{2+}$

As can be seen in Figure 29 below, in the absence of DNA the emission near 400 nm (attributed to the pyrene) and near 680 nm (attributed to the ruthenium center) nm are both appreciable. In the presence of DNA the emission around 400 nm decreased slightly, and, unlike the results seen in Figure 26 b, the emission at 680 nm is greatly enhanced. This enhancement of emission upon exposure to DNA suggests that the complex is capable of undergoing DNA mediated fluorescence enhancement and furthermore the complex is binding to DNA. It appears that energy absorbed from pyrene may be transferred upon binding to DNA, as evident by a slight quenching in the emission of pyrene seen in Figure 29.

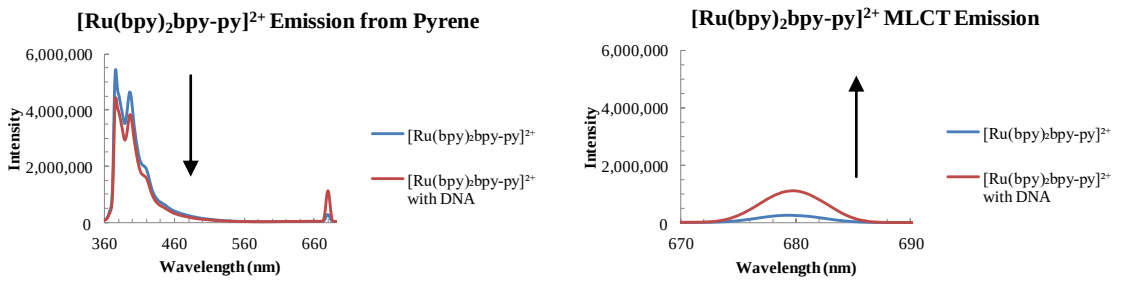

Figure 29. Luminescence enhancement by excitation at 339 nm for 15 µM $[Ru(bpy)_2bpy\text{-}py]^{2+}$.

Competitive Binding Experiments

The competitive binding experiments are another type of fluorometric experiment that were briefly introduced earlier. These experiments are also able to determine if DNA binding is occurring. In this experiment three molecules are used to determine if a complex is binding to DNA. This works by using a dye that is known to bind to DNA, such as EB. This known DNA binder is first allowed to interact with DNA, and then the complex which is being investigated for its ability to bind to DNA is titrated into the solution. If the complex under investigation binds to DNA, it will compete with the dye for space on the double helix, thereby displacing some of the EB and reducing its emission.

The cause of EB's low emission when it is by itself in aqueous solution is due to quenching effects when a proton from water is transferred to the excited state of EB. As DNA is titrated into an aqueous solution of EB, its emission is recovered due to DNA shielding the molecule from the solvent. This shielding occurs because EB intercalates into the base pairs of DNA, where it is protected from interacting with the solvent. In order to establish how EB's emission changed in the presence of DNA, known amounts of EB were titrated into a fixed concentration of DNA. The emission of EB was monitored and the results of this experiment were used to determine a working concentration of EB for the competitive binding experiments.

The results of this experiment are in the Figure 30. Unless otherwise noted the competitive binding experiments using EB were all performed using 520 nm as the excitation wavelength.

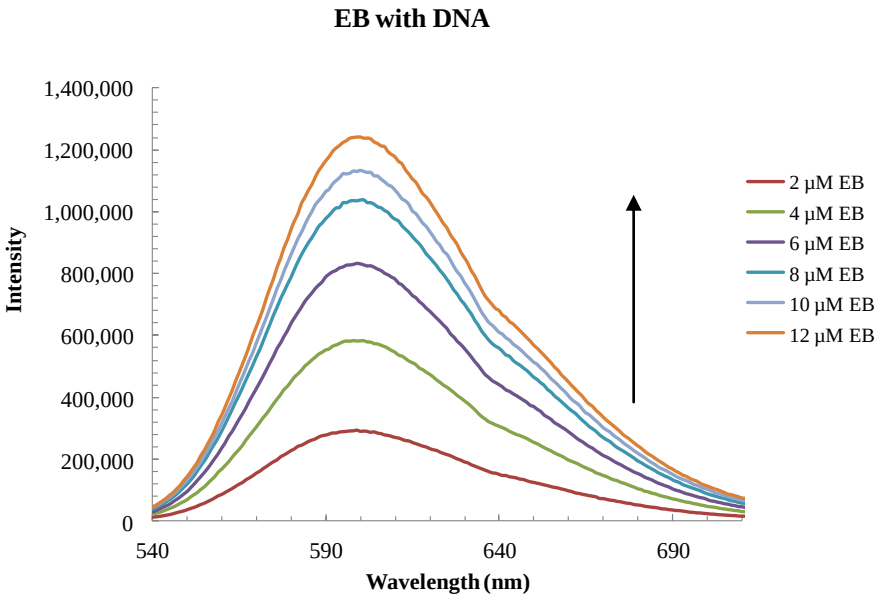

Figure 30. Titration of EB into DNA. For each experiment 25 µM DNA was used. The emission of EB increased as more of the molecule was added to solution.

The literature shows that of 1 molecule of EB is bound for every 4 or 5 nucleotides (or 1 molecule of EB per 2.4 base pairs). (Waring, 1965) In order to ensure that the DNA was saturated with EB for the competitive binding titrations 10 µM of EB and 25 µM DNA was used in all of the experiments.

When a third species that is capable of binding to DNA is added to a mixture of ethidium bromide and DNA, the emission of ethidium bromide decreases with the amount of secondary binder added. (Baguley, et al. 1981) (Iizuka, et al. 2014) This quenching may occur due to the third species displacing some EB from its protected environment within DNA. The competitive binding experiment can show if a complex is binding to DNA and it can also provide a measure to the strength of binding through calculation of an apparent binding constant, K_{app}, as described

in equation 4. The results of the competitive binding experiments with the complexes under study in this work can be seen in Figures 31 through 36.

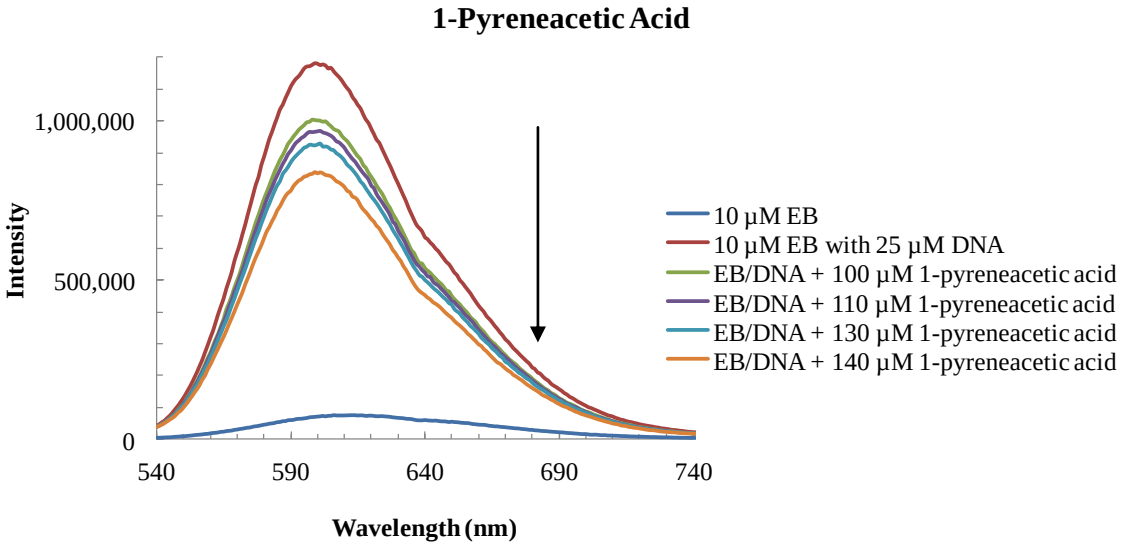

Figure 31. Competative binding titration of 1-pyreneacetic acid

When 1-pyreneacetic acid was studied for competitive binding it caused a concentration dependent decrease in EB's emission. Comparatively greater concentrations of 1-pyreneacetic acid were needed to promote an appreciable decrease in the intensity of EB. The apparent binding constant for 1-pyreneacetic acid was calculated from equation 4 to be 5.1×10^5 M^{-1}. Figure 32 shows competitive binding experiments using lower concentrations of 1-pyreneacetic acid, confirming that this molecule is considerably less effective than $[Ru(bpy)_2DPPZ]^{2+}$ or $[Ru(bpy)_2bpy\text{-}py]^{2+}$ at displacing EB from DNA as can be observed in the results to follow.

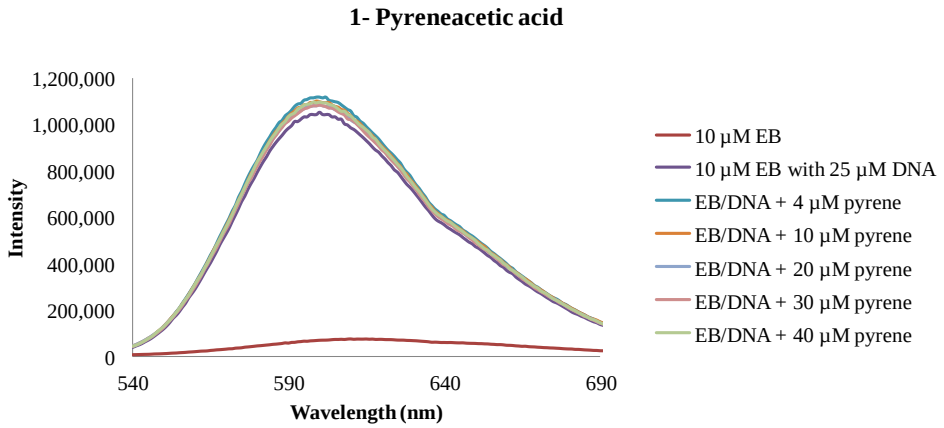

Figure 32. Low concentration of 1-Pyreneacetic acid for competitive binding with excitation at 520 nm.

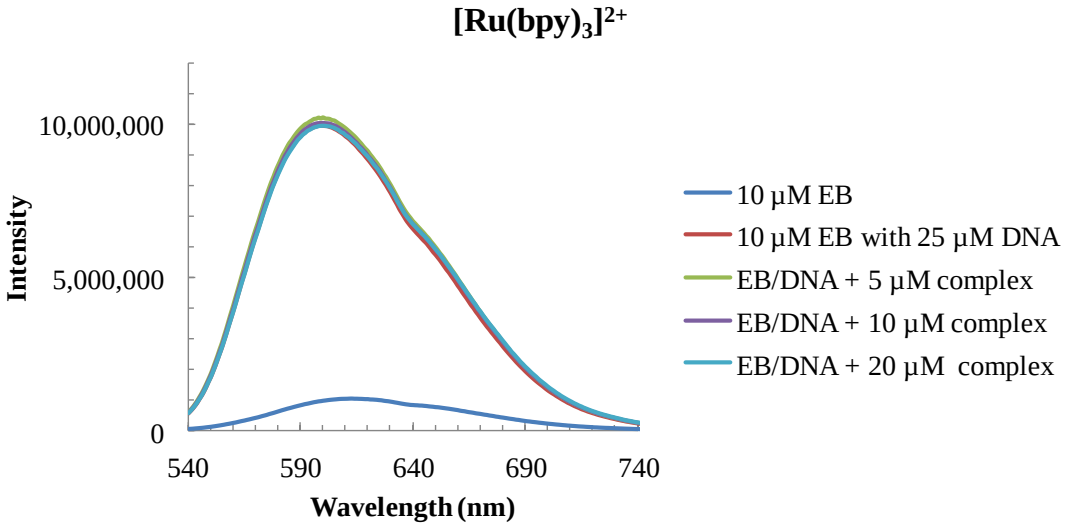

Figure 33. Competative binding titration of $[Ru(bpy)_3]^{2+}$

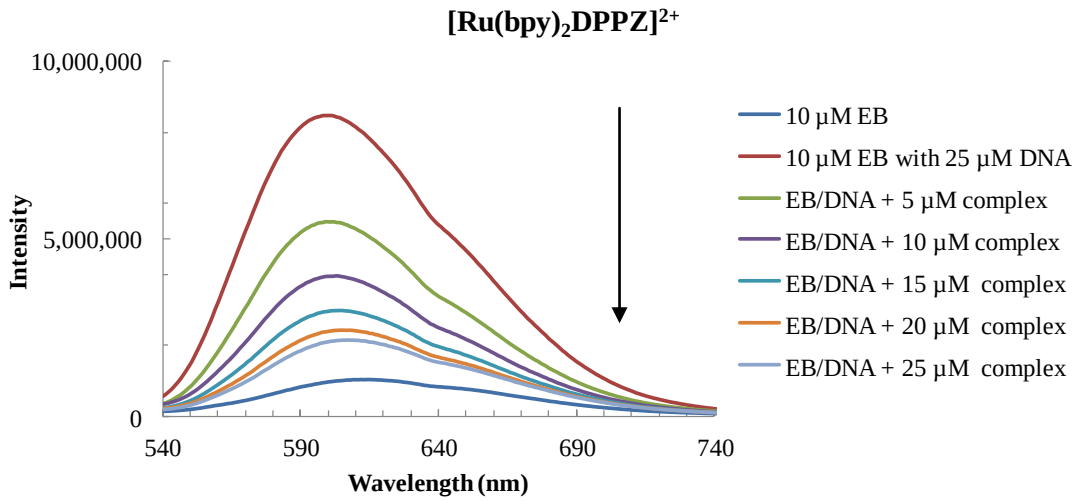

Figure 34. Competative binding titration of $[Ru(bpy)_2DPPZ]^{2+}$

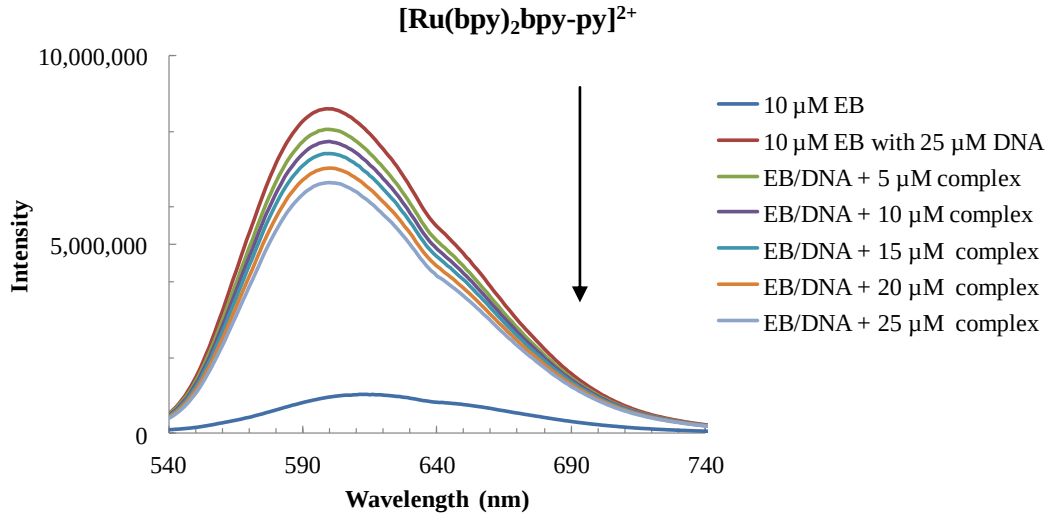

Figure 35. Competative binding titration of $[Ru(bpy)_2bpy\text{-}py]^{2+}$.

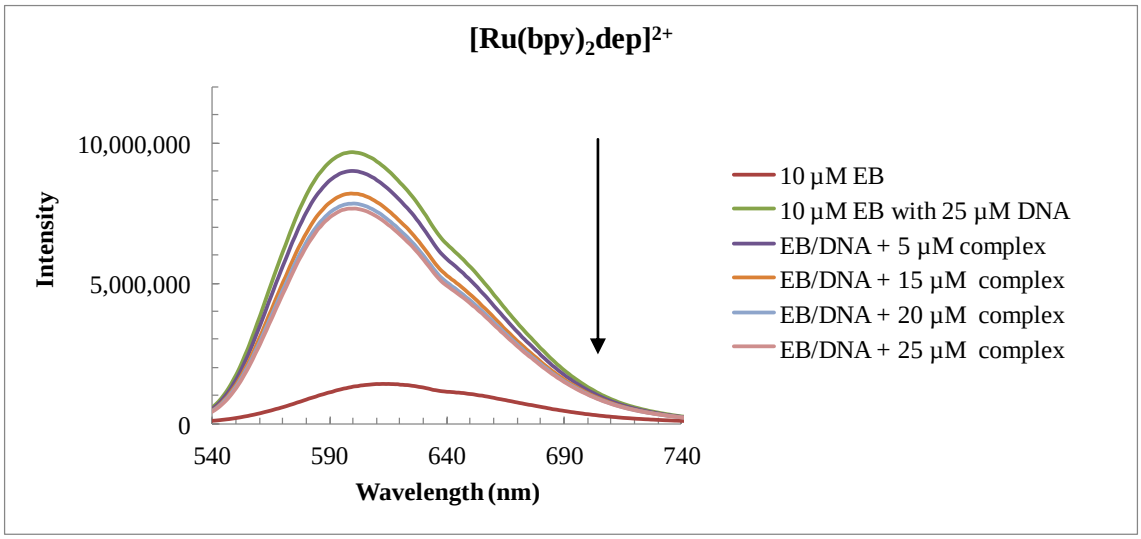

Figure 36. Competitive binding experiment for $[Ru(bpy)_2dep]^{2+}$

The results of the competitive binding titrations show that the controls $[Ru(bpy)_3]^{2+}$ and $[Ru(bpy)_2DPPZ]^{2+}$ behave as predicted. $[Ru(bpy)_3]^{2+}$ does not diminish the intensity of EB's emission and therefore the complex is not competing for space on DNA. $[Ru(bpy)_2DPPZ]^{2+}$ does cause a decrease in EB's emission and does so in a concentration dependent manner. This indicates that the control is competitively binding to DNA. The complex $[Ru(bpy)_2bpy\text{-}py]^{2+}$ also causes a decrease in the emission of EB and therefore is shown to be binding to DNA. Apparent binding constants for $[Ru(bpy)_2DPPZ]^{2+}$ and $[Ru(bpy)_2bpy\text{-}py]^{2+}$, were calculated to be $5.0 \times 10^7\ M^{-1}$ and $9.9 \times 10^6\ M^{-1}$ respectively. The binding constant obtained for $[Ru(bpy)_2DPPZ]^{2+}$ agrees with literature values. (Dalton, Glazier, Leung, Win, Megatulski, & Burgmayer, 2008) Furthermore the apparent binding constants calculated for $[Ru(bpy)_2DPPZ]^{2+}$ and $[Ru(bpy)_2bpy\text{-}py]^{2+}$ from the competitive binding experiments are in line with the binding constants obtained from the isothermal binding titrations. (Dalton, et al. 2008) $[Ru(bpy)_2bpy\text{-}py]^{2+}$ does not bind as strongly to DNA as $[Ru(bpy)_2DPPZ]^{2+}$ however $[Ru(bpy)_2bpy\text{-}py]^{2+}$ does bind to DNA.

Addition of $[Ru(bpy)_2dep]^{2+}$ into a solution of EB and DNA resulted in a decrease in EB emission, indicating that the complex also competitively binds to DNA. This is in contrast to the result obtained from the isothermal binding study in Figure 22 and the fluorescence enhancement experiment in Figure 26. In the previously presented studies the complex was shown not to bind to DNA. This new result was unexpected due to the fact that $[Ru(bpy)_2dep]^{2+}$ lacks an aromatic moiety capable of intercalation, making groove binding the more feasible mode of interaction. Since EB binds to DNA through intercalation it is not clear how a groove binder would be able to displace an intercalator. A study performed by Pal et al investigated simultaneous binding of the minor groove binder Hoechst 33258 and intercalator, EB, with DNA. (Banerjee & Pal, 2007) The group found that despite their different modes of binding, both small molecules were able to bind to DNA. Furthermore, the group used fluorescence resonance energy transfer (FRET) to show that when Hoechst 33258 and EB are bound to DNA in the correct orientation, energy transfer between the two molecules is possible. (Banerjee & Pal, 2007) Therefore when the presumed groove binder, $[Ru(bpy)_2dep]^{2+}$, is added to EB bound DNA it is possible that energy transfer is occurring which can account for EB's decrease in emission.

When both Hoechst 33258 and EB are bound to DNA, Hoechst 33258 may cause quenching of EB's emission. Therefore in order to study possible energy transfer between the two molecules when exposed to DNA the emission properties of EB were studied with simultaneous DNA binding of in the presence and absence of Hoechst 33258. (Suh and Chaires 1995) The competitive binding titration with Hoechst 33258 was performed with excitation at two different wavelengths. Excitation at 520 nm will excite EB while excitation at 339 nm will excite Hoechst 33258. When Hoechst 33258 is excited at 339 nm it will emit around 510 nm. This is close to the region where EB is able to be excited. In this way, the emission of light from

Hoechst 33258 may cause excitation of EB bound to DNA through energy transfer. The results of this experiment can be found in Figure 37.

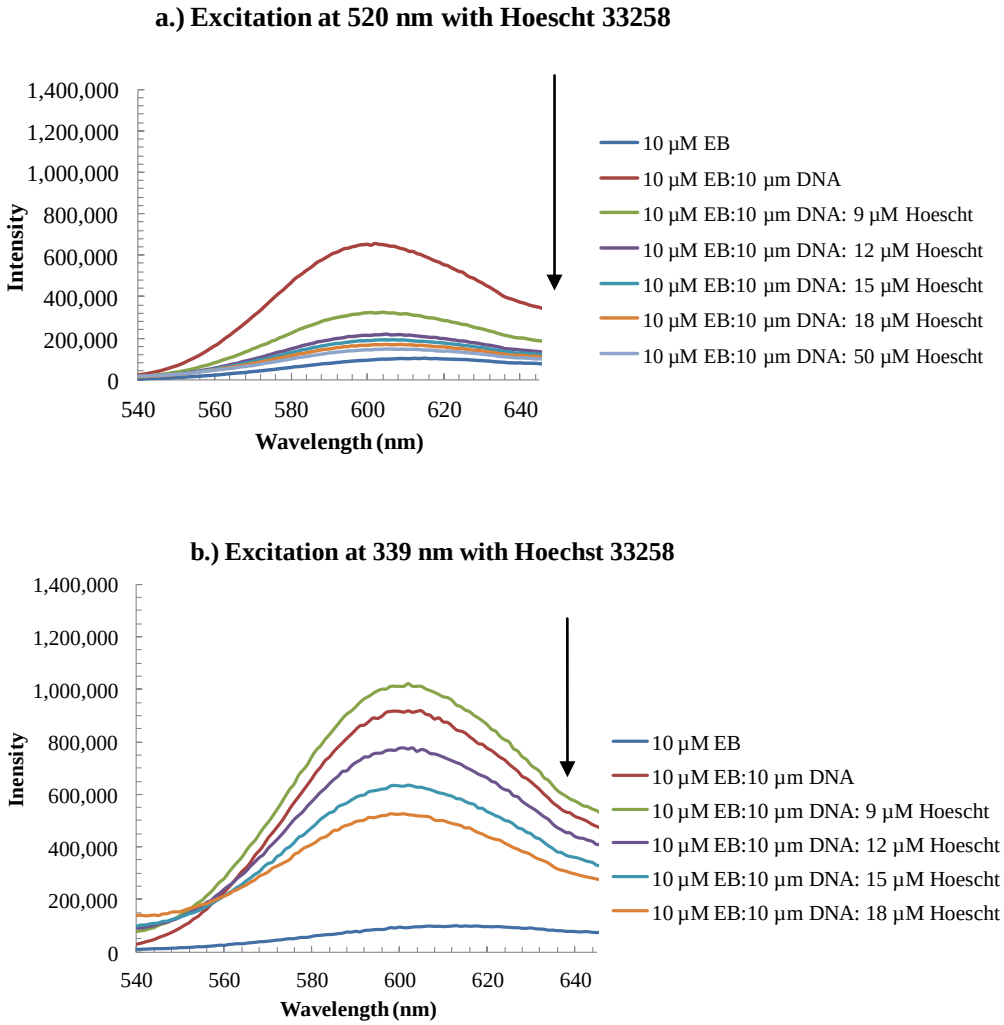

Figure 37. Competitive binding titration of Hoechst 33258 with EB. Solutions excited at a.) 520 nm and b.) 339 nm. Emission of 10 µM EB was collected and then 10 µM of DNA was titrated into the solution. Varying amounts of Hoecsht 33258 added to this solution.

Control experiments were performed by exciting Hoechst 33258 by itself and with either EB or DNA at 520 nm and 339 nm and none of the solutions emitted. Figure 37 a.) shows that as Hoechst 33258 was titrated into a solution of EB and DNA, the minor groove binder

decreased the emission of EB. This result shows that both molecules are binding to DNA. Since competition for space on DNA between the two small molecules is not the cause for EB's decrease in emission, some other energetic process must be occurring. In an attempt to provide more information about how energy transfer between EB and Hoecsht 33258 may occur the same solutions were excited at 339 nm (see Figure 37 b) a region where Hoechst 33258 is capable of absorbing light but EB does not strongly absorb. If EB emits in these solutions, it must undergo excitation from light emitted by Hoechst 33258 bound nearby on DNA. As the concentration of Hoechst 33258 is increased, the emission of EB with DNA decreased. This result also shows that Hoechst 33258's emission can excite EB bound to DNA. As evident through the EB's emission. What is not clear from this set of experiments is why in Figure 37 a.) EB's emission decreases as Hoeschst 33258 is added. The groove binder would not be able to accept energy emitted in this region. Furthermore in Figure 37 b.) if EB is being excited from light emitted by Hoescht 33258, it is not clear why EB's emission incrementally decreases as the concentration of Hoescht 33258 increases.

The results of the competitive binding experiments with $[Ru(bpy)_2dep]^{2+}$ and Hoechst 33258 make it difficult to determine what mode of binding any of the molecules undergo. $[Ru(bpy)_2dep]^{2+}$ is postulated to be a groove or electrostatic binder and Hoechst 33258 is a known groove binder, yet both of these molecules were able to cause a kind of competition with EB (a known intercalator) when bound to DNA. While these molecules most likely did not compete with EB for space on DNA, rather they probably affected the transfer of energy in and around the molecules simultaneously bound to DNA, thereby affecting EB's emission. (Banerjee & Pal, 2007) The competitive binding experiments performed with $[Ru(bpy)_2bpy\text{-}py]^{2+}$ and EB showed that this complex could be an intercalator because it displaces EB from DNA. This

conclusion is difficult to draw from competitive binding experiments because it is possible that both $[Ru(bpy)_2bpy\text{-}py]^{2+}$ and $[Ru(bpy)_2dep]^{2+}$ reduce EB's emission by similar mechanisms that do not involve physical displacement of EB. Therefore the competitive binding experiments with Hoescht 33258 and $[Ru(bpy)_2dep]^{2+}$ bring into question if the mode of binding can be discerned from this set of experiments. The results from the competitive binding experiment with Hoescht 33258 and EB left unanswered questions as to how the transfer of energy may be occurring between the small molecules and DNA. Furthermore, a spectroscopic experiment that provides more conclusive evidence about the mode of binding to DNA is needed; examples of such an experiment would be thermal denaturation experiments or FRET experiments.

In order to further investigate the spectroscopic effects of intercalation and groove binding with DNA Fluorescence Resonance Energy Transfer (FRET) experiments were performed. FRET works when there is spectral overlap between the emission bands of a donor molecule and absorption bands of acceptor molecule similar to what was observed when the emission of Hoechst 33258 excited EB. (Suh and Chaires 1995) The donor molecule absorbs energy from light, and then transfers this energy to the acceptor. The acceptor can then undergo emissive processes resulting from the transferred energy. In order for this to occur the two molecules must be close contact (~10-100Å) and their transition dipole orientation must be approximately parallel. (Suh and Chaires 1995) (LePecq and Paoletti 1967) The nature of intercalative binding of a complex with DNA necessitates that the two molecules are in contact and satisfies many of the other conditions that make FRET possible (such as the orientation of their transition dipoles). DNA absorbs energy around 260 nm. When a complex or molecule intercalates into DNA it can receive this energy from DNA and then undergo fluorescence. Chaires et al peformed FRET experiments with the minor groove binder Hoechst 33258 with

DNA and the molecule is not able to undergo this type of energy transfer because the nature of its groove binding places the molecule too far from the base pairs of DNA for FRET to occur. (Suh and Chaires 1995) While the FRET experiments offered the possibility of obtaining more conclusive evidence about the mode of DNA binding, control experiments were not successful and therefore this avenue of investigation was abandoned. The FRET experiment could still provide information about the mode of DNA binding of the complexes used in this work once the control experiments are optimized.

3.4 Determination of DNA Binding Mode Through Viscometry

While the spectroscopic experiments described above indicate that $[Ru(bpy)_2bpy\text{-}py]^{2+}$, $[Ru(bpy)_2dep]^{2+}$ and 1-pyreneacetic acid are binding to DNA, their mode of binding is still not entirely clear. Results from the fluorometric competitive binding show that both known intercalators and groove binders are able to produce similar results. This complicates assignment of the mode of DNA binding through the use of spectroscopic experiments alone. The use of viscosity measurements is a classic way to determine whether or not DNA binding occurs in an intercalative fashion, as molecules that intercalate increase the contour length of the DNA and consequently increase the viscosity of a DNA-containing solution. (Cohen and Eisenberg 1969) Viscosity data is plotted as intrinsic viscosity $(\eta/\eta_\circ)^{1/3}$ vs. the ratio of complex to DNA in accordance with the theory of Cohen and Eisenberg. (Cohen and Eisenberg 1969) The intrinsic viscosity is defined as the viscosity of a solution resulting from the solute. (Cohen & Eisenberg, 1969) In this experiment the solute is the DNA with and without complex. An initial intrinsic viscosity is obtained by comparing the viscosity of the buffer alone to the viscosity of the buffer of the DNA solutions. (Cohen & Eisenberg, 1969) Intercalation is said to occur when a plot of the change in viscosity of DNA vs. the ratio of complex to DNA produces data poitns that could

be fit to a line with a positive slope. This indicates that the viscosity increases and changes proportionally with the amount of complex or ligand added and this confirms that binding by intercalation is occuring. A result indicating that intercalation is not occuring would yield data points that could be fit to a line with a slope of zero. In Eq. 1, η is the viscosity of DNA and complex, t_f is the average flow time of the respective trial in seconds, t_o is the flow time of the buffer in seconds. $\eta_\circ$ is the viscosity of the DNA solution .

$$\eta = t_f - t_{o/} t_o \quad (1)$$

When the amount of time it takes for a solution of DNA and complex to flow through the viscometer increases, this is an indication that intercalation is occurring. A series of viscosity experiments were performed using controls and the complexes or small molecules under investigation in order to determine more definitively if their mode of binding was through intercalation. In the literature two different types of viscometers are commonly used for this series of experiments, the Ostwald and semi-micro viscometer. The semi-micro viscometer is preferable to use when small quantities of solution are being studied, as was the case for this series of experiments, however results obtained from either viscometer are comparable and both Ostwald and semi-micro viscometers were used in this work. Due to the differences in experimental conditions found in the literature for viscosity experiments a variety of concentration ranges for both controls and complexes/molecules under study were performed. This approach was used to optimize the absolute concentrations to obtain the ratios in the ideal range to observe any changes in viscosity (around 0.2). It was determined that it is best to achieve this ratio using relatively concentrated solutions of complex (around 1-2 mM) and DNA around 0.3 – 0.9 mM x BP. (Ganeshpandian, Loganathan, Suresh, Riyasdeen, Akbarsha, & Palaniandaver, 2014) (Ganeshpandian, Loganathan, Suresh, Riyasdeen, Akbarsha, &

Palaniandaver, 2014) The volume of complex or small molecule added to solutions of DNA in these viscosity experiments ranges from the tens to hundreds of microliters. Due to this small quantity of analyte added, experiments were repeated using a semi-micro viscometer which can offer greater experimental sensitivity in this range. The data collected using the Ostwald viscometer is being presented first and can be seen in the Figures 38 below.

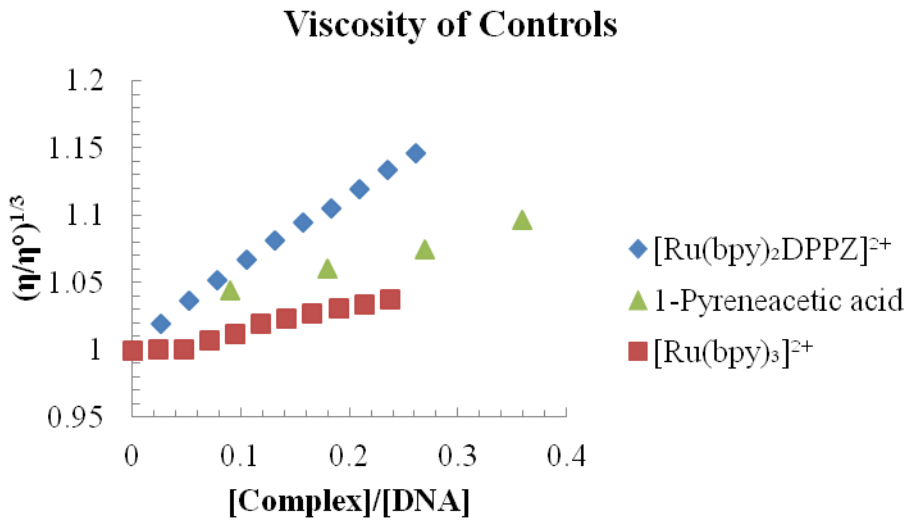

Figure 38. Viscosity experiments with Ostwald viscometer using 0.9 mM x BP DNA for solutions of $[Ru(bpy)_2DPPZ]^{2+}$ (2.35 mM) or $[Ru(bpy)_3]^{2+}$ (2.13 mM). For 1-pyreneacetic acid 0.3 mM x BP DNA was used with 2.33 mM 1-pyreneacetic acid.

In Figure 38 the controls $[Ru(bpy)_2DPPZ]^{2+}$ and $[Ru(bpy)_3]^{2+}$ behaved as expected. (Liu, et al. 2012) (Haq, et al. 1995) $[Ru(bpy)_2DPPZ]^{2+}$ appeared to cause an increase in the viscosity of DNA in a concentration dependent manner. (Haq, et al. 1995) $[Ru(bpy)_3]^{2+}$ when added to DNA yielded only a small change in its viscosity, the expected result for the non-intercalative complex would be no change in viscosity however the small change observed may be attributed to temperature fluctuations during the experiment. (Liu, et al. 2012) 1-pyreneacetic acid produced a result intermediate to the two controls. It is obviously causing the viscosity of DNA

to increase as it is added, but not to as great of an extent as the known intercalator, $[Ru(bpy)_2DPPZ]^{2+}$.

The complex $[Ru(bpy)_2bpy\text{-}py]^{2+}$ has limited solubility in aqueous solutions as well as acetonitrile which complicates the viscosity studies that require more concentrated solutions. When preliminary viscosity experiments were being performed using $[Ru(bpy)_2bpy\text{-}py]^{2+}$, the glass viscometer was found to be stained with complex after the experimentation. It was determined that DMF was able to solubilize the complex and as a result viscosity experiments were performed using this solvent in Figure 39.

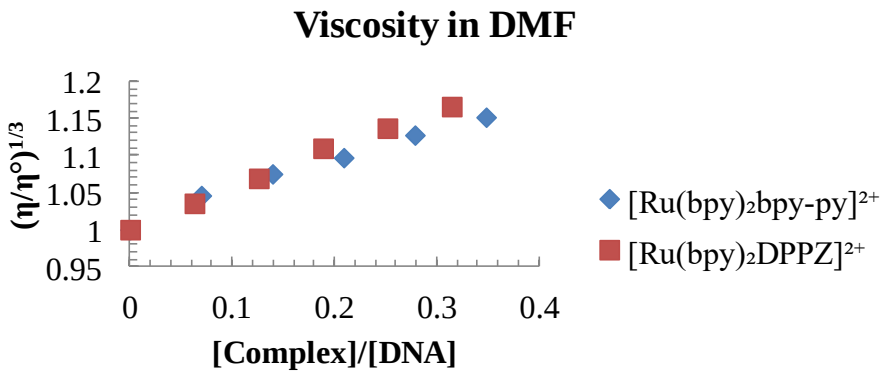

Figure 39. Viscosity performed using 0.3 mM x BP DNA and 0.9 mM $[Ru(bpy)_2DPPZ]^{2+}$ or $[Ru(bpy)_2bpy\text{-}py]^{2+}$ prepared in DMF.

The results in Figure 39 were obtained using $[Ru(bpy)_2bpy\text{-}py]^{2+}$ and $[Ru(bpy)_2DPPZ]^{2+}$ prepared in DMF. Both complexes cause an increase in the viscosity of DNA that is consistent with intercalation. The solvents, DMF, acetonitrile and a solution of 10% DMF in ACN were also tested as controls for their ability to change the viscosity of DNA and the results can be seen in Figure 40.

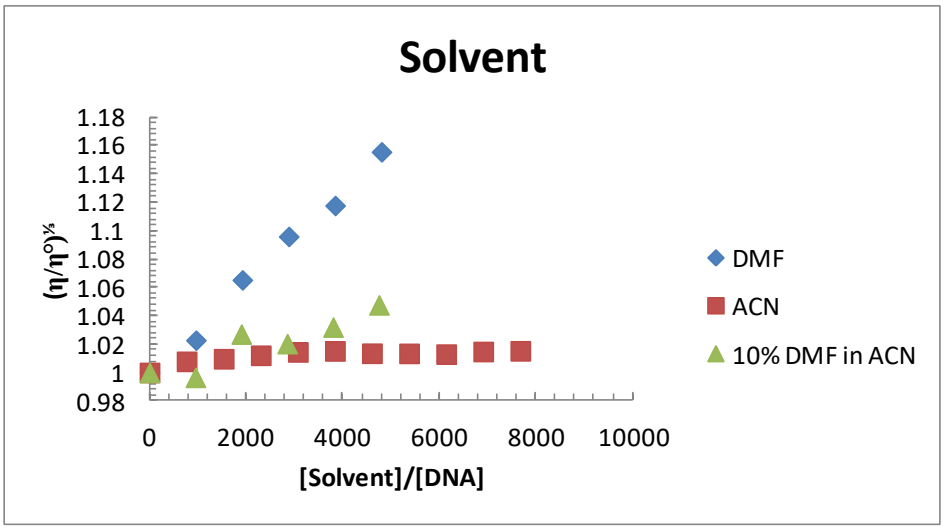

Figure 40. Viscosity performed using 0.3 mM x BP DNA and either DMF, ACN or a solution of 10% DMF in ACN.

DMF by itself was titrated into a solution of DNA and it produced a marked increase in its viscosity. This solvent lacks any kind of aromatic structure, making it an unlikely candidate to intercalate into DNA. The dramatic change in viscosity of DNA upon addition of DMF is most likely due to its inherent viscosity and mixing effects with the 10 mM phosphate buffer solution used in the experiment. In order to minimize the effects of DMF while still taking advantage of its solubilizing properties, solutions of complex were made using only 10% DMF. All of the complexes tested produced an increase in the viscosity of DNA in 10% DMF, even the known non-intercalator $[Ru(bpy)_3]^{2+}$. This indicates that even 10% DMF is too much to yield valid results. The viscosity results for 10% DMF in ACN in Figure 40 show that this mixture of solvents causes an increase in viscosity an is capable of skewing viscosity results. In order to ensure that ACN (a solvent commonly used to solublize complexes for viscosity experiments) does not cause an increase in viscosity similar to that observed for DMF, a solution of ACN and buffer with DNA was tested and no increase in viscosity was observed. The viscosity experiments presented in Figure 41 a and b were conducted using complex or small molecule

prepared in acetonitrile solutions in order to improve solubility but avoid the complications experienced with DMF.

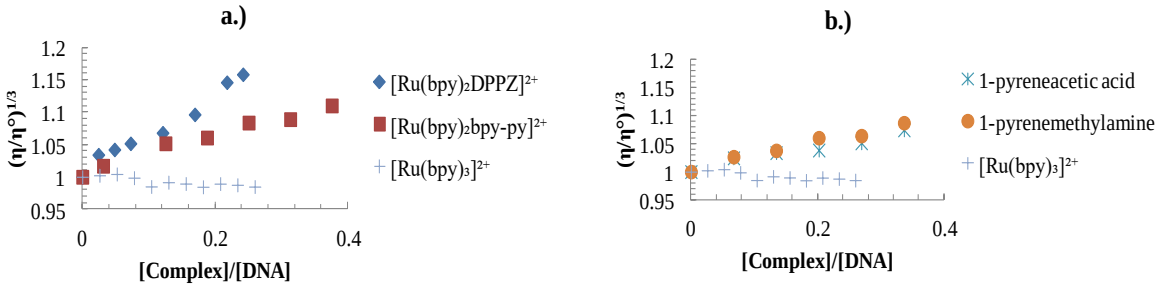

Figure 41. Viscosity experiments perfromed using 0.3 mM x BP DNA. All complexes or small molecules were prepared using acetonitrile. Concentrations are as follows: $[Ru(bpy)_2DPPZ]^{2+}$ 0.7 mM, $[Ru(bpy)_2bpy\text{-}py]^{2+}$ 0.9 mM, $[Ru(bpy)_3]^{2+}$ 0.9 mM, both 1-pyrenemethylamine and 1-pyreneacetic acid were prepared to 1.0 mM.

For the remaining experiments in acetonitrile special care was taken to mix the solutions thoroughly and ensure that $[Ru(bpy)_2bpy\text{-}py]^{2+}$ in particular was in solution. In this experiment $[Ru(bpy)_2DPPZ]^{2+}$ caused an increase in viscosity of DNA and the data points obtained could be fit to a line with a positive slope. This is the expected result for the control complex, which is a known DNA intercalator. $[Ru(bpy)_3]^{2+}$ did not cause a change in the viscosity of DNA as it was titrated into the buffered DNA solution. This finding is the expected result for the known non-intercalator. $[Ru(bpy)_2bpy\text{-}py]^{2+}$ resulted in a increase in the viscosity of DNA, but to a lesser extent when compared to $[Ru(bpy)_2DPPZ]^{2+}$. A similar result was obtained for 1-pyreneacetic acid and 1-pyrenemethylamine. Both of these small molecules produced an increase in the viscosity of DNA, but to a lesser extent than $[Ru(bpy)_2DPPZ]^{2+}$.

The experiment in Figure 41 was repeated to confirm the reproducability of the results. The results of the duplicated experiment can be found in Figure 42.

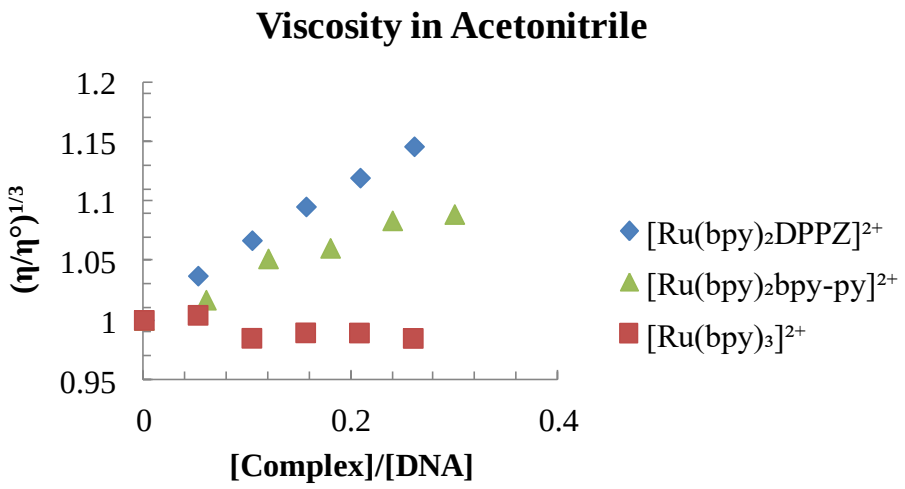

Figure 42. Viscosity experiments using complexes prepared in Acetonitrile. For $[Ru(bpy)_2bpy\text{-}py]^{2+}$ (0.9 mM) and 0.3 mM x BP DNA. $[Ru(bpy)_2DPPZ]^{2+}$ (2.4 mM) and 0.9 mM x BP DNA and $[Ru(bpy)_3]^{2+}$ (2.5 mM) and 1.0 mM x BP DNA.

The results in Figure 42 confirmed that $[Ru(bpy)_2DPPZ]^{2+}$ yields a change in viscosity that is consistent with an intercalator while $[Ru(bpy)_3]^{2+}$ does not cause intercalation as is evident by points that could be fit to a flat line. $[Ru(bpy)_2bpy\text{-}py]^{2+}$ produced a change in viscosity intermediate to the two controls, indicating that it is intercalating into DNA but to a lesser degree than $[Ru(bpy)_2DPPZ]^{2+}$.

A summary of the results from the various binding experiments can be found in Table 1 below.

Table 1. Summary of Results From DNA Binding Experiments

	Isothermal	**Fluorescence Enhancement**	**Competative Binding**	**Viscosity**
$[Ru(bpy)_2DPPZ]^{2+}$	$2.9 \times 10^6\ M^{-1}$	Binds*	$5.0 \times 10^7\ M^{-1}$	Intercalates
$[Ru(bpy)_2bpy\text{-}py]^{2+}$	$8.0 \times 10^6\ M^{-1}$	-	$9.9 \times 10^6\ M^{-1}$	Intercalates
1-pyreneacetic acid	-	-	$5.1 \times 10^6\ M^{-1}$	Intercalates
$[Ru(bpy)_2dep]^{2+}$	-	-	$1.6 \times 10^6\ M^{-1}$	NT

*binding constant not calculated, NT- Not tested

The experiments for $[Ru(bpy)_2DPPZ]^{2+}$ provide the expected results. The UV-Vis isothermal binding experiments and competative binding experiments show that $[Ru(bpy)_2DPPZ]^{2+}$ binds to DNA and viscosity results indicate that the mode of binding is through intercalation. A binding constant was not derived from the fluorescence enhacement experiment because there was no corresponding value to compare to for the complex of interest, $[Ru(bpy)_2bpy\text{-}py]^{2+}$. The binding constants for $[Ru(bpy)_2bpy\text{-}py]^{2+}$ from the UV-Vis isothermal binding and competative binding experiments are in good agreement and show that the complex is binding to DNA but with a lower strength when compared to $[Ru(bpy)_2DPPZ]^{2+}$. The viscosity experiments for both 1-pyreneacetic acid and $[Ru(bpy)_2bpy\text{-}py]^{2+}$ yielded similar results and showed that both compounds bind through intercalation but to a lesser degree than the positive control $[Ru(bpy)_2DPPZ]^{2+}$. The competative binding results for 1-pyreneacetic acid and $[Ru(bpy)_2dep]^{2+}$ showed that both compounds bind to DNA, which was an unexpected result for $[Ru(bpy)_2dep]^{2+}$. $[Ru(bpy)_2dep]^{2+}$ lacks an extended aromatic functional group that would be able to intercalate into DNA so this result is atypical. Viscosity experimentation was not performed on $[Ru(bpy)_2dep]^{2+}$ and needs to be performed in the future works in order to determine if the complex is capable of intercalating. If $[Ru(bpy)_2dep]^{2+}$ were to yield a viscosity result indicative of intercalation it would be presumed to bind to DNA through partial intercalation of one of its bpy ligands.

3.5- Photocleavage of DNA

Once a complex or molecule has been shown to bind to DNA, its ability to damage DNA can be studied. Several different pathways exist by which the energy absorbed by complexes can cause the degradation of DNA through photocleavage. Many of these pathways involve the generation of reactive oxygen species (ROS) such as the hydroxyl radical and superoxide. In oxygen dependant photocleavage pathways inhibitor studies can be performed to determine which forms of ROSs are involved in the mechanism of DNA degradation. (Caitino, Mella and Cardenas-Jiron 2014) Photocleavage of DNA can also occur without oxygen, for example the excited state of some ruthenium complexes causes the oxidatation of guanine on DNA which breaks down the DNA strand. (Knoll & Turro, 2015)

The ability for a complex to damage DNA can be determined by using photocleavage experiments. Since each of the complexes or molecules previously studied absorb either UV, visible light or a combination of both they are all excellent candidates to be studied for their ability to damage DNA through photocleavage. In a typical photocleavage experiment 8 or 12 samples are tested, each of the samples consisting of supercoiled plasmid DNA. Generally one sample will act as a control and is made up of only plasmid DNA in buffer. The other samples tested will contain varying amounts of the complex being tested for its ability to photocleave in addition to plasmid DNA. After the samples are prepared each will be irradiated with UV light. After irradiation, the samples are loaded onto a mold or gel made up of the starch agarose that has had ethhidium bromide added to it. The gel is then loaded into an electrophoresis chamber and a current is applied so that the negatively charged DNA travels down the gel towards a positive terminal. After the current is applied the gel can be imaged to see how the plasmid DNA migrated. The ethidium bromide that was put into the gel mixture is able to bind to DNA

through intercalation. When the DNA bound ethidium bromide is exposed to UV light it will emit light in a manner similar to the competative binding experiments discussed previously. Only ethidium bromide bound to DNA will be able to emit or be visualized and so one can determine where the DNA has migrated on the gel. Different forms of DNA will have different migration patterns. Three different forms of DNA may be present on a gel, and they correspond to varying degrees of damage to DNA. Form I is intact supercoiled DNA that has not been photocleaved. Intact supercoiled DNA is able to travel the farthest down the gel. This is because undamaged supercoiled DNA condenses to a ball like shape which is best able to travel through the pores made within the agarose gel. When scission of DNA occurs on one strand, the result is nicked DNA, Form II, and it is less compact than the intact DNA, as a result Form II has slower mobility through the agarose gel and will not travel as far as Form I. (Tan, et al., 2007) When scission occurs on both strands, linear DNA results and is termed Form III. This form of DNA has a mobility intermediate to that of the intact and the nicked DNA and as a result will appear in between Form I and II when imaged on the gel. (Tan, et al., 2007)

In all the gels that follow, the wells are labeled 1 through 8 from left to right. Well 1 always contains only DNA and serves as a control for each experiment. Figure 43 below shows the photocleavage of $[Ru(bpy)_3]^{2+}$ (a control known not to photocleave DNA) and $[Ru(bpy)_2bpy\text{-}py]^{2+}$. Intact Form I DNA is labeled SC for supercoiled.

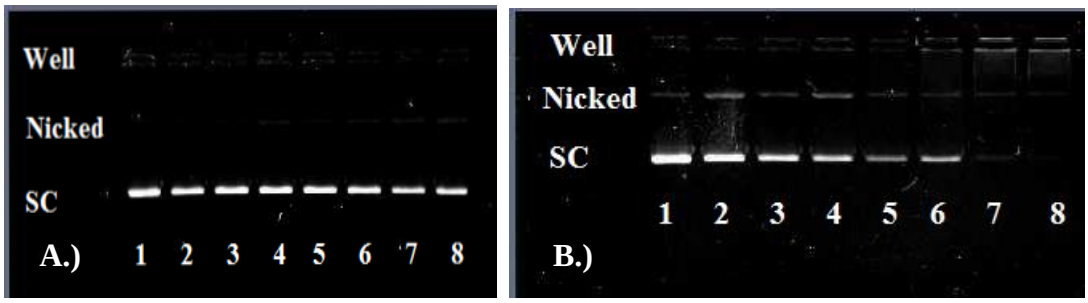

Figure 43. Photocleavage experiments with A.) $[Ru(bpy)_3]^{2+}$ and B.) $[Ru(bpy)_2bpy\text{-}py]^{2+}$. From wells 1 through 8 the concentration of complex is 0, 16, 64, 112, 160, 208 and 258 μM.

In Figure 43 a Form I, supercoiled DNA is present, which indicates that all of the DNA is intact and undamaged (faint illumination in the nicked lane can be seen and is explained by a small amount of nicked DNA being present in most commercially available pBR322 DNA). In contrast to this result $[Ru(bpy)_2bpy\text{-}py]^{2+}$ appears to cause some degree of damage to DNA as evident in the nicked bands seen in wells 2 through 6. The wells containing samples with higher concentrations of complex show the DNA remaining in the well as can be seen in lanes 7 and 8. DNA remaining in the well after electrophoresis is an atypical result. Researchers Rajendiran et al. described a similar result in some of their DNA photocleavage experiments. The group postulated that a complex-DNA-ethidium bromide adduct forms which causes the sample to remain in the well and indicates that the DNA has not traveled down the gel. (Rajendiran, Murali, Suresh, Sinha, Somasundaram, & Palaniandavar, 2008) The illumination of a band in the well indicates that EB is able to bind to DNA, however for some reason the mobility of the DNA is affected. The only way for EB to fluoresce on a gel is for it to interacalate into DNA. If a complex or molecule were to block access on DNA from EB, then imaging would not be possbile. This is one scenario that could cause bands to be absent on a gel. Another possible cause for bands to be missing or for the DNA to not move out of the well is because when the

complex binds to DNA it could stiffen the DNA so much that it is unable to move out of the well.

The gels shown in Figure 43 were made using a 1% solution of agarose, which is a common concentration found in the literature. The greater the concentration of agarose used, the smaller the pore size. Due to the fact that it appears that the presence of the complex is causing the DNA to be trapped in the well, a lower concentration of agarose (0.7%) was used in an attempt to increase the pore size in order to remedy the mobility issues. The results of this experiment can be found in Figure 44 a.

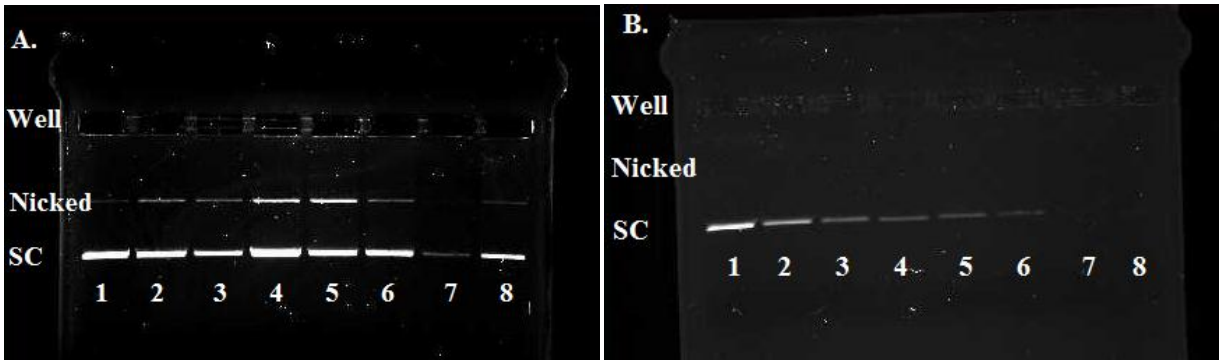

Figure 44. Photocleavage experiments with a.) $[Ru(bpy)_2bpy\text{-}py]^{2+}$ exposed to light b.) experiment performed in the dark. Both trials used 0.7% agarose gels. From wells 1 through 8 the concentration of complex is 0, 16, 64, 112, 160, 208 and 258 μM.

The 0.7% agarose concentration was chosen because if the gel is made any more dilute it lacks integrity and falls apart when handled. The results show that more of the DNA is able to be imaged outside of the well than when 1% agarose is used. This increased mobility of the DNA is likely due to the larger pore sizes in the 0.7% agarose, indicating that the interaction of $[Ru(bpy)_2bpy\text{-}py]^{2+}$ with DNA causes the mobility of the DNA to change dramatically. The presence of nicked DNA makes clear that the complex is able to photocleave DNA, yet at higher concentrations of complex the bands of DNA become more difficult to image.

To investigate if the damage $[Ru(bpy)_2bpy\text{-}py]^2$ caused to DNA was the result of a light driven process the same experiment with $[Ru(bpy)_2bpy\text{-}py]^2$ and DNA was run in the dark and the results are presented in Figure 44 b. There is no nicked DNA present on this gel, indicating that the complex is not able to cleave DNA in the dark this suggests that $[Ru(bpy)_2bpy\text{-}py]^{2+}$ damages DNA through a light mediated process. Figure 45 a reveals that as the concentration of $[Ru(bpy)_2bpy\text{-}py]^{2+}$ increases the amount of DNA imaged decreases.

While the quantification of the amount of DNA present in the bands is not able to be determined visually, a general rule is that the intensity of the bands present in a given lane should approximate that of the control (lane 1). When examining Figure 44 a, bands are not observed in the wells containing higher concentrations of complex however there is reduced intensity of the supercoiled bands imaged in lanes 7 and 8 compared to the control (lane 1). Futhermore there are no nicked bands in well 7 or 8 so it appears that some of the DNA is not being imaged. In Figure 44 b it is even more clear that the amount of DNA imaged decreases as the concentration of complex increases. As this mobility issue persists even when the experiment is run in the dark, it can be attributed to the interaction between the complex and DNA and not to any light-mediated process.

When bands of DNA are trapped in the wells of the gel or are not illuminated as expected, this makes it difficult to conduct other experiments that are aimed towards investigating the DNA photocleavage mechanism. In turning to the literature to try and help explain and troubleshoot why some bands do not appear on gels with $[Ru(bpy)_2bpy\text{-}py]^{2+}$ and DNA, work conducted by Palaniandavar et. al. was found to produce similar results. Their research group studied a series of mixed ligand Ru(II) complexes containing a mixture of benzimidazoles, 1,10-phenantrholine and DPPZ. (Rajendiran, et al. 2008) The agarose gels used

to image the photocleavage products also showed DNA being trapped in the wells at higher concentrations of complex. (Rajendiran, et al. 2008) They surmized that the complexes formed adducts with DNA that impeded its mobility. (Rajendiran, et al. 2008) At higher concentrations of complex the group also noticed that the DNA was not able to be imaged at all. The group concluded that this was occuring due to the complexes under investigation displacing the EB from DNA and preventing it from being visualized. (Rajendiran, et al. 2008) The results of the fluoroscence competitive binding experiments with $[Ru(bpy)_2bpy\text{-}py]^{2+}$ showed that the complex is capable of competing with EB for space on DNA, however the same experiments showed that $[Ru(bpy)_2DPPZ]^{2+}$ competes with EB to an even greater extent. Despite this observation, electrophoretic experiments with $[Ru(bpy)_2DPPZ]^{2+}$ do not cause the same problem with DNA being trapped in the well or hindering the emission of EB. It is possible that some different electronic process maybe occuring between $[Ru(bpy)_2bpy\text{-}py]^{2+}$ and EB.

In order to better visualize the bands of DNA from the photocleavage experiments, a series of alternate staining techniques were carreied out. Hoechst 33258 can also be used as a gel stain that will bind to DNA via groove binding, versus EB that intercalates. In either scenario, when the gel is exposed to UV light, the dye absorbs the energy and then emits, which is how the bands of DNA are ultimately imaged. One theory as to why some of the bands "vanish" when studying $[Ru(bpy)_2bpy\text{-}py]^{2+}$, is that the complex is displacing EB or quenching EB's emissive process. Since Hoechst 33258 binds to DNA differently than EB, it may not be displaced or quenched by $[Ru(bpy)_2bpy\text{-}py]^{2+}$ making it a more suitable stain. A study was conducted by running two gels and staining one with Hoechst 33258 and the other with ethidium bromide for comparison. The results of the study can be found in Figure 45.

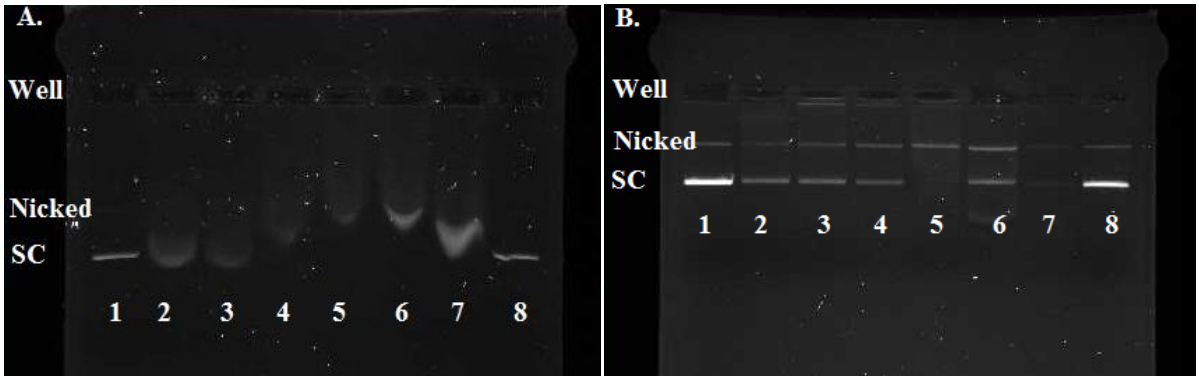

Figure 45. Photocleavage experiment using $[Ru(bpy)_2bpy\text{-}py]^{2+}$. Wells 1 and 8 contain only supercoiled DNA, wells 2 through 7 contain 13, 27, 40, 54, 68, 81 µM $[Ru(bpy)_2bpy\text{-}py]^{2+}$ respectively. a.) stained with Hoechst 33258 b.) stained with EB.

In the photocleavage experiments presented in Figure 45, the control wells for each experiment do not show appreciable nicked DNA, indicating that the DNA used for the experiment was intact. For the experiment using Hoechst 33258 as a stain, it is very difficult to discern nicked or supercoiled DNA when $[Ru(bpy)_2bpy\text{-}py]^{2+}$ is present due to considerable streaking of bands imaged. It should be noted however that bands are imaged, which is not always the case when EB is used as the dye. Due to the streaking of bands the expierment was repeated and the results can be seen in Figure 46.

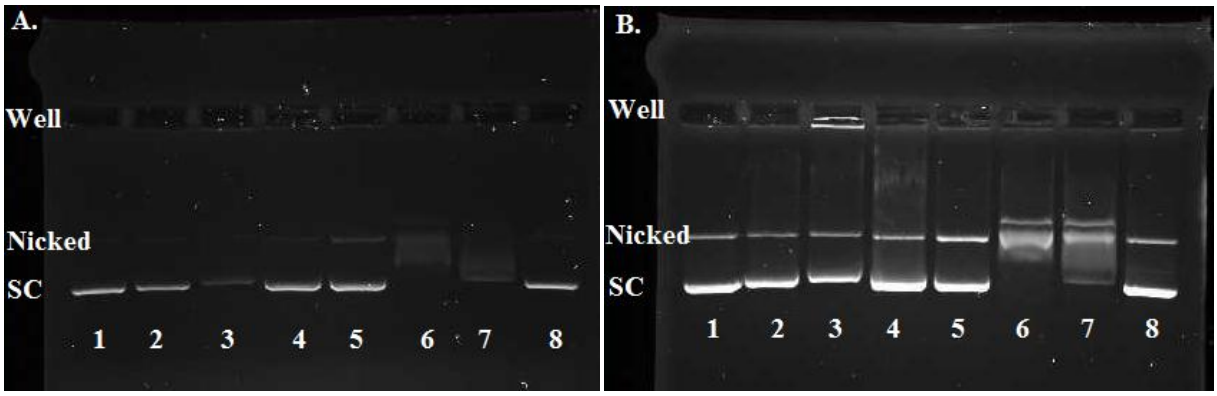

Figure 46. Photocleavage experiment using $[Ru(bpy)_2bpy\text{-}py]^{2+}$, $[Ru(bpy)_3]^{2+}$ and $[Ru(bpy)_2DPPZ]^{2+}$. Wells 1 and 8 contain only supercoiled DNA, wells 2 and 3 respectively contain 7 and 70 µM $[Ru(bpy)_2bpy\text{-}py]^{2+}$, wells 4 and 5 respectively contain 19 and 190 µM $[Ru(bpy)_3]^{2+}$ and wells 6 and 7 respectively contain 14 and 140 µM of $[Ru(bpy)_2DPPZ]^{2+}$. a.) stained using Hoechst 33258. b.) stained by EB post stain.

A study was conducted using a series of complexes, including controls. The controls in Figure 46 are wells, 1 and 8, for both of the experiments and each shows minimal nicked DNA. In one experiment the gels were again stained using Hoechst 33258 added directly to the gel mixture. While the streaking was improved from the experiment in Figure 45 a, almost no DNA was imaged in lane 3 corresponding to $[Ru(bpy)_2bpy\text{-}py]^{2+}$. Furthermore the intensity of the bands imaged for the complex are weaker than the control, indicating that some of the DNA is not accounted for. This result limits the usefulness of Hoescht 33258 as a stain in this set of experiments.

The second study in Figure 46 b was conducted using EB, however instead of the dye being added to the agarose directly prior to setting (as has been done for all ethidium dyed gels up to this point) it was added after illumination and running the gel. This method is known as post staining. If competion of $[Ru(bpy)_2bpy\text{-}py]^{2+}$ with EB is what was causing the bands of

DNA to not be imaged then post staining with ethidium bromide may be a way around this problem. In the post stain $[Ru(bpy)_2bpy\text{-}py]^{2+}$ is first exposed to DNA and allowed to bind. The gel is submerged into a buffer solution and the electric potential is applied. Afterwards the gel is removed and added to a buffered solution of EB. The EB should be able to bind to any unoccupied sites on DNA, thereby allowing the bands to be imaged. The gel is soaked in an EB solution for a period of time and then rinsed with water to remove excess dye. In Figure 46 b which was post-stained with EB, the bands are streaking and the control, $[Ru(bpy)_3]^{2+}$ appears to be producing nicked DNA in wells 4 and 5 which is not the expected result. It is likely that these are experimental anomolies and as a result ethidium bromide post staining was abandoned. No set of experimental conditions was found to stop the bands of DNA exposed to $[Ru(bpy)_2bpy\text{-}py]^{2+}$ from vanishing or remaining in the well after electrophoresis. The best conditions for imaging DNA with $[Ru(bpy)_2bpy\text{-}py]^{2+}$ were to use 0.7% agarose with ethidium bromide added directly to the gel.

The complex $[Ru(bpy)_2bpy\text{-}py]^{2+}$ appears to cause photocleavage of DNA based on the results presented above. Since viscosity experiments showed that 1-pyreneacetic acid intercalates into DNA, pyrene molecules were studied for their ability to photocleave DNA on their own. If the pyrene can photocleave DNA by itself then the question arises of whether there is any added benefit to attaching it to a ruthenium center. To help answer these questions a series of pyrene molecules such as 1-pyreneacetic acid and bpy-py were also studied for their ability to photocleave DNA. The results of their photocleavage experiments are presented in Figure 47.

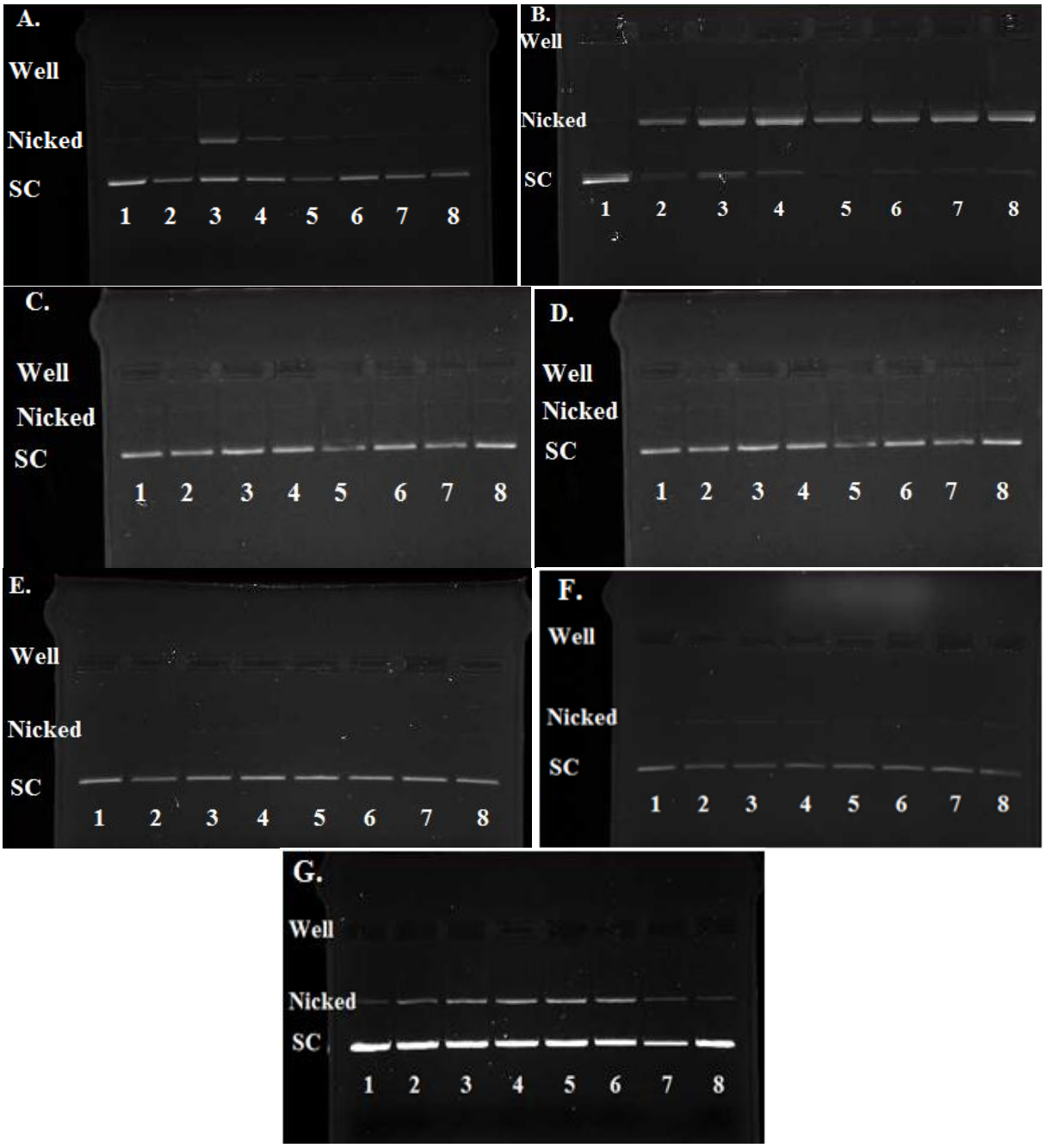

Figure 47. Photocleavage experiments using modified pyrenes. a) experiment conducted using concentration of 1-pyreneacetic acid 0, 10, 5, 12, 18, 31 and 43μM from wells 1 through 8. b) experiment conducted using 1-pyreneacetic acid 0, 2, 3, 4, 5, 5, 7, 6 μM from wells 1 through 8. c) experiment conducted in the dark using 1-pyreneacetic acid 0, 2, 3, 4, 5, 5, 7, 6 μM from wells 1 through 8. d) experiment using bpy-py at concentrations 0, 4, 9, 15, 26, 37, 67, 77 μM from

wells 1 through 8. e) 1-pyrenecarboxylic acid at concentrations 0, 10, 25, 40, 70, 98, 130, 150 µM f) 1-aminopyrene at concentrations 0, 11, 29, 46, 81, 116, 150 and 185 µM. g) 1-pyrenemethylamine at concentrations 0, 6, 17, 27, 46, 66, 86, 0 µM.

For each of the controls in Figure 47 (well 1 of each gel) only supercoiled DNA is imaged which is the expected result. In Figure 47 a the experiment was conducted using 1-pyreneacetic acid at increased concentrations and shows photocleavage as evident by nicked bands however this is only observed at 1-pyreneacetic acid around 5 µM. This shows that 1-pyreneacetic acid is a good photocleaver at low concentrations. When lower pyrene concentrations were used almost all nicked DNA is observed with 1-pyreneacetic acid (Figure 47 b). The higher concentrations of 1-pyreneacetic acid may cause the formation of dimers which prevent its association with DNA and therefore decrease the amount of photocleavage observed. (Lukes, Ilcin, Kollar, Hrdlovic, & Chmela, 2010) The experiment in Figure 47 c was conducted with 1-pyreneacetic acid at the same concentrations used in Figure 47 b however in this experiment the gel was not exposed to light. No damaged DNA was observed, indicating that 1-pyreneacetic acid damages DNA through a light driven process.

The ligand bpy-py was examined for its ability to photocleavage DNA in Figure 47 d at concentrations around where 1-pyreneacetic acid was shown to cleave in addition to somewhat higher concentrations. Under these conditions only supercoiled DNA was observed, therefore the ligand is unable to photocleave DNA. It is possible that the hydrophobic regions of both the bpy and pyrene portions of the ligand prevented it from getting close to DNA and therefore binding and subsequent photocleavage were not possible. Furthermore, neither 1-pyreneacetic acid nor the bpy-py ligand appear to be causing the DNA to be trapped in the well as is observed with $[Ru(bpy)_2bpy\text{-}py]^{2+}$. This result indicates that the reason $[Ru(bpy)_2bpy\text{-}py]^{2+}$ causes DNA

to be trapped in the well or not be imaged is not due to the binding of its pyrene moeity by itself. In some instances ruthenium complexes can undergo bifunctional DNA binding. For example Lecomte et. al. studied a ruthenium polypyridyl complex linked with an alkyl chain to aminochloroquinoline. The group surmised that one end of the complex binded superfically to the surface of DNA while the other end binded more deeply through intercalation. A similar bifunctional binding behavior could be occuring between $[Ru(bpy)_2bpy\text{-}py]^{2+}$ and DNA. This type of binding behaviour could help explain why the $[Ru(bpy)_2bpy\text{-}py]^{2+}$ causes gel imaging problems while bpy-py and 1-pyreneacetic acid do not. The exact cause of the imaging problems with $[Ru(bpy)_2bpy\text{-}py]^{2+}$ have been difficult to pinpoint.

Two related pyrene molecules, 1-pyrenecarboxylic acid and 1-aminopyrene were also studied for their ability to photocleave DNA in Figure 47 e and f. Neither of these molecules produced appreciable photocleavage. However, 1-pyrenemethylamine (Figure 47 g) was found to cause nicked DNA consistent with photocleavage when present in a concentration range of 6-66 μM.

While further study is needed to determine why some pyrene molecules photocleave and others do not, it is clear that 1-pyreneacetic acid at low concentrations causes appreciable damage to DNA. In order to better understand the mechanism of degradation, an inhibitor study was conducted using the molecule. Reactive oxygen species (ROS) are often involved in the degradation of DNA in light driven processes. (Guo & Wei, 2009) DMSO is a scavanger for hydroxyl radicals and was used to perform an inhibitor study with 1-pyreneacetic acid. It would be desireable to perform a similar inhibitor study on $[Ru(bpy)_2bpy\text{-}py]^{2+}$ since this complex was also shown to photocleave DNA. Due to the fact that $[Ru(bpy)_2bpy\text{-}py]^{2+}$ has inherent mobility issues and is difficult to image with DNA in gels, the information obtained from an inhibitor

study would be difficult to attribute to the inhibitor, or problems naturally associated with using the complex. Thefore, until more consistent bands were able to be developed using $[Ru(bpy)_2bpy\text{-}py]^{2+}$ with DNA, an inhibitor study for this complex was not conducted. The results of the study using 1-pyreneacetic acid failed because the DNA used was already completely nicked as evident by only nicked bands being imaged in the control well, well 1. This made it impossible to attribute any of the observed photocleavage to the 1-pyreneacetic acid, due to the fact that the control well failed to give the expected result. Future studies involving a series of reactive oxygen species inhibitors should be carried out on 1-pyreneacetic acid in order to help determine what chemical process is causing the molecule to photocleavae DNA. Ideally inhibitor studies should also be conducted using the complex of interest, $[Ru(bpy)_2bpy\text{-}py]^{2+}$, however as previously mentioned, until reliable gels can be produced that do not have the vanishing bands or problems with the samples getting trapped in the well, conducting meaningful inhibitor studies would be challenging.

4.0 Conclusion

4.1 Synthesis

The objective of the synthetic work was to create $[Ru(bpy)_2bpy\text{-}py]^{2+}$ [9] shown in Figure 17 and reaction Scheme 3. In order to make this complex it was first necessary to synthesize the pyrene modified bipyridine ligand, bpy-py [6], which was developed from the reactions in Schemes 1 and 2. Two different reaction pathways were used to generate the protected bpy [3]. After purification the pathway using TPP resulted in a yield of 26% compared to 48% for the reaction using the acid chloride. The deprotection of [3] proceeded with high purity but the synthesis of [6] was more complicated due to the product's low solubility. Bpy-py [6] contains both a hydrophobic pyrene group as well as polar amides and pyridine nitrogens. The yield of

this molecule was quite low, likely because of losses during extractions due to its amphiphilic nature. The low solubility of bpy-py [6] presented challenges during the synthesis of $[Ru(bpy)_2bpy\text{-}py]^{2+}$ [9]. Instead of using the typical solvent, ethylene glycol, for the metal complex formation, 2-methyl-1-propanol was ultimately chosen because it dissolved the reactants and it provided a high enough reflux temperature to drive product formation. Once synthesized $[Ru(bpy)_2bpy\text{-}py]^{2+}$ [9] required a multistep purification using aluminum oxide column chromatography, filtering, extractions and recrystallization. After purification $[Ru(bpy)_2bpy\text{-}py]^{2+}$ [9] was isolated in high purity but in low yield. Due to the lengthy purification procedure and low overall yield, another synthetic route was investigated to synthesize [9]. The alternate synthesis reacted 1-pyrenebutyric acid n-hydroxy succinimide ester [5] with $[Ru(bpy)_2dep]^{2+}$ [8], the rationale behind this approach was that the difference in polarity between the two reactants would make extractions and other purification steps more successful. However, unreacted 1-pyrenebutyric acid n-hydroxy succinimide ester [5] could not be removed from $[Ru(bpy)_2bpy\text{-}py]^{2+}$ [9] and so this synthetic route was abandoned. While this synthetic approach was not useful for making $[Ru(bpy)_2bpy\text{-}py]^{2+}$ [9], it did synthesize an analog $[Ru(bpy)_2dep]^{2+}$ [8] which was used in the DNA binding and photocleavage studies.

4.2 DNA Binding

The DNA binding experiments were able to provide information on the binding properties of the complexes and molecules studied in this work. The isothermal binding titrations using absorbance spectroscopy were useful for providing evidence of DNA binding for $[Ru(bpy)_2bpy\text{-}py]^{2+}$ [9]. A hypochromic shift in the absorbance of $[Ru(bpy)_2bpy\text{-}py]^{2+}$ [9] centered around 339 nm as DNA was added indicated that [9] was binding to DNA and a binding constant of $8.0 \times 10^5\ M^{-1}$ was calculated. The absorbance occurring at 339 nm in $[Ru(bpy)_2bpy\text{-}$

py]$^{2+}$ [9] is attributed to transitions involving the pyrene portion of the complex. The fact that the absorbance of 339 nm changed as DNA was added to the complex suggests that the pyrene moiety is the region of the complex interacting with DNA. When the isothermal fluorescence titration was performed on [Ru(bpy)$_2$bpy-py]$^{2+}$ [9] the results were less straightforward. When excited at the MLCT of [Ru(bpy)$_2$bpy-py]$^{2+}$ [9] no increase in the complex's emission was observed upon addition of DNA. This result is not entirely unexpected due to the structure of the pyrene moiety which is presumed to bind with DNA. Emission enhancement is thought to occur when a protonatable group on the intercalating end of the complex or molecule is shielded from the quenching effects of water molecules. [Ru(bpy)$_2$bpy-py]$^{2+}$ [9] lacks any protonatable groups on its pyrene and this explains why it did not undergo any change in emission intensity as DNA was added. However, when the fluorescence enhancement experiment was conducted with solutions of [Ru(bpy)$_2$bpy-py]$^{2+}$ [9] with DNA and the excitation wavelength 339 nm was used, an increase in emission intensity was observed. Excitation at 339 nm is presumed to excite an electron on pyrene centered molecular orbitals. The enhanced emission resulting from excitation at 339 nm when [Ru(bpy)$_2$bpy-py]$^{2+}$ [9] is exposed to DNA further supports that the pyrene is associated with DNA in order for its emission intensity to increase. Further studies are necessary to evaluate what type of electronic processes could be occurring to result in emission enhancement when the complex is excited at 339 nm but not when it is excited at wavelengths responsible for its MLCT. Isothermal binding titrations using both absorbance and fluorescence spectroscopy indicated that neither [Ru(bpy)$_2$dep]$^{2+}$ [8] nor 1-pyreneacetic acid bind to DNA.

Fluorometric competitive binding experiments were conducted to further evaluate the binding properties of the complexes and molecules. In contrast to the results obtained from the isothermal binding titrations previously discussed, [Ru(bpy)$_2$dep]$^{2+}$ [8], [Ru(bpy)$_2$bpy-py]$^{2+}$ [9]

and 1-pyreneacetic acid were all shown to bind to DNA. A reduction in the emission intensity of EB was observed when increasing amounts of either [8], [9], or 1-pyreneacetic acid were added to solutions containing EB bound to DNA. This finding suggests that neither the fluorescence nor absorbance isothermal binding titrations performed previously were sensitive enough to detect the binding of $[Ru(bpy)_2dep]^{2+}$ [8] or 1-pyreneacetic acid. The differences in binding behavior obtained from the three different spectroscopic methods used shows that a lack of spectral change does not equate to a lack of DNA binding.

The spectroscopic binding studies show that $[Ru(bpy)_2bpy\text{-}py]^{2+}$ [9] binds to DNA however they do not provide conclusive evidence as to the mode of binding. Viscosity experiments are one of the few DNA binding experiments that can determine if binding occurs through intercalation. The viscosity experiments were performed using comparatively higher concentrations of complex, in order to improve solubility of $[Ru(bpy)_2bpy\text{-}py]^{2+}$ [9], some viscosity experiments were performed using DMF. While the use of DMF improved the solubility of the complex, further investigation found that DMF by itself was capable of increasing the viscosity of buffered DNA solution. When solutions of $[Ru(bpy)_2bpy\text{-}py]^{2+}$ [9] were prepared in acetonitrile and sonicated for several hours the complex went into solution and allowed for viscosity experiments to be performed using the more traditional solvent. Acetonitrile did not affect the viscosity of the buffered DNA solutions as DMF did. The viscosity experiments showed that $[Ru(bpy)_2bpy\text{-}py]^{2+}$ [9] and 1-pyreneacetic acid intercalate into DNA but to a lesser extent when compared to classical intercalators such as $[Ru(bpy)_2DPPZ]^{2+}$.

4.3 Photocleavage

Based on spectroscopic and hydrodynamic experimentation both $[Ru(bpy)_2bpy\text{-}py]^{2+}$ [9] and 1-pyreneacetic acid bind to DNA and the mode of binding is through intercalation. Photocleavage experiments were performed to evaluate if each was able to damage DNA. Gels performed using 1-pyreneacetic acid resulted in only nicked DNA, no undamaged supercoiled DNA remained, which indicates that the compound is an effective photocleaver. The photocleavage results for $[Ru(bpy)_2bpy\text{-}py]^{2+}$ [9] were more complicated. Some of the gels produced results that suggest $[Ru(bpy)_2bpy\text{-}py]^{2+}$ [9] photocleaves DNA, however at higher concentrations of [9] the mobility and imaging of DNA is impeded by a yet undefined process. Possible reasons for the imaging problems are due to electronic interactions between $[Ru(bpy)_2bpy\text{-}py]^{2+}$ [9] and DNA or that [9] causes physical changes to DNA through adduct formation that hinders its ability to move throughout the gel.

5.0 Future Work

The goal of this work was to study DNA binding and photocleavage of a novel ruthenium polypyridyl complex containing an alkyl chain separating the metal center from an extended aromatic region presumed to bind to DNA. A new direction for this project would be to study complexes similar to $[Ru(bpy)_2bpy\text{-}py]^{2+}$ but with shorter alkyl chains separating the metal center and pyrene. Decreasing the alkyl chain from 6 carbons to 4 and 2 carbons may drastically effect the chemical properties of the complexes. One of the synthetic challenges when working with $[Ru(bpy)_2bpy\text{-}py]^{2+}$ was its solubility issues. Reducing the alkyl chain length may help improve solubility by reducing the hydrophobicity of the resutling complexes. One theory as to why $[Ru(bpy)_2bpy\text{-}py]^{2+}$ may have problems being imaged in photocleavage experiments is due to adduct formation or the possibility of bifunctional DNA binding. Reducing the chain length

may make it more difficult for the resulting complexes to bind to DNA in a bifunctional mode and therby help mitigate the gel problems experienced with $[Ru(bpy)_2bpy\text{-}py]^{2+}$.

While the viscosity experiments showed that $[Ru(bpy)_2bpy\text{-}py]^{2+}$ binds to DNA through intercalation, it is possible that the complex binds to DNA in more than one mode. DNA thermal denaturation experiments can be performed to further support that $[Ru(bpy)_2bpy\text{-}py]^{2+}$ binds through intercalation. When a complex intercalates into DNA it also causes a stiffening of the helix and this results in an increased temperature necessary to denature the DNA. (Dalton, Glazier, Leung, Win, Megatulski, & Burgmayer, 2008) In these DNA melting experiments a solution of DNA and complex is slowly heated. As the solution is heated, the absorbance at 260 nm is monitored. This is the wavelength at which the base pairs of DNA absorb. As the DNA denatures with heat, the absorbance will increase. A sigmoidal curve is plotted and the midpoint corresponds to the melting temperature. (Dalton, Glazier, Leung, Win, Megatulski, & Burgmayer, 2008) In some instance when more than one mode of DNA binding occurs a biphasic melting curve will be obtained. If $[Ru(bpy)_2bpy\text{-}py]^{2+}$ binds in two modes it could be through intercalation of the pyrene as has been previously estabilished as well as slight intercalation of one of the unmodified bpy ligands.

To gain a better understanding of some of the results obtained in this work further experimentation is suggested. The results for $[Ru(bpy)_2dep]^{2+}$ [8] from the competitive binding experiments using EB showed that the complex was able to compete with EB bound to DNA. $[Ru(bpy)_2dep]^{2+}$ lacks an extended aromatic region that would intercalate into DNA thereby competing with EB for space on DNA. It is not likely that $[Ru(bpy)_2dep]^{2+}$ intercalates and since similar experiments using Hoechst 33258 (a known groove binder) both appear to decrease the emission intensity of EB, the competitive binding experiment cannot conclusively prove that

binding to DNA occurs through intercalation. In order to show that $[Ru(bpy)_2dep]^{2+}$ does not bind through intercalation viscosity experiments using the complex should be performed.

In order to better understand the results from the competitive binding of Hoechst 33258 with DNA and EB a variation on the previously performed experiments should be conducted. In the new experiment sample solutions would be incubated differently. For example, in one variation DNA solutions would have increasing amounts of Hoechst 33258 added, mixed and then allowed to sit for a period of time. After the incubation period then the EB would be added to the solutions and the emission would be monitored by excitation at 339 nm and 520 nm. The experiment would then be repeated only EB and DNA would be incubated for a period of time prior to adding increasing amounts of Hoechst 33258. If the solutions in which Hoescht 33258 and DNA were incubated prior to addition of EB produce weaker emission than the EB/DNA incubated solutions this could suggest that Hoechst 33258 physically blocks DNA binding site access to EB. Since Hoechst 33258 cannot intercalate itself, instead it may act as a blockade preventing EB from intercalating.

Another direction this project could expand to is studying the effects of different terminal aromatic groups on the complex's ability to bind to and photocleave DNA. By chainging the pyrene moiety on $[Ru(bpy)_2bpy\text{-}py]^{2+}$ for another extended aromatic hydrocarbon such as bpy the photochemistry of the complex would change. Pyrenes are strong UV chromophores on their own, therefore removing this portion of the complex could decrease the new complex's ability to absorb light and damage DNA. One complication previously discussed when working with pyrenes is that they can form dimers at higher concentrations. Whether dimer formation could be complicating some of the experiments in this study is unknown. By synthesizing complexes structurally similar to $[Ru(bpy)_2bpy\text{-}py]^{2+}$ a greater understanding for the photochemistry, DNA

binding behavior and photocleavage performance of the whole series of complexes could be realized.

Works Cited

Abdel-Shafi, A. A., Worrall, D. R., & Ershov, A. Y. (2004). *Dalton Trans.* , 30-36.

Ambroise, A., & Maiya, B. G. (2000). *Inorg. Chem.* , *39*, 4256-4263.

Arounaguiri, S., & Maiya, B. G. (1996). *Inorg. Chem.* , *35*, 4267.

Baguley, B. C., Denny, W. A., Atwell, G. J., & Cain, B. F. (1981). *J. Med. Chem* , *24*, 170-177.

Banerjee, D., & Pal, S. K. (2007). *J. of Phys. Chem. Letters B.* , *111*, 5047-5052.

Barone, G., Terenzi, A., Lauria, A., Almerico, A. M., Leal, J. M., Busto, N., et al. (2013). *Coord. Chem. Rev.* , *257*, 2848-2862.

Barril, P., & Nates, S. (2012). Introduction to Agarose and Polyacrylamide Gel Electrophoresis Matricies With Respect to Their Detection Sensitivities. In P. Barril, S. Nates, & S. Magdeldin (Ed.), *Gel Electrophoresis- Principles and Basics* (pp. 1-14). InTech.

Barton, J. (1986). *Science* , *233*, 727-734.

Barton, J. K., Dannenberg, J. J., & Raphael, A. L. (1982). *J. Am. Chem. Soc.* , *104*, 4967-4969.

Barton, J. K., Goldberg, J. M., Kumar, K. V., & Turro, N. J. (1986). J. Am. Chem. Soc. *108*, 2081-2088.

Bassani, D. M., Wirz, J., Hochstrasser, R., & Leupin, W. (1996). Synthesis of pyrene-acridine bis-intercalators and effects of binding to DNA. *J. of Photochem. and Photobiol. A: Chemistry* , *100*, 65-76.

Basu, P., & Burgmayer, S. J. (2011). *Coord. Chem. Revs.* , *255*, 1016-1038.

Becker, W. M., Kleinsmith, L. J., & Hardin, J. (2006). Phages: Model Systems For Studying Genes. In W. M. Becker, L. J. Kleinsmith, & J. Hardin, *The World Of The Cell* (pp. 515-517). San Francisco: Pearson Education, Inc.

Bellon, S. F., & Lippard, S. J. (1990). *Biophys. Chem.* , *35*, 179-188.

Belvedere, A., Bosca, F., Catalfo, A., Cuquerella, M. C., Guidi, G., & Miranda, M. A. (2002). *Chem. Res. Toxicol.* , *15*, 1142-1149.

Biver, T., Seco, D., & Venturrini, M. (2008). *Coord. Chem. Revs.* , *252*, 1163-1172.

Bouskila, A., Drahi, B., Amouyal, E., Sasaki, I., & Gaudemer, A. (2004). *J. of Photochem. and Photobiol. A: Chem , 163*, 381-388.

Bresloff, J. L., & Crothers, D. M. (1975). *J. Mol. Biol. , 95*, 102-123.

Brun, A. M., & Harriman, A. (1992). *J. Am. Chem. Soc. , 114*, 3656-3660.

Caitino, E. L., Mella, A., & Cardenas-Jiron, G. I. (2014). *Journal of Photochemistry and Photobiology A: Chemistry , 294*, 68-74.

Carter, M. T., Rodriguez, M., & Bard, A. J. (1989). *J. Am. Chem. Soc. , 111*, 8901-8911.

Chen, X., Gao, F., Yang, W.-Y., Sun, J., Zhou, Z.-X., & Ji, L.-N. (2011). *Inorganica Chimica Acta , 378*, 140-147.

Chouai, A., Wicke, S. E., Turro, C., Bacsa, J., Dunbar, K. R., Wang, D., et al. (2005). *Inorg. Chem. , 44*, 5996-6003.

Cohen, G., & Eisenberg, H. (1969). *Biopolymers , 8*, 45-55.

Cosa, G., Focsaneanu, K. S., McLean, J. N., McNamee, J. P., & Scaiano, J. C. (2001). *Photochem. & Photobiol. , 73* (6), 585-599.

Crul, M., van Waardenburg, R. C., Beijnen, J. H., & Schellens, J. M. (2002). *Cancer Treat. Revs. , 28*, 291-303.

Cutillas, N., Yellol, G. S., Haro, C., Vincente, C., & Rodriguez, V. (2013). *Coord. Chem. Rev , 257*, 2784-2797.

Dalton, S. R., Glazier, S., Leung, B., Win, S., Megatulski, C., & Burgmayer, S. J. (2008). *J. Biol. Inorg. Chem. , 13*, 1133-1148.

DeFlaun, M. F., & Paul, J. H. (1986). *J. of Microbiological Methods* , 265-270.

Dong, S., Fu, P. P., Shirsat, R. N., Hwang, H.-M., Leszczynski, J., & Yu, H. (2002). *Chem. Res. Toxicol. , 15*, 400-407.

Dong, S., Hwang, H.-M., Shi, X., Holloway, L., & Yu, H. (2000). *Chem. Res. Toxicol. , 13*, 585-593.

Dunn, D. A., Lin, V. H., & Kochevar, I. E. (1992). Base-Selective Oxidation and Cleavage of DNA by Photochemical Cosensitized Electron Transfer. *Biochemistry , 31*, 11620-11625.

Eggleston, D. J., Goldsby, K. A., Hodgson, D. J., & Meyer, T. J. (1985). *Inorg. Chem. , 24*, 4573-4580.

Eriksson, M., Leijon, M., Hiort, C., Norden, B., & Graslund, A. (1992). *J. Am. Chem. Soc. , 14*, 4933-4934.

Erkkila, K. E., Odom, D. T., & Barton, J. K. (1999). *cHEM. rEV. , 99*, 2777-2795.

Fackler, J. P., Broomhead, J. A., Young, C. G., & Hood, P. (1982). *Inorg. Syn. , 21*, 127-128.

FDA. (2012, April 10). *FDA Drug Safety Communication: Updated information about the risk of blood clots in women taking birth control pills containing drospirenone*. Retrieved February 12, 2016, from http://www.fda.gov/Drugs/DrugSafety/ucm299305.htm

Fede, A., Billeter, M., Leupin, W., & Wuthrich, K. (1993). *Structure , 1*, 177-186.

Fornander, L. H., Billeter, M., Lincoln, P., & Noran, B. (2013). *J. of Phys. Chem. B. , 117*, 5820-5830.

Foster, P., Ramaswamy, V., Arlexo, P., Bernsten, T., Betts, R., Fahey, D. W., et al. (2007). Changes in Atmospheric Constituents and in Radiative Forcing. In: Climate Change 2007: The Physical Science Basis. *Contribution of Working Group I to the Fourth Assessment Report of the Intergovernmental Panel on Climate Change.* Cambridge, UK; New York, NY: Cambridge University Press.

Friedman, A. E., Chambron, J.-C., Sauvage, J.-P., Turro, N. J., & Barton, J. K. (1990). *J. Am. Chem. Soc. , 112*, 4960-4962.

Fromherz, P., & Rieger, B. (1986). *J. Am. Chem. Soc. , 108*, 5361-5362.

Ganeshpandian, M., Loganathan, R., Suresh, E., Riyasdeen, A., Akbarsha, M. A., & Palaniandaver, M. (2014). *Dalton Trans. , 43*, 1203.

Guo, L.-H., & Wei, Y. (2009). *Environmental Toxiciology and Chemistry , 28* (5), 940-945.

Gust, R., Beck, W., Jaouen, G., & Schonenberger, H. (2009). *Coord. Chem. Rev. , 253*, 2742-2759.

Haq, I., Lincoln, P., Suh, D., Norden, B., Chowdhry, B. Z., & Chaires, J. B. (1995). *J. Am. Chem. Soc. , 117*, 4788-4796.

Hariharan, M., Joseph, J., & Ramaiah, D. (2006). *J. Phys. Chem. B. , 110*, 24678-24686.

Hartley, J. A., Weber, J., Wyatt, M. D., Bordenick, N., & Lee, M. (1995). *Bioorg. and Med. Chem. , 3* (6), 623-629.

Hartshorn, R. M., & Barton, J. K. (1992). *J. Am. Chem. Soc. , 114*, 5919-5925.

Haworth, I. S., Elcock, A. H., Freeman, J., Rodger, A., & Richards, W. G. (1991). *J. Biomol. Struct. Dyn. , 9*, 23-43.

Herman, B., Centonze Frohlich, V. E., Lakowicz, J. R., Fellers, T. J., & Davidson, M. W. (2012). *Fluorescence Resonance Energy Transfer (FRET) Microscopy.* Retrieved Aug 29, 2016, from Olympus: http://www.olympusmicro.com/primer/techniques/fluorescence/fret/fretintro.html

Holder, A., Swavey, S., & Brewer, K. J. (2004). *Inorg. Chem. , 43* (1), 303-308.

Holmlin, R. E., & Barton, J. K. (1995). *Inorg. Chem. , 34*, 7.

Jain, A., Slebodnick, C., Winkel, B. S., & Brewer, K. J. (2008). *Journal of Inorg. Biochem. , 102*, 1854-1861.

Jakupec, M. A., Galanski, M., & Keppler, B. K. (2003). *Rev. Physiol. Biochem. Pharmacol. , 146*, 1-.

Jennette, K. W., Lippard, S. J., Vassiliades, G. A., & Bauer, W. R. (1974). *Proc. Natl. Acad. Sci. , 71* (10), 3839-3843.

Johnson, I. D., & Davidson, M. W. (2012). *Jablonski Energy Diagram*. Retrieved Aug 16, 2016, from http://www.olympusmicro.com/primer/java/jablonski/jabintro/

Juris, A., Barigeletti, F., Campagna, S., Balzani, V., Belser, P., & Zelewsky, A. (1988). *Coord. Chem. Revs. , 84*, 85.

Katz, S. A., Parfitt, C., & Purdy, R. (1970). *J. Chem. Educ. , 47* (10), 721-722.

Kelly, J. M., McConnell, J., OhUigin, C., Tossi, A. B., Mesmaeker, A. K.-D., Masschelein, A., et al. (1987). *J. Chem. Soc. Chem. Commun. , 1149*, 1821-1823.

Kim, K.-W., Roh, J. K., Wee, H.-J., & Kim, C. (2016). Carboplatin. In *Cancer Drug Discovery Science and History* (p. 90). Springer.

Knoll, J. D., & Turro, C. (2015). *Coordination Chemistry Reviews , 282-283*, 110-126.

Komatsuzaki, N., Katoh, R., Himeda, Y., Sugihara, H., Arakawa, H., & Kasuga, K. (2000). *J. Chem. Soc. Dalton Trans.* , 3053-3054.

Kumar, K. A., Reddy, K. L., & Satyanarayana, S. (2010). *Transi. Met. Chem , 35*, 713-720.

Lecomte, J.-P., Mesmaeker, A. K.-D., Demeunynck, M., & Lhomme, J. (1993). *J. Chem. Soc. Faraday Trans. , 89* (17), 3261-3269.

Lee, M., Rhodes, A. L., Wyatt, M. D., Forrow, S., & Hartley, J. A. (1993). *Biochemistry , 32*, 4237-4245.

LePecq, J. B., & Paoletti, C. (1967). *J. Mol. Biol. , 27*, 87-106.

Lerner, M. B., Resczenski, J. M., Amin, A., Johnson, R. R., Goldsmith, J. I., & Johnson, A. C. (2012). *J. of Am. Chem. Soc. , 134*, 14318-14321.

Li, B., Mao, B., Liu, T.-M., Xu, J., Dourondin, A., Amin, S., et al. (1995). *Chem. Res. Toxicol. , 8*, 396-402.

Liu, J. G., Zhang, Q.-L., Shi, X.-F., & Ji, L.-N. (2001). *Inorg. Chem. , 40*, 5045-5050.

Liu, J.-G., Ye, B.-H., Li, H., Zhen, Q.-X., Ji, L.-N., & Fu, Y.-H. (1999). *J. of Inorg. Biochem. , 76*, 265-271.

Liu, Y.-J., Liang, Z.-H., Li, Z.-Z., Yao, J.-H., & Huang, H.-L. (2011). *J. of Organometallic Chem. , 696*, 2728-2735.

Liu, Z., Lu, Y., Rosenstein, B., Lebwohl, M., & Wei, H. (1995). *Biochemistry , 37*, 10307-10312.

Lootiens, F. G., McLaughin, I. W., & Diekmann, S. (1991). *Biochemistry , 30*, 182-189.

Lukes, V., Ilcin, M., Kollar, J., Hrdlovic, P., & Chmela, S. (2010). *Chemical Physics , 377*, 123-131.

Maity, B., Roy, M., Saha, S., & Chakravarty, A. R. (2009). *Organometallics , 28*, 1495-1505.

Mariappan, M., Suenaga, M., Mukhopadhyay, A., Raghavaiah, P., & Maiya, B. G. (2011). *Inorganica Chimica Acta , 376*, 340-349.

Meyer-Almes, F. J., & Dietmar, p. (1993). *Biochemistry , 95*, 4246-4253.

Miao, R., Mongelli, M. T., Ziegler, D. F., Winkel, B. S., & Brewer, K. J. (2006). *Inorg. Chem. , 45*, 40413-10415.

Mongelli, M., Heinecke, J., Shatara, M., Okyere, B., Winkel, B. S., & Brewer, K. J. (2006). *Journal of Inorg. Biochem. , 100*, 1983-1987.

Moucheron, C., Mesmaeker, A. K.-D., & Kelly, J. M. (1997). *J. of Photochem. and Photobiol. B: Bio. , 40*, 91-106.

Murphy, C. J., & Barton, J. K. (n.d.). *Metho. in. Enzymology* .

Murphy, C. J., & Barton, J. K. (1993). *Meth. in Enzymology , 226*, 576-594.

Murphy, C. J., & Barton, J. K. (1993). *Methods in Enzymology , 226*, 576-594.

Myrick, M. l., DeArmond, M. K., & Blakley, R. L. (1989). *Inorg. Chem , 28*, 4077.

Niko, Y., Kawauchi, S., & Konishi, G.-I. (2011). *Tetrahedron Letters , 52*, 4843-4847.

Nishiyama, N., Kato, Y., Sugiyama, Y., & Kataka, K. (2001). Cisplatin-loaded-polymer-metal Complex Micelle With Time-modulated Decaying Property As A Novel Drug Delivery System. *Pharm. Res. , 18*, 1035-1041.

O'Connor, D., Shafirovich, V. Y., & Geacintov, N. E. (1994). *J. Phys. Chem. , 98*, 9831-9839.

Olmstead, J. I. (n.d.).

Olmstead, J. I., & Kearns, D. R. (1977). *Biochemistry , 16* (16), 3647-3654.

Paoletti, J., & Le Pecq, J. B. (1971). *J. Mol. Biol. , 59*, 43-62.

Peterson, H. C. (2001). The "Exxon Valdez" Oil Spill in Alaska: Acute, Indirect and Chronic Effects on the Ecosystem. *Advances in Marine Biology , 39*, 1-103.

Poteet, S. A., Majewski, M. B., Breitbach, G. S., Griffith, C. A., Singh, S., Armstrong, D. W., et al. (2013). *J. Am. Chem. Soc. , 135*, 2419-2422.

Putta, V. R., Mallepally, R. R., Avudoddi, S., Yata, P. K., Chintakuntla, N., Nachorla, D., et al. (2015). *Analytical Biochemistry , 485*, 49-58.

Rajalakshmi, S., Weyhermuller, T., Freddy, A. J., Vasanthi, H. R., & Nair, B. U. (2011). *Eu. J. of Med. Chem. , 46*, 608-617.

Rajendiran, V., Murali, M., Suresh, E., Sinha, S., Somasundaram, K., & Palaniandavar, M. (2008). *Dalton Transactions* , 148-163.

Rehmann, J. P., & Barton, J. K. (1990). *Biochem. , 29*, 1709-1709.

Reichmann, M. E., Rice, S. A., Thomas, C. A., & Doty, P. (1954). *J. of the Am. Chem. Soc. , 76* (11), 3047-3053.

Reinhardt, C. G., Roques, B. P., & Le Pecq, J. B. (1982). *Biochem. and Biophys. Res. Comm. , 104* (4), 1376-1385.

Rice, J. E., Hosted, T. J., & Lavoie, E. J. (1984). *Cancer Lett. , 24*, 327-333.

Riley, C. M., Sternson, L. A., Repta, A. J., & Slyter, S. A. (1983). *Anal. Biochem. , 130*, 203-214.

Rosenberg, B. (1978). *Biochimie , 60*, 1037-1038.

Sabatani, E., Nikol, H. D., Gray, H. B., & Anson, F. C. (1996). *J. Am. Chem. Soc. , 118*, 1158-1163.

Samuni, A., Chevion, M., & Czapski, G. (1981). *J. of Biol. Chem. , 256* (24), 12632-12635.

Satyanarayana, S., Dabrowiak, J. C., & Chaires, J. B. (1992). *Biochemistry , 31* (39), 9319-9324.

Scarla, P. V., & Shafer, R. H. (1991). *J. of Biological Chemistry , 266* (9), 5417-5423.

Scovell, W. M., & O'Connor, T. (1977). *J. Am. Chem. Soc. , 99* (1), 120-126.

Services, U. D. (2014). *U.S. Department of Health and Human Services. Smoking and Cancer (Fact Sheet).* Atlanta, GA: US Dept of Health and Human Services, Centers for Disease Control and Prevention, National Center for Chronic Disease Prevention and Health Promotion, Office on Smoking and Health .

Sibirtsev, V. (2005). *Biochemistry (Moscow) , 70* (4), 449-457.

Singer, N. (2009, September 26). Health Concerns over Popular Contraceptives. *New York Times* .

Smith, J., Keene, F. R., Li, F., & Collins, J. G. (2013). In *Comprehensive Inorganic Chemistry II* (pp. 709-750).

Stemp, E. D., Holmlin, R. E., & Barton, J. K. (2000). *Inorganica Chimica Acta , 297*, 88-97.

Strianese, M. P. (2016). *Coord. Chem. Rev. , 318*, 16-28.

Suh, D., & Chaires, J. B. (1995). *Bioorganic & Medicinal Chemistry , 3* (6), 723-728.

Sun, Y., Collins, S. N., Joyce, L. E., & Turro, C. (2010). *Inorg. Chem. , 49*, 4257-4262.

Sundquist, W. L., & Lippard, S. J. (1990). *Coordination Chemistry Reviews , 100*, 293-322.

Sutherland, J. C., Lin, B., Monteleone, D. C., Mugavero, J., Sutherland, B. M., & Trunk, J. (1987). *Analytical Biochemistry , 163*, 446-457.

Swavey, S., & Wilson, D. (2015). *Inorganica Chimica Acta , 426*, 45-49.

Tan, L.-F., Chao, H., Zhen, K.-C., Fei, J.-J., Wang, F., Zhou, Y.-F., et al. (2007). *Polyhedron , 26*, 5458-5468.

Tortorello, M. (2012, March 14). The New York Times. *Is It Safe To Play Yet?*

Toyooka, T., & Ibuki, Y. (2007). *Environmental Toxicology and Pharmacology , 23*, 256-263.

Tse, W. C., & Boger, D. L. (2004). *Chem. and Biol. , 11*, 1607-1617.

Tullius, T. (1989). *Annu. Rev. Biophys. Biophys. Chem.* , 213-37.

Turro, C., Bossman, S. H., Jenkins, Y., Barton, J. K., & Turro, N. J. (1995). *J. Am. Chem. Soc. , 117*, 9026-9032.

Turro, N. J., Barton, J. K., & Tomalia, D. A. (1991). *Acc. Chem. Res. , 40*, 332-340.

Wang, D., & Lippard, S. J. (2005). *Nature Reviews Drug Discovery , 4* (4), 307-320.

Wang, L., Bian, G., Wang, L., Dong, L., Chen, H., & Xia, T. (2005). *Spectrochimica Acta Part A , 61*, 1201-1205.

Xiong, Y., & Ji, L.-N. (1999). *Coord. Chem. Rev. , 185-186*, 711-733.

Xue, W., & Warshawsky, D. (2005). *Toxicol. and Appl. Pharma. , 206*, 73-93.

Zelent, B., Vanderkooi, J. M., Coleman, R. G., Gryczynski, I., & Gryczynski, Z. (2006). *Biophysical Journal , 91*, 3864-3871.

Zhang, C. X., & Lippard, S. J. (2003). New Metal Complexes as Potential Therapeutics. *Current Opinion in Chemical Biology , 7*, 481-489.

Zhang, Y., Zhou, H.-Y., Shi, P., Yang, Q., Tang, L.-J., Jiang, J.-H., et al. (2016). *Analytica Chimica Acta* , 5.

Zhen, Q.-X., Ye, B.-H., Zhang, Q.-L., Liu, J.-G., Li, H., Ji, L.-N., et al. (1999). *J. of Inorg. Biochem. , 76*, 47-57.

Appendix 1: ^{1}H-NMR and ESI-MS of Synthesized Molecules

tert-butyl (6-([2,2'-bipyridine]-5-carboxamido)hexyl)carbamate [3] from acid chloride [2]

ESI-MS

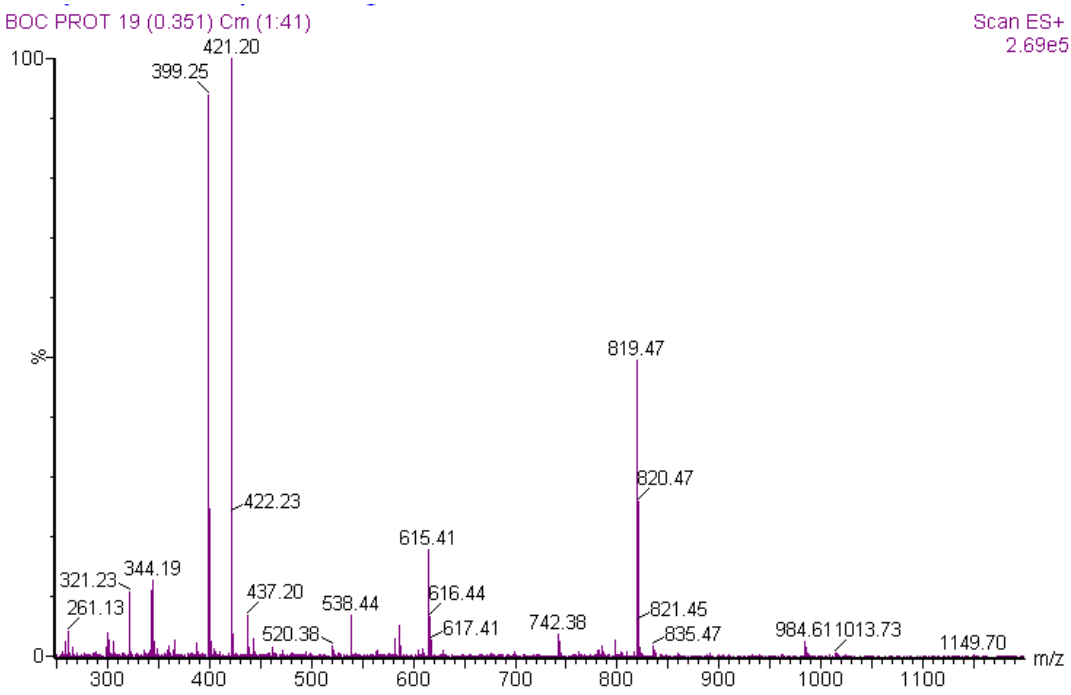

^{1}H-NMR

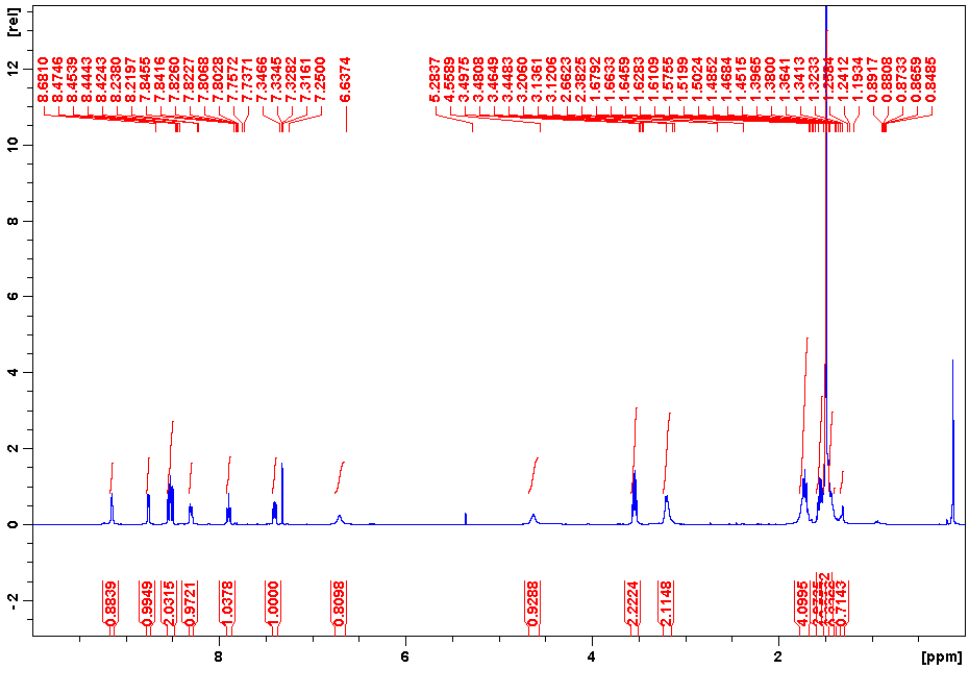

tert-butyl (6-([2,2'-bipyridine]-5-carboxamido)hexyl)carbamate [3] from TPP synthesis

ESI-MS

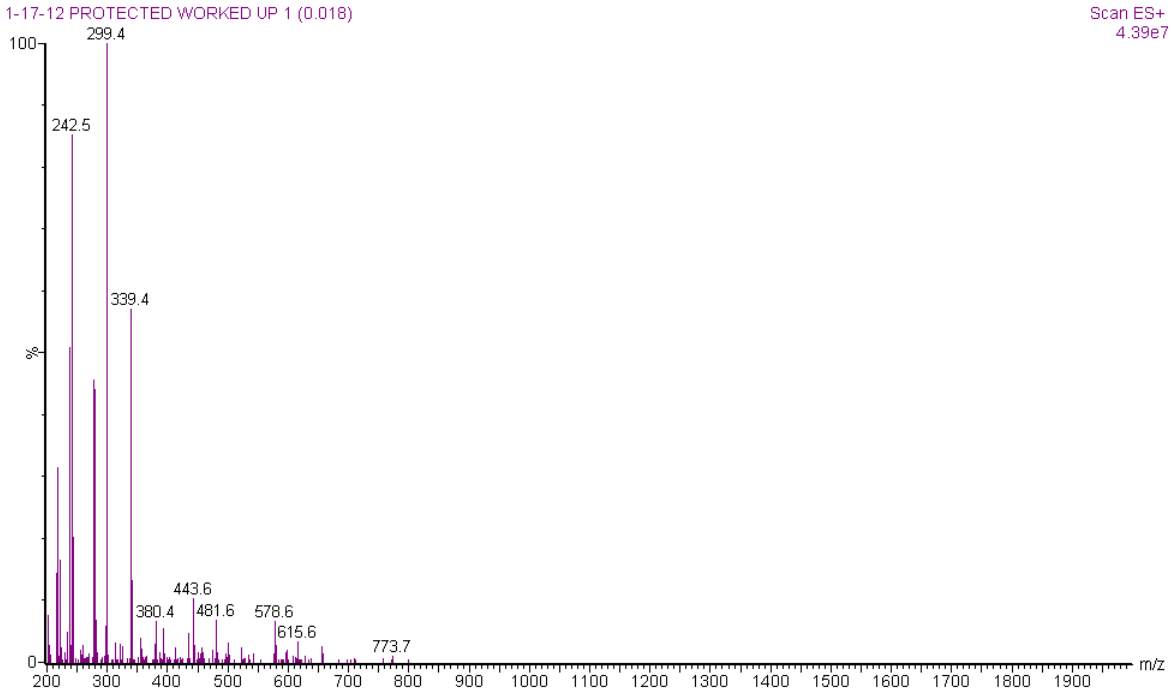

^{1}H-NMR

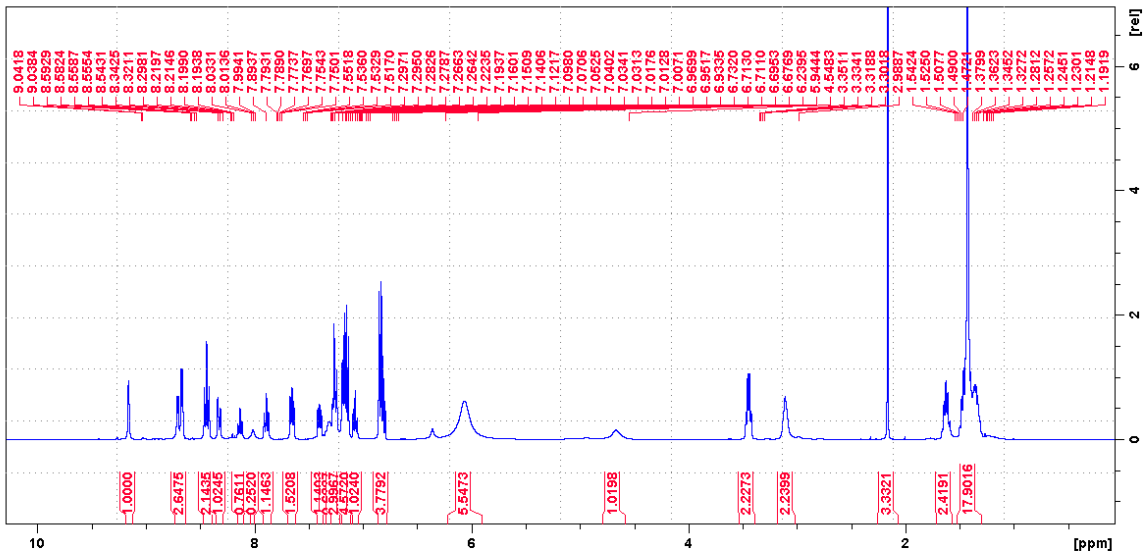

N-(6-aminohexyl)-[2,2'-bipyridine]-5-carboxamide [4]- from acid chloride [2]

ESI-MS

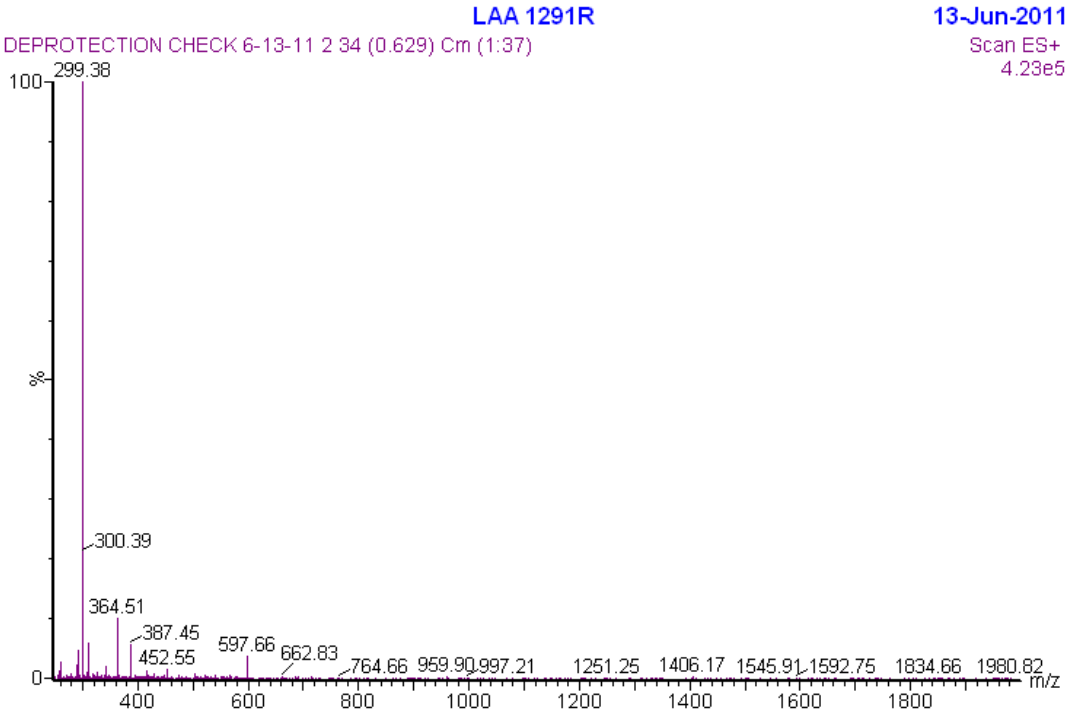

^{1}H-NMR

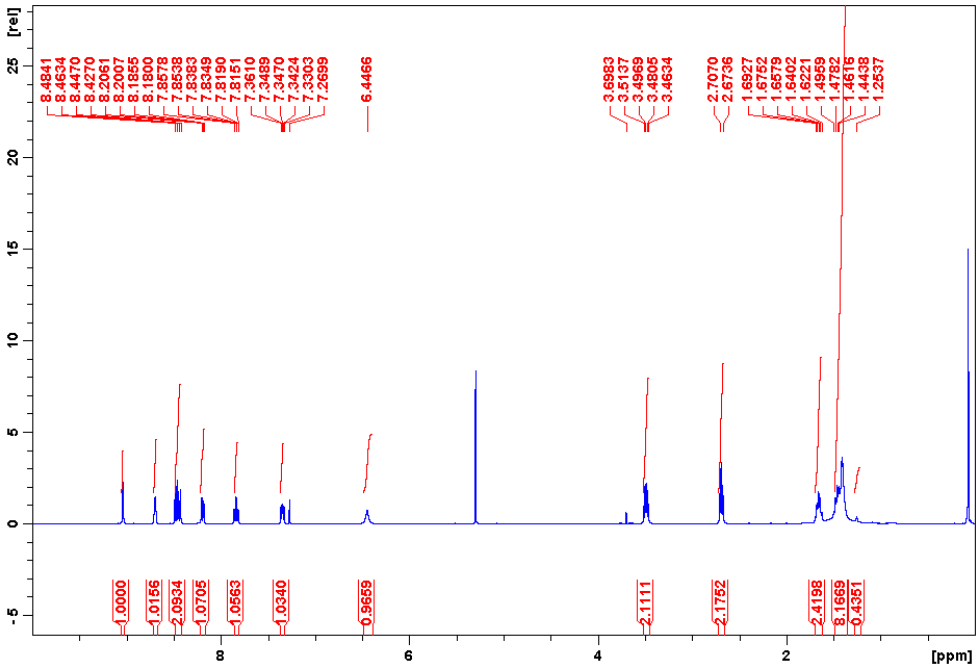

N-(6-aminohexyl)-[2,2'-bipyridine]-5-carboxamide [4]- from TPP Synthesis

ESI-MS

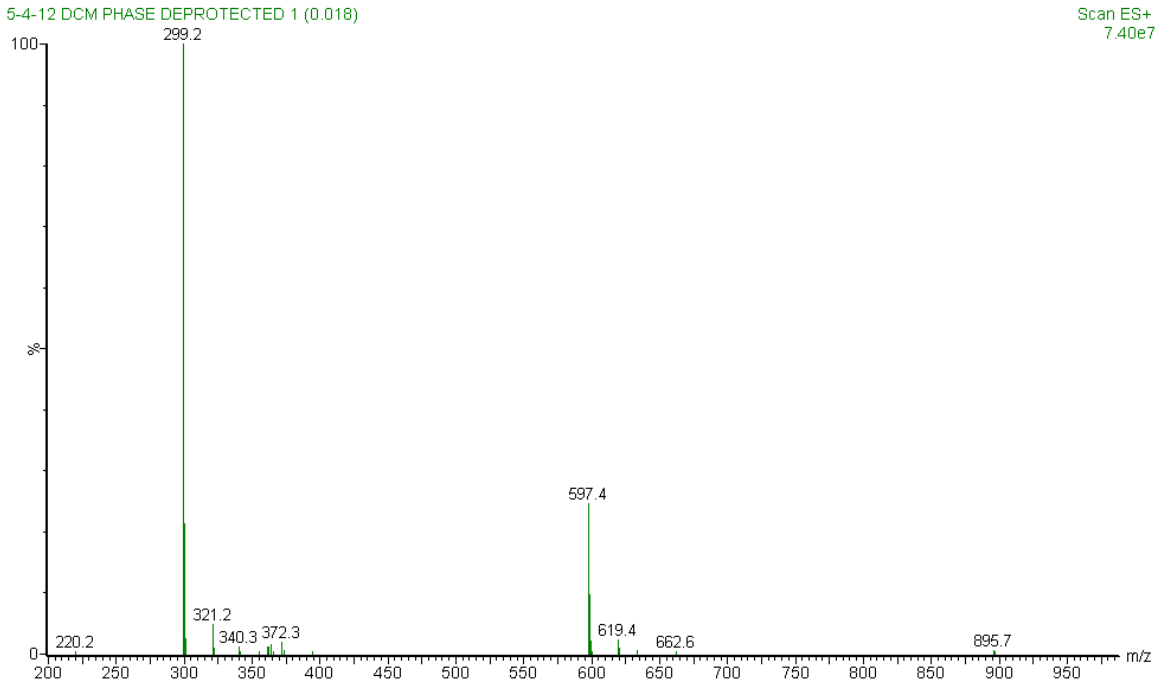

^{1}H-NMR

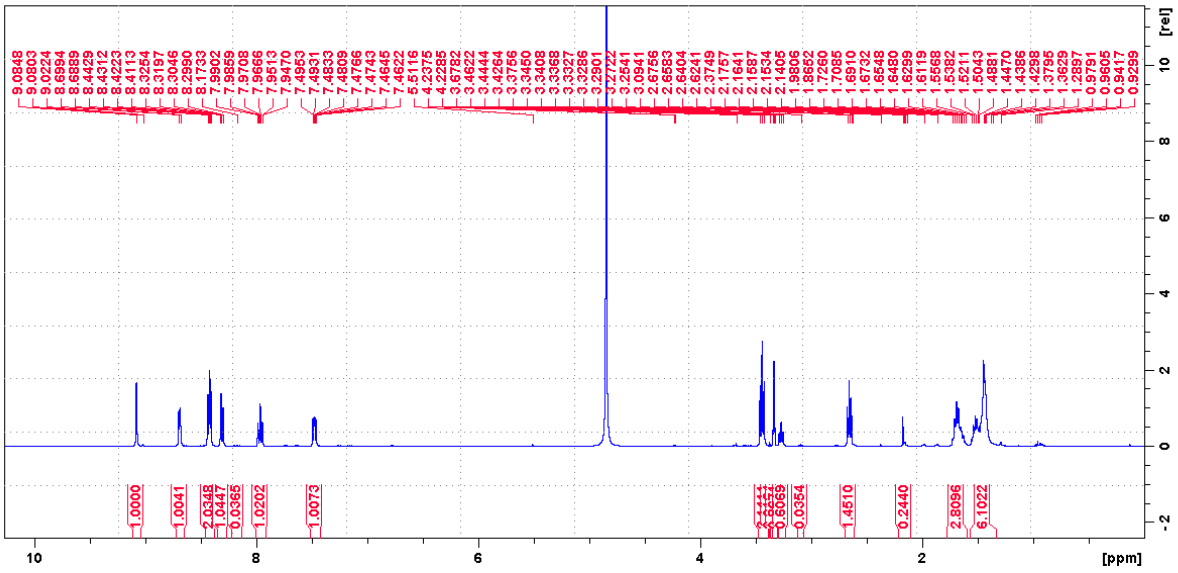

***N*- (6-(4-(pyren-1-yl)butanamido)hexyl)-[2,2'-bipyridine]-5-carboxamide (bpy-py) [6]**

ESI-MS

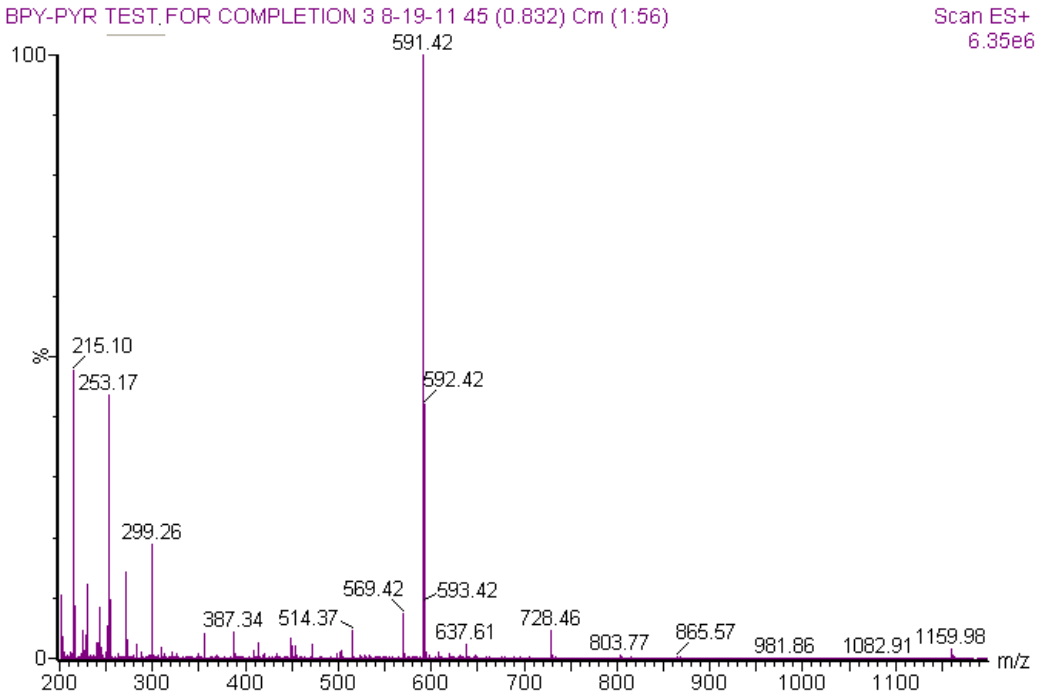

^{1}H-NMR

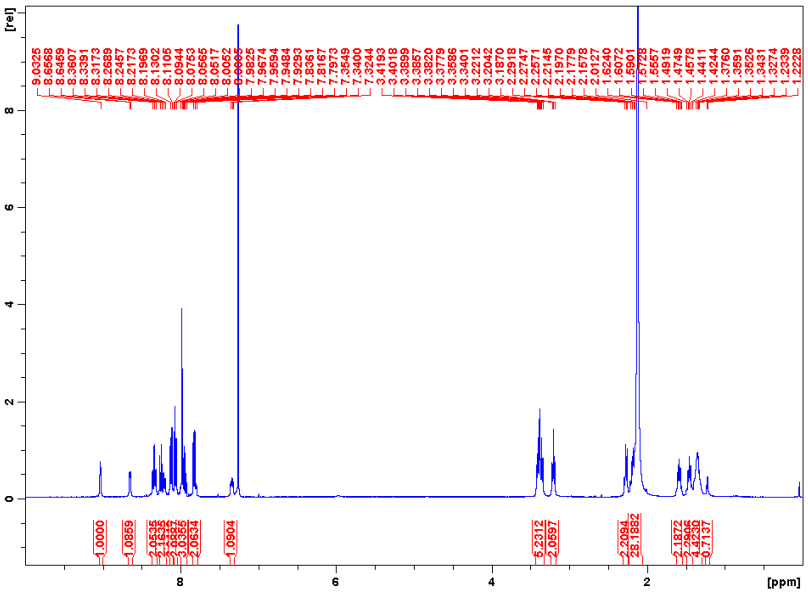

[Ru(bpy)$_2$dep]$^{2+}$ [8]

ESI-MS

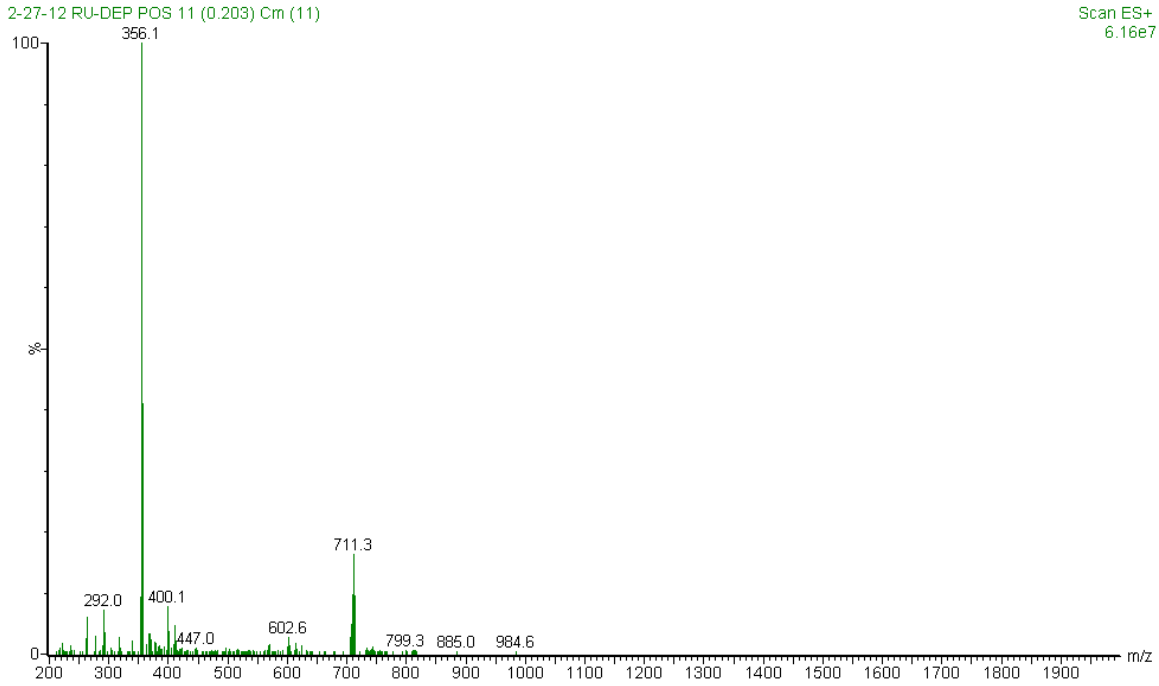

^{1}H-NMR

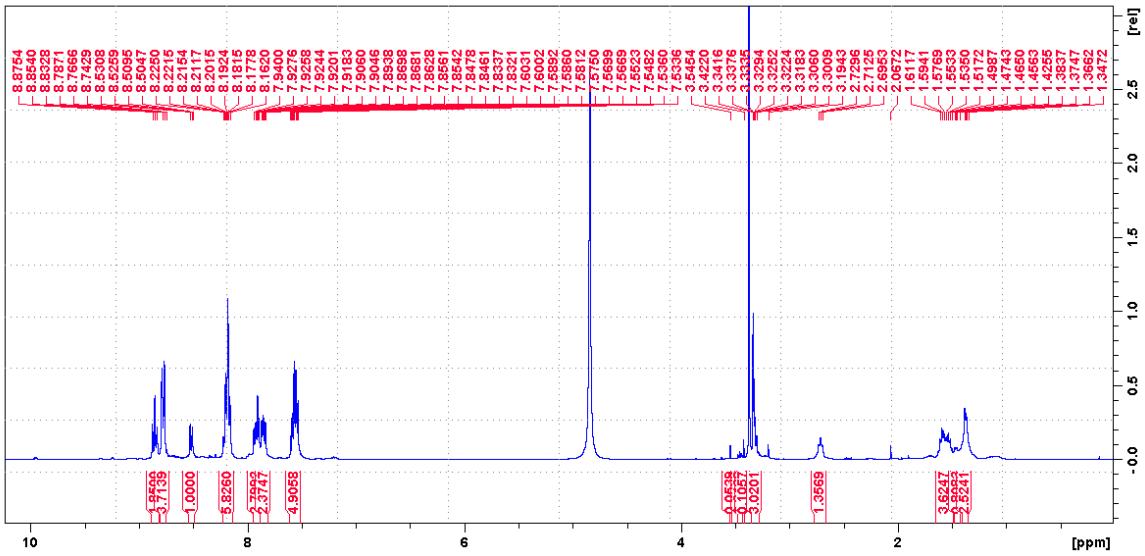

[Ru(bpy)$_2$bpy-py]$^{2+}$ [9]

ESI-MS

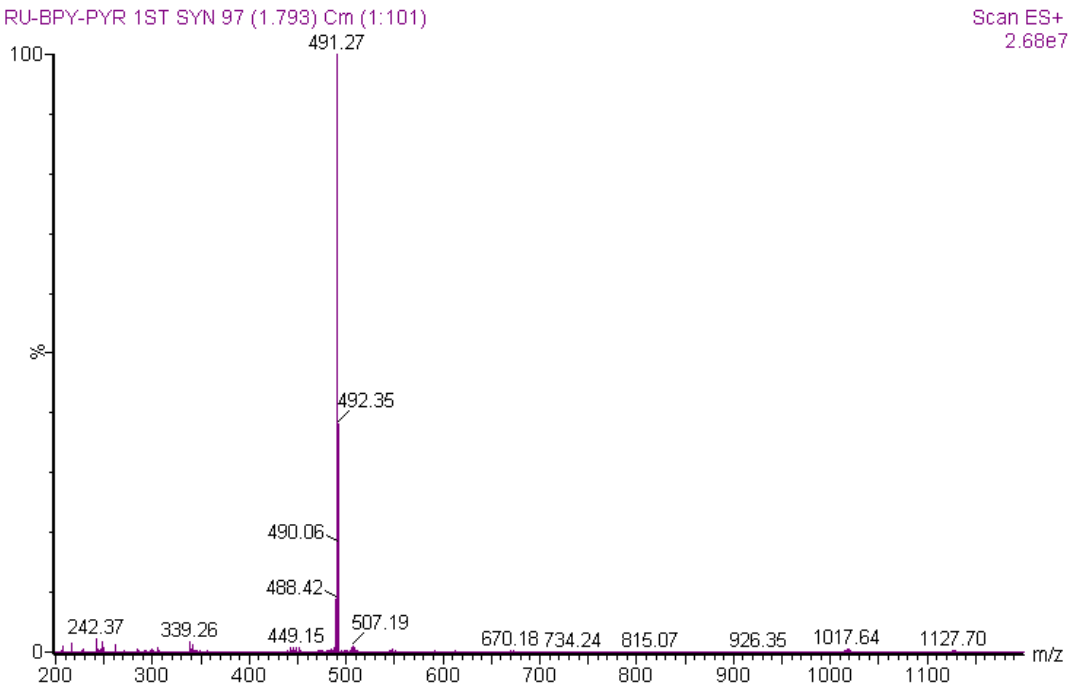
RU-BPY-PYR 1ST SYN 97 (1.793) Cm (1:101)
Scan ES+
2.68e7
491.27
492.35
490.06
488.42
242.37
339.26
449.15
507.19
670.18
734.24
815.07
926.35
1017.64
1127.70
m/z
%

^{1}H-NMR

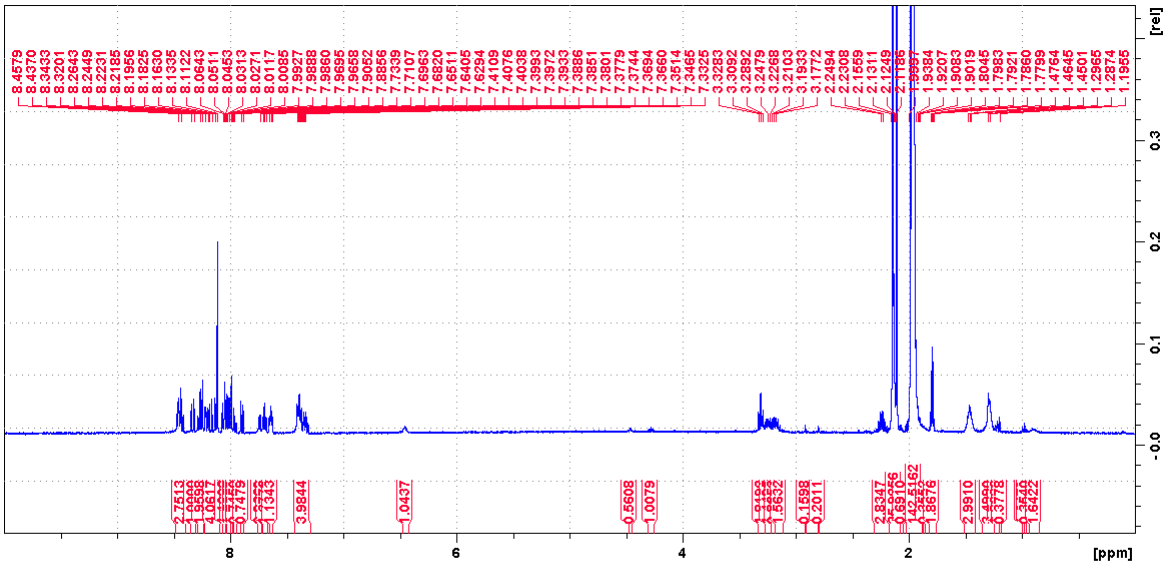
[rel]
[ppm]

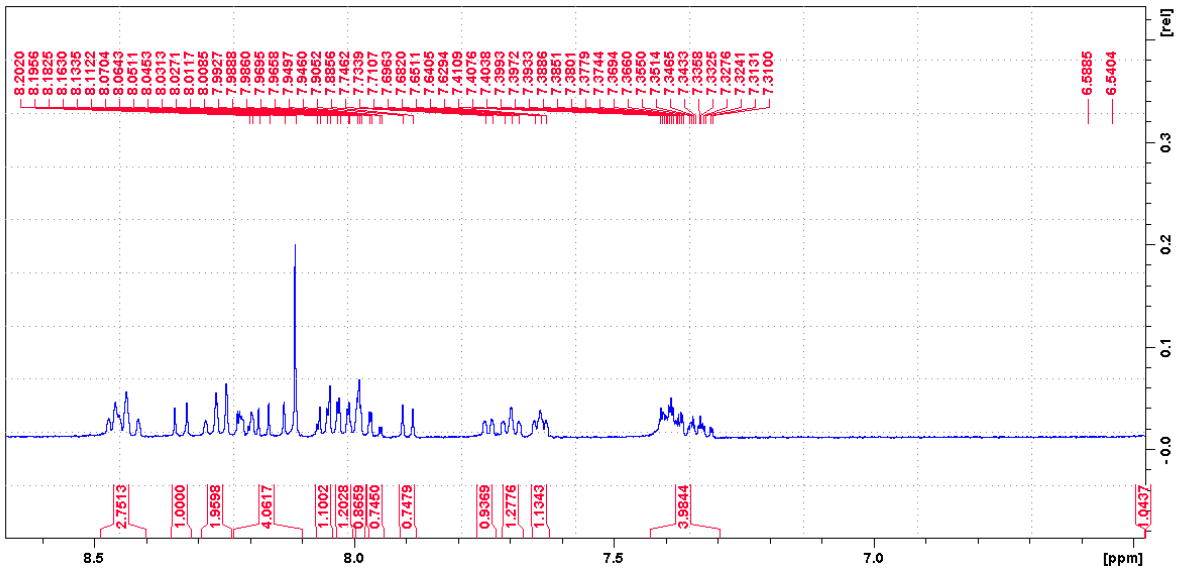
8.2020
8.1956
8.1825
8.1630
8.1336
8.1122
8.0704
8.0643
8.0511
8.0453
8.0313
8.0271
8.0117
8.0085
7.9927
7.9888
7.9860
7.9696
7.9668
7.9497
7.9460
7.9062
7.8866
7.7462
7.7432
7.7139
7.7107
7.6963
7.6870
7.6511
7.6485
7.6234
7.4109
7.4076
7.4038
7.3993
7.3972
7.3933
7.3886
7.3851
7.3801
7.3779
7.3744
7.3694
7.3660
7.3550
7.3514
7.3485
7.3433
7.3388
7.3325
7.3276
7.3241
7.3131
7.3100
6.5885
6.5404
[rel]
0.3
0.2
0.1
-0.0
2.7613
1.0000
1.9598
4.0617
1.1002
1.2028
0.3659
0.7480
0.7479
0.9369
1.2776
1.1343
3.9844
1.0437
8.5
8.0
7.5
7.0
[ppm]